THESIS REPORT
Master's Degree

SYSTEMS RESEARCH CENTER

Supported by the National Science Foundation Engineering Research Center Program (NSFD CD 8803012), the University of Maryland, Harvard University, and Industry

Dynamic Modeling and Analysis of Intermittent Turning Process

by W. Xu
Advisor: G. Zhang

M.S. 91-2

Abstract

Title of Thesis: Dynamic Modeling and Analysis of Intermittent Turning Process

Name of degree candidate: Weiyuan Xu

Degree and Year: Masters of Science, 1991

Thesis directed by: Dr. Guangming Zhang, Assistant Professor
Department of Mechanical Engineering and Systems Research Center

Increasing attention has been paid to the intermittent cutting process in modern metal machining industry. Research has been done in this thesis to develop a system model which can describe the intermittent turning process more precisely. In the development of the system model, the intermittent turning process is mathematically formulated and analyzed as a system associated with three periods, namely, the impact, cutting, and noncutting periods. The main methodologies used in this investigation are (1) applying modern control theory to perform dynamic cutting analysis in the cutting and noncutting periods, (2) employing wave propagation theory to study the impact force during the impact period, and (3) using numerical simulation and finite element method to examine the impact process and its effect on the machining performance. In this thesis, emphasis is focused on the effect of impact on the tool motion and the effect of the workpiece damping on the machining performance. The research results indicate that the impact between cutting tool and

workpiece at the every beginning of each cutting period is the main cause leading to mechanical failures of tool during the intermittent machining. Laboratory experiments have been conducted, and the obtained results show a general, good agreement with the results predicted by the developed system model. An attempt has been made to construct a stability boundary map, which could be useful in practical applications.

DYNAMIC MODELING AND ANALYSIS OF INTERMITTENT TURNING PROCESS

by

Weiyuan Xu

Thesis submitted to the Faculty of the Graduate School
of The University of Maryland in partial fulfillment
of the requirements for the degree of
Master of Science
1991

Advisory Committee:

Assistant Professor Guangming Zhang, Chairman/Advisor
Professor Andre Tits
Professor Jackson Yang

ACKNOWLEDGEMENT

I would like to express my thanks to my advisor, Dr. G. M. Zhang who always found time in his busy schedules to provide the encouragement and set the goals needed to complete such a project. I also appreciate the constructive criticism and suggestions which he provided at times when I strayed a bit off track. I would like to thank Professors A. Tits and J. Yang for their support throughout the course of this research.

I would like to thank my wife for her love, encouragement and financial support during my study in this school, without which I probably would never have reached this point. Also, I want to thank all my friends for their help.

TABLE OF CONTENTS

LIST OF FIGURES

LIST OF TABLES

NOMENCLATURE

A	= system matrix of the system dynamic equations, 4 $\times$ 4
A	= cross section area of the tool holder
a	= exponent representing nonlinearity between force and cutting speed
B	= input matrix of the system dynamic equation, 4 x 2
b	= exponent representing nonlinearity between force and mass
c	= exponent representing nonlinearity between force and K_2
$c_{1,2}$	= damping factor of the two principal modes
d	= depth of cut, mm
E	= modulus of elasticity for tension
F	= cutting force
F_o	= magnitude of the impact force
f	= feed, mm/rev
$G(j\omega)$	= open-loop transfer function in the complex domain
$g_1(s)$	= Laplace form of structural dynamics of mode 1
$g_2(s)$	= Laplace form of structural dynamics of mode 2
K_2	= material property coefficient function
$k_{1,2}$	= static stiffness of the two principal modes
k_c	= cutting stiffness
k_v	= gain factor related to cutting velocity variation
k_p	= gain factor related to penetration rate
l	= length of the tool holder
m	= equivalent mass of toolpost structure
M_{eq}	= equivalent mass of impactor

$M(j\omega)$ = closed-loop transfer function in the complex domain

$M(s)$ = closed-loop transfer function in the Laplace domain

N = spindle speed of a lathe

NUM = number of slots distributed along the circumference

P = transformation matrix, 4 x 4

$p(t)$ = force function

$Q(t)$ = state vector in the eigenvector space, 4 x 1

$q_{1,2}$ = displacement of the cutting tool in two principal directions

$\dot{q}_{1,2}$ = velocity of the cutting tool in two principal directions

R = nose radius of an impactor

$S_{x,y,z}$ = allowable strength properties of material in three orthogonal directions

T = time duration of one cycle of the intermittent cutting

t_o = time duration of impact period

$u(t)$ = chip thickness

u_i = deformation of the mass in the i^{th} direction

$u_o(t)$ = normal chip thickness

$\underline{u}(t)$ = matrix form of input function, 2 x 1

v = cutting speed, m/sec

v_{rel} = relative cutting speed between cutting tool and workpiece

w = width of cut

$\underline{x}(t)$ = state vector representing two principal modes, 4 x 1

$y(t)$ = displacement of the tool in the normal direction

$y_{res}(t)$ = surface modulation produced in the previous revolution

z = deformation in z direction

z_o = maximum displacement of the tool in tangential direction

$z(t)$ = displacement of the tool in the tangential direction

α = approach

α_1 = directional angle of the first principal mode

μ = overlap factor

ν = Poisson's ratio

θ = directional angle of the dynamic cutting force component

ρ = mass density

σ = normal stress

σ_{ii} = normal stress in principal direction

σ_{ij} = shear stress between i and j principal directions

σ_e = equivalent stress

σ_1 = real part of the first eigenvalue

σ_2 = real part of the second eigenvalue

$\omega_{n1,n2}$ = fundamental angular frequencies

$\omega_{i1,i2}$ = low and upper limits of angular frequency bandwidth for stability

ξ = constant in the calculation of impact force

$\xi_{1,2}$ = damping ratio of the system respecting to cutting and noncuttiing periods

CHAPTER 1
INTRODUCTION

The turning process is used widely in industry and has countless applications. Traditionally, the process has been used to reduce the diameter of a cylindrical workpiece, or to change a workpiece of non-circular to that of circular cross-section. This is done by rotating the workpiece about the axis of the machine's spindle and removing the workpiece material with the cutting tool which is fed in the axial direction.

The ever increasing competition in product functionality has forced product designer to seriously design the product components. The complexity of product geometry has been significantly increased during the past decades. Nowadays it is not uncommon to find holes, key-ways, slots, and other unique discontinuous geometries (such as the skirt on a piston) that are located on the circumference of a workpiece. Consequently, the use of the turning process has been extended to machine the workpiece without continuous machining surfaces. Since the cutting tool engages and leaves the workpiece alternatively, this type of turning processes is called the intermittent turning process.

Many industries make use of the intermittent turning process. they range from one as simple as the furniture industry to the auto industry, or to the high-tech aerospace industry. The reasons for the increase of using intermittent turning processes are mainly due to the following two factors:

First, new applications required for many new branches of industry, such as "the space age industry", have risen considerably. The machine parts used in these new branches not only have more specific quality and technology requirements, but also require the geometries of machine parts which are more complex to perform specific tasks.

Second, reduction of the chip product, consequently the reduction of machining time, is another factor for the increasing significance of applying intermittent machining although not many people have realized this implicit requirement. Today, the casting and forging techniques have become so precise that the machine parts can be shaped by a minima amount of cutting. As a result, some holes and slots or some non-continuous surfaces are pre-made on the workpiece before the workpiece undergoes machining.

In order to understand the mechanics of the intermittent turning process, or for any metal cutting process for that matter, one must have an understanding of both types of cutting, the continuous cutting and intermittent cutting. A major difference between the two is the cutting force generated during machining. In the continuous cutting process, the nominal cutting force is assumed to be a constant. In the intermittent turning process, the cutting force varies with the occurrence of cutting periods and non-cutting periods alternatively.

To have a deep understanding of the machining process , it is a common practice to develop a process model. Usually, the material properties of the workpiece, and the cutting conditions such as feed, spindle speed and the depth of cut, are treated as inputs to the process model. The outputs are the interests of machining performance, such as the cutting force and machined surface geometry. By developing the process model, the design of a machining operation can be improved by examining the input-output relations of the model rather than by a trialand-error method, which has been a traditional method used on the shop floor. On the other hand, the performance of a new machining operation, (a new workpiece material or new productivity constraints), can be maximized using the process model without even machining an actual workpiece. For this reason, numerous research has been done for the continuous turning process as well as the intermittent turning process.

The primary research objective of this thesis work is to search for the cause and origin of the phenomena observed during the intermittent cutting operation. In this thesis, mechanistically based models are developed that are able to predict the effect of various process variables on the performance measures of interests such as cutting forces, tool breakages, and surface accuracy. In light of these objectives, the main phases of this thesis work deal with modeling, analysis of system dynamics (finite element analysis), simulation, and experimental verification.

This thesis is organized as follows. There are six chapters to the thesis. Chapter 2 gives an overview of the relevant literature. There is fairly extensive literature pertaining to the turning process because the turning process is considered as the basis of most cutting operations. An attempt has been made to present a comprehensive picture in order to put this thesis in proper perspective.

Chapter 3 describes the basic methodology used in this thesis. The intermittent turning process is divided into three periods, namely impact period, cutting period and non-cutting period. A two-degree-of-freedom model is used in this thesis to describe the cutting and non-cutting periods. The impact period is treated as a transient period between the cutting and non-cutting periods. The wave propagation theory is applied in this thesis to describe the impact force and the relationship between the impact force and the cutting speed, chip load, and the position of the cutting tool.

In Chapter 4, the main focus is placed on model analysis of the intermittent turning process. System stability analysis is performed in this chapter. The effect of cutting speed, chap load and the intermittent frequency on system stability is studied in this chapter.

Chapter 5 presents a study of using numerical method to simulate tool motion both in the normal and tangential direction under some special conditions. The surface finish of workpiece is studied based on the simulation results. The experimental results and system performance indices are discussed in this chapter. In addition, finite element method is employed to analyze the impact process. As the most powerful method to deal with impact situation, the very complicated impact situation is viewed as a static situation in a very short time duration. The strain and stress distribution and variation in the impact period are expressed.

Chapter 6 summarizes the thesis and provides recommendations on the continuing research in this field.

CHAPTER 2
LITERATURE REVIEW

A review of the literature pertaining to studies of the continuous and intermittent turning processes can be divided into two basic areas. These two basic areas are analyses for the prediction of the cutting force system and surface topography, and analyses devoted to examining the dynamic characteristics of the impact between the tool and workpiece, leading to the prediction and control of tool breakages. The first area has been primarily devoted to the development of models, based on fundamental relationships, which may be used to predict a wide variety of process performance measures. These models, based on first principles are generally referred to as being mechanistic due to their limited dependence on experimentally obtained data. The second area of research has proven to be useful in predicting the dynamic characteristics of the impact force for a given set of machining parameters.

2.1 Continuous Turning Process

The continuous turning process has served as one of the basic machining processes in machining science. From the analytical and experimental studies, many scientists have made the contributions to this area. Most of the efforts directed to the continuous turning process were focused on describing the cutting tool chatter, which has been classified into three main categories, i.e., forced vibration or chatter, self-excited without regeneration chatter, and self-excited with regeneration chatter [26].

Generally, forced vibration is caused by an excitation force which has its origin outside the cutting zone, such as from a vibrating base, or from rotational unbalance in the workpiece being machined or in gears or shafts of the machine tool under operation. The main characteristic of the forced vibration is that the predominant frequency components of the forced vibration of the cutting tool are usually equal to the frequency components of the excitation force. To avoid the forced vibration in continuous machining processes, accurate balancing, mounting of vibration isolators are some of the popular methods used in workshops.

The two types of self-excited chatter, namely, the chatter with and without regeneration, have attracted many scientists. In the self-excited chatter, the excitation force acts on the cutting tool, and the force affecting the motion of the cutting tool is governed by the motion itself. The self-excited chatter with regeneration means that the exciting force varies with magnitude of the overlap caused by the prior cutting revolution. The self-excited chatter is a primary type of chatter encountered in continuous cutting processes. In practice, it is the basic performance limitation of cutting during a continuous cutting process.

Over the years, many mathematical models have been proposed to describe the continuous cutting system [63]. Several system analysis techniques have been developed to attack chatter problems. For example, in order to explain the occurrence of system instability when cutting speed and depth of cut are increased during machining, study on the system dynamics has been carried out by using the developed system models and analysis techniques. Significant progress for modeling development of the continuous turning process has been made in the following areas.

2.1.1 Machining System Modeling

Since the effects of these vibrations mentioned above are evidenced by poor surface finish, accelerated tool wear, dimensional inaccuracies, and acoustic pollution, much work has been done on investigation of the link between the cutting process and the machine tool structure. During the past two decades, attempts have been made to apply control theory which stemmed from electrical engineering to the field of metal cutting research, especially in the study of turning machining operations [26,27,28,31]. The basic assumptions which open the door of metal cutting research to control theory were dealing with how to define the tool motion during machining. Merritt first applied the control theory approach in this area [39]. He described the system model by the loop gains under two assumptions: 1) the tool motion occurs only in the direction of the uncut chip thickness; and 2) The dynamic characteristics of the tool motion at every point along the width of cut are identical. The three dynamic equations [39] ,which were used to develop a system model for the machining operation, are

1. Dynamic chip load equation,
2. Dynamic cutting force equation, and
3. Dynamic machine tool structural equation(s).

Based on these three equations, a mathematical model was formulated to describe the continuous machining process. The block diagram of a generalized machining system model is shown in Fig. 2.1.

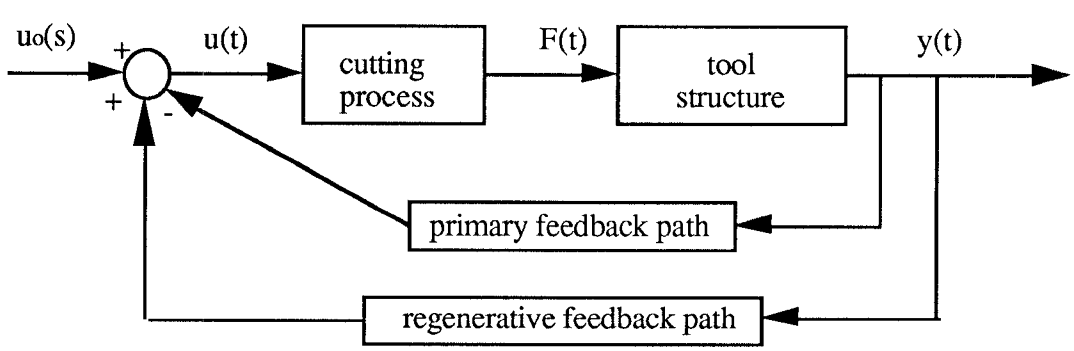

Fig.2.1 Turning Machining System

Since then, many researchers have done some significant work based on the control approach. Nachtigal and Cook first demonstrated the applicability of an active control scheme to a turning operation [24]. The designed controller during machining actuated the tool tip for the purpose of quenching any relative motion between the workpiece and the toolpost of a lathe, based on the detected cutting force signal. Kline, Glaser, and Nachtigal also applied the same active control scheme to a boring machining operation [17,27]. The designed controller in their work consisted of two hydraulic chambers and a servovalve. Based on the detected force and torque signals, the controller actuated the tool tip to compensate the tool displacement from its dynamic equilibrium. The work reported in [63] treated the regenerative feedback path in the Merritt's model as a second input. Such a modification in the system modeling allowed a non-linear system model to be dealt with as a linear system. In addition, a two degree-of-freedom system was used to perform analysis of the system dynamics. The random excitation caused by nonhomogeneity of the workpiece material hardness was also investigated in [63]. The block diagram shown in Fig. 2.2 is taken from [63].

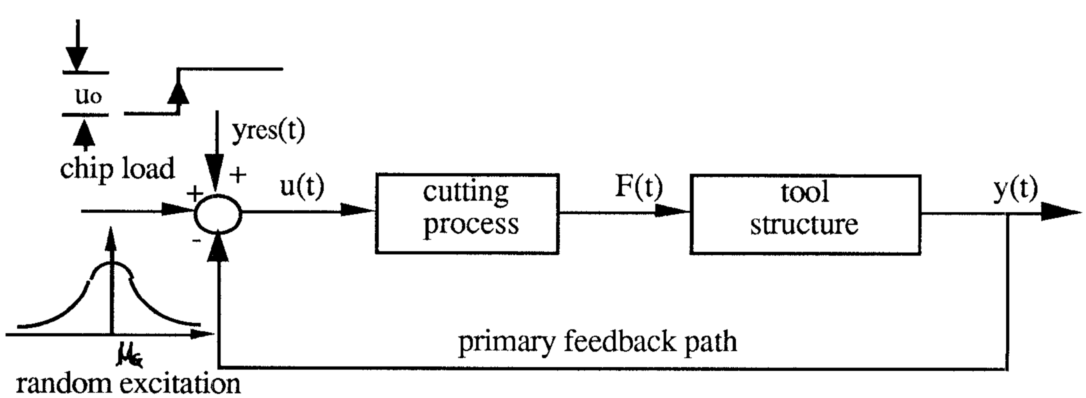

Fig. 2.2 Turning Machining System with Random Excitation

These progresses made by the researchers enable the prediction of system stability as well as the creation of the operation criteria for the continuous turning process. Difficulties, however, are met when these models are used to deal with the intermittent turning process.

2.1.2 Models of Machine Tool Structures

The dynamic behavior of the machine tool is of great concern when strict tolerances on surface characteristics must be met in the final product. For example, the dynamic response of the cutting process in conjunction with the dynamic response of the machine tool structure can result in instability. From a mechanical design point of view, a tool consists of two parts, i.e., a tool holder and a tool insert. During machining, the tool holder is fastened rigidly at one end and fitted with a cutting tool at the free end. Therefore, the structural dynamics of a tool during machining can be dealt with as a prismatic beam structure. A mathematical description based on Timoshenko formulation to describe the transverse vibration through a partial differential equation approach [50] is shown as follow:

$$m[\frac{\partial^2 y(x,t)}{\partial t^2} + c\frac{\partial y(x,t)}{\partial t}] + EI\frac{\partial^4 y(x,t)}{\partial t^4} = 0 \qquad (2.1)$$

with boundary and end conditions

$$\frac{\partial y}{\partial x}(0,t) = 0 \qquad EI\frac{\partial^3 y}{\partial x^3}(l,t) = -F(t)$$

$$y(0,t) = 0 \qquad \frac{\partial^2 y}{\partial x^2}(l,t) = 0$$

where m=mass per unit length of the tool holder, c=damping factor, E=modules of elasticity of the tool holder material, I=moment of inertia of the cross-section area, y(x,t)=deflection of the tool holder at a point x along the axis, and F(t)= force acting at the free end.

In general, the process of solving Eq. (2.1) identifies the natural frequency and natural modes of the tool holder structure.

$$\omega_i^2 = \xi_i \sqrt{\frac{EI}{\rho A}} \tag{2.2}$$

where ρ is the material density; A is the cross-section area; ξ_i are eigenvalues of the transcendental characteristics equation.

$$\cosh \xi_i l \cos \xi_i l = -1 \qquad i = 1, 2, \ldots \tag{2.3}$$

The Timoshenko' approach treats beam structures as continuous systems. Using the infinite degrees of freedom method, the approach accurately describes the dynamics of beam structures. However, due to the complexity of machining systems, a discrete system modeling approach is usually used in the study of system dynamics in the domain of machining science.

It has been observed that the fundamental mode of the tool holder structure plays a predominant role in the dynamic behavior during machining. Past experiences have shown that a two-degree-of-freedom model for the tool holder structure provides a reasonable way to predict the tool motion during machining. Using two-degree-of-freedom system models, the discrete system modeling approach is capable of evaluating the tool motion in the both directions, normal and tangential to the machined surface, and forms a basis for the simulation of the surface topography of the workpiece.

In this thesis work, both continuous and discrete system modeling approach are used. Taking the advantage of explicit, the tool motion during the cutting and non-cutting period is evaluated using a discrete system model. For an accurate prediction, the impact process is studied based on a continuous system model.

2.1.3 Cutting Force Models

The scientific basis for cutting mechanics has been the subject of many investigations. It is a well-accepted fact that the cutting mechanics in any machining operation where single-point tools are used is similar to the cutting mechanics in the lathe machining operation. In the beginning stage of the cutting force study, it was simply assumed that the cutting force was proportional to the instantaneous chip load [31,49].

$$F=k_s * A \tag{2.4}$$

Where k_s is proportionality coefficient, which is mainly a function of workpiece material, tool geometry, and cutting conditions. There were numerous experimental tests in the past to study the proportionality coefficient k_s. In early 1960's, Kronenberg [31] proposed that the cutting force be decomposed into three components, i.e., components of the tangential cutting force, the radial force and the feed force. It would be easy to obtain the measurements of these three components during machining tests. Upon knowing the three force components, the resultant cutting force can be evaluated by

$$F = \sqrt{p_1^2 + p_2^2 + p_3^2} = k_1 * f * d \sqrt{1 + k_2^2 + k_3^2} \tag{2.5}$$

where F=resultant force, p_1=tangential force component=k_1*f*d, p_2=radial force component=k_2*p_1, p_3=feed force component=k_3*p_1, f=feed, d=depth of cut, and k_1,

k_2 and k_3 are three proportionality coefficients which are functions of the workpiece material, tool geometry, and cutting conditions. These coefficients can be experimentally determined [31].

A few examples are presented to outline the previous study in the area of cutting dynamics. Hallam and Allasopp developed an integration method for the evaluation of the chip load during machining. Afterward, they assumed that the cutting force generated during machining be proportional to the chip load. In fact, they attempted to establish a mechanistic link between the cutting force and the cutting parameters such as the depth of cut, feed, and tool nose radius [20]. Although their work provided much insight of cutting mechanics from the cutting geometrical point of view, their derived mechanistic cutting force model did not fit over all the cutting parameters.

Tobias, et al. [47,54], suggested that cutting force be a function of chip area as well as a function of the penetration rate and the cutting speed variation.

$$F=k_c\, u+k_v\, v_z+k_p\, v_y \tag{2.6}$$

where k_c, k_v, and k_p are proportionality coefficients, v_z is the cutting velocity, v_y is the penetration rate, and u is the chip load. The suggestion about k_p was confirmed by Smith and Tobias [21] and later by Parker [6]. In order to determine the coefficient of penetration rate, they proposed the following equation.

$$k_p = -\frac{c_p k_c}{N} \tag{2.7}$$

where N is the spindle speed selected, k_c = cutting stiffness, and c_p = penetration factor.

Recognizing the effect of the part of tool vibration in the direction tangential to the machined surface, researchers further introduced a new cutting force component into the evaluation of the cutting force produced during machining [63]. This new component is called "tangential cutting force component." Consequently, the cutting force equation is modified as follow.

$$F(t)=k_c\, u+k_v\, v_z+k_p\, v_y+k_t\, z \qquad (2.8)$$

where z is the displacement of the cutting tool in the tangential direction, and k_t is the proportionality coefficient describing the effect of the tangential displacement. A method to determine the coefficient k_t was proposed in [63].

2.2 Intermittent Turning Process

Since the need for intermittent turning process increases, people tried to imitate research methods used in the area of continuous turning processes for the study of intermittent turning processes. As mentioned above, the intermittent turning process consists of cutting periods and non-cutting periods. It is reasonable to assume that all the methods used for studying the continuous turning process can be applied to the study of cutting dynamics during the cutting periods of an intermittent turning process. However, questions arise such as "What is the effect of the impact occurring at every beginning of the cutting period on tool motion? What is the influence of the metal fatigue on the occurrence of tool breakage during the intermittent turning process?", and etc. Evidently, a new research area has been established for studying the intermittent turning process.

Progress of the intermittent turning process research has been remarkable. The dynamics of intermittent cutting were first investigated by Zorev (1963 and 1970), Andreev (1974), Bhatia et al. (1979), and Tlusty and Ismail (1981 and 1983). they recognized the existence of thermal cracking, and mechanical fatigue during the intermittent turning process. Their research was focused on the determination of tool life, mainly through experimentation. Analytical approaches to study the cutting dynamics of the intermittent turning process became available in 1980s. Recognizing the inadequacy of the time-invariant system parameters, Kapoor (1985) developed and used a time-varying parameter model, based on Mathiew equation, to determine the stability boundary conditions of the intermittent turning process. Stability charts were constructed to aid in the proper selection of cutting parameters which maintain stability of the machining process.

Due to the increased machining speeds used on the shop floor, tool failure due to sudden impact has posed a new challenge to the manufacturing community. In addition, the frequent occurrence of sudden tool failure at high speed machining limits experimental studies of the intermittent turning process. To reduce the high cost associated with the tool insert replacement, recent advance reported in (Zhang, et al., 1989) was to study the mechanism of premature tool failure through computer simulation. Instead of carrying out actual cutting tests, tool motion during machining was evaluated through simulation, based on a developed time-varying parameter model. A failure criterion based on the concept of maximum overshoot was used to predict the rate of tool breakage. As preliminary study, in order to make the problem more distinct and handy, an assumption was set that the impact between the rotating workpiece and the vibrating tool is mainly due to the dynamic chip load variation at the start of every cutting period to allow a one-degree-of-freedom system to be developed [63]. With this assumption, the nominal chip load during the machining process can be represented by a rectangular wave function. The magnitude of the wave force was determined by the nominal chip load. The pattern of the wave form was determined by the shape of the discontinuous geometries located on the circumference of workpiece. The system model is shown in Fig. 2.3.

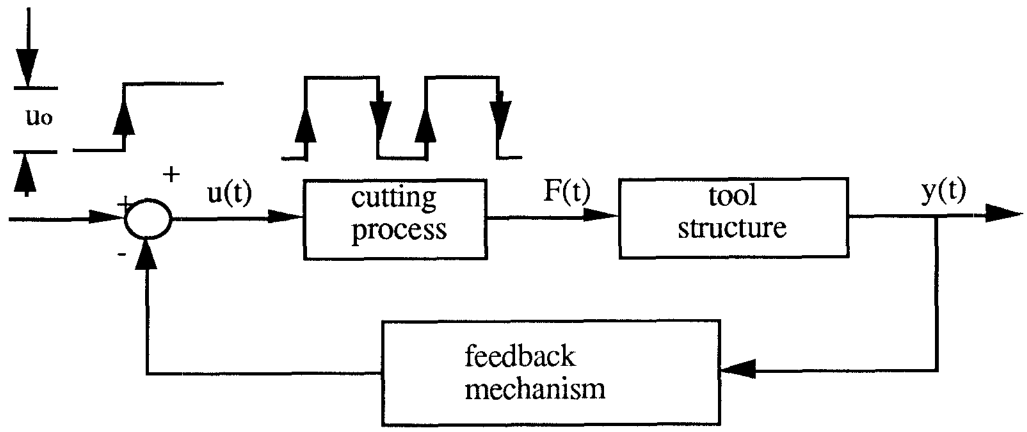

Fig. 2.3 Intermittent Turning Machining System

CHAPTER 3

BASIC METHODOLOGY

This chapter outlines the basic methodology used in this thesis for modeling and analyzing the intermittent turning process. There are two parts in this chapter.

The first part describes a modeling process to formulate the intermittent turning process. A new model for describing the intermittent turning process is developed. The model is a two-degree-of-freedom model based on the state-space approach in the modern control theory. Different from the previous approaches, the approach developed in this thesis treats the intermittent turning process as a process composing with three periods; cutting period, non-cutting period and impact period. Although the impact duration is a very short time period compared with the cutting period and non-cutting period, its importance on the machining system performance should be recognized, especially when the cutting speed is high. In this thesis, the impact duration is treated as a transient period between the cutting period and non-cutting period. The dynamic analysis of this transient process makes it possible to look into the relationship between the impact force and the machining parameters.

The second part of this chapter presents the modeling procedure of the intermittent turning process with emphasis on the formulation of the impact force developed during machining. The Newton's law of impact is used to establish an impact model to imitate the impact phenomenon observed during machining. Theories of elastic-plastic deformation and wave propagation are used to model the impact force and to estimate the time duration of the impact period.

3.1 Formulation of the Intermittent Turning Process

Traditionally, a machining operation system is considered to be a dynamic system. The machining system characterizes the process in which the generation of the cutting force during machining causes tool vibratory motion, which produces surface modulation.

Figures 3.1a and 3.1b present two typical models, which are represented by a one-degree-of-freedom and a two-degree-of-freedom systems. A major difference between these two models is determination of the tool motion in the direction normal to the machined surface. In a two-degree-of-freedom system, this motion is determined by the two shown modes, as opposed to this motion is determined solely by the mode shown in Figs. 3.1a. Generally speaking, a two-degree-of-freedom model is more acceptable for the study of machining system dynamics.

The block diagram shown in Fig. 3.2 is a general conceptual representation of the machining system model. The block diagram shows that the machining system model can be decomposed into two subsystems and a feedback mechanism. The two subsystems are the cutting process and the structural dynamics of machine tool. The feedback mechanism forms the link between the two subsystems.

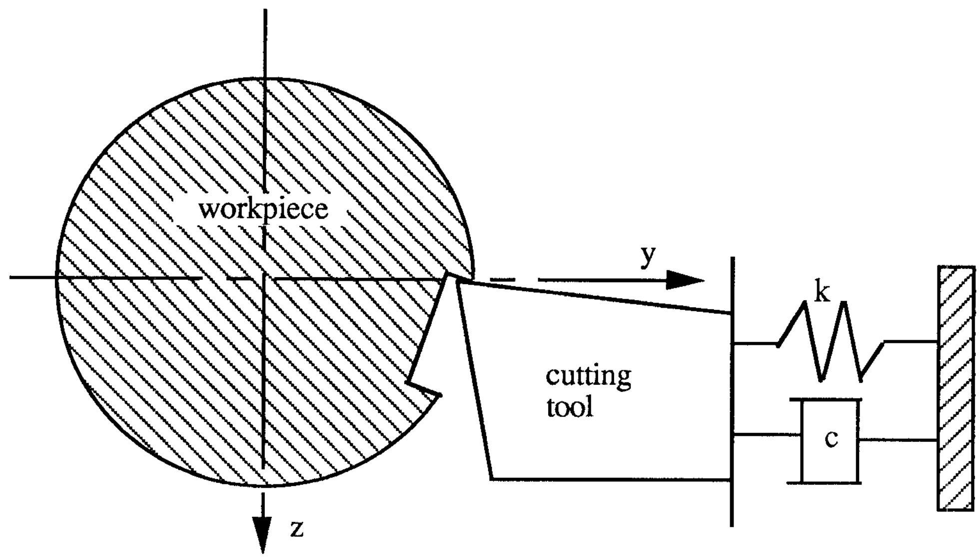

Fig. 3.1a System with One Degree of Freedom

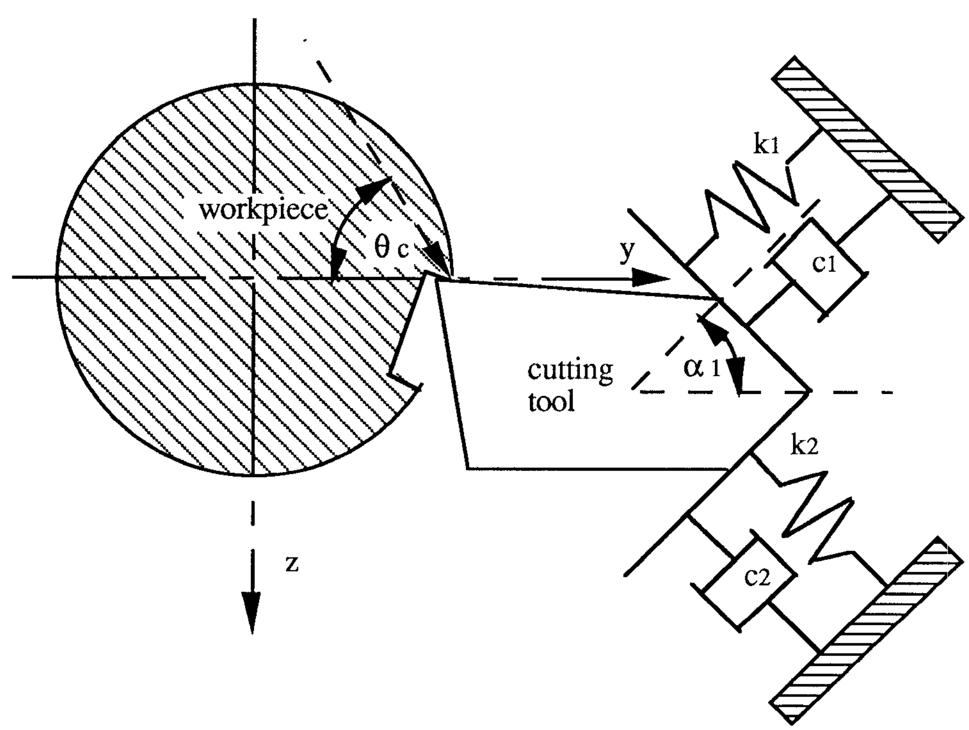

Fig. 3.1b System with Two Degree of Freedom

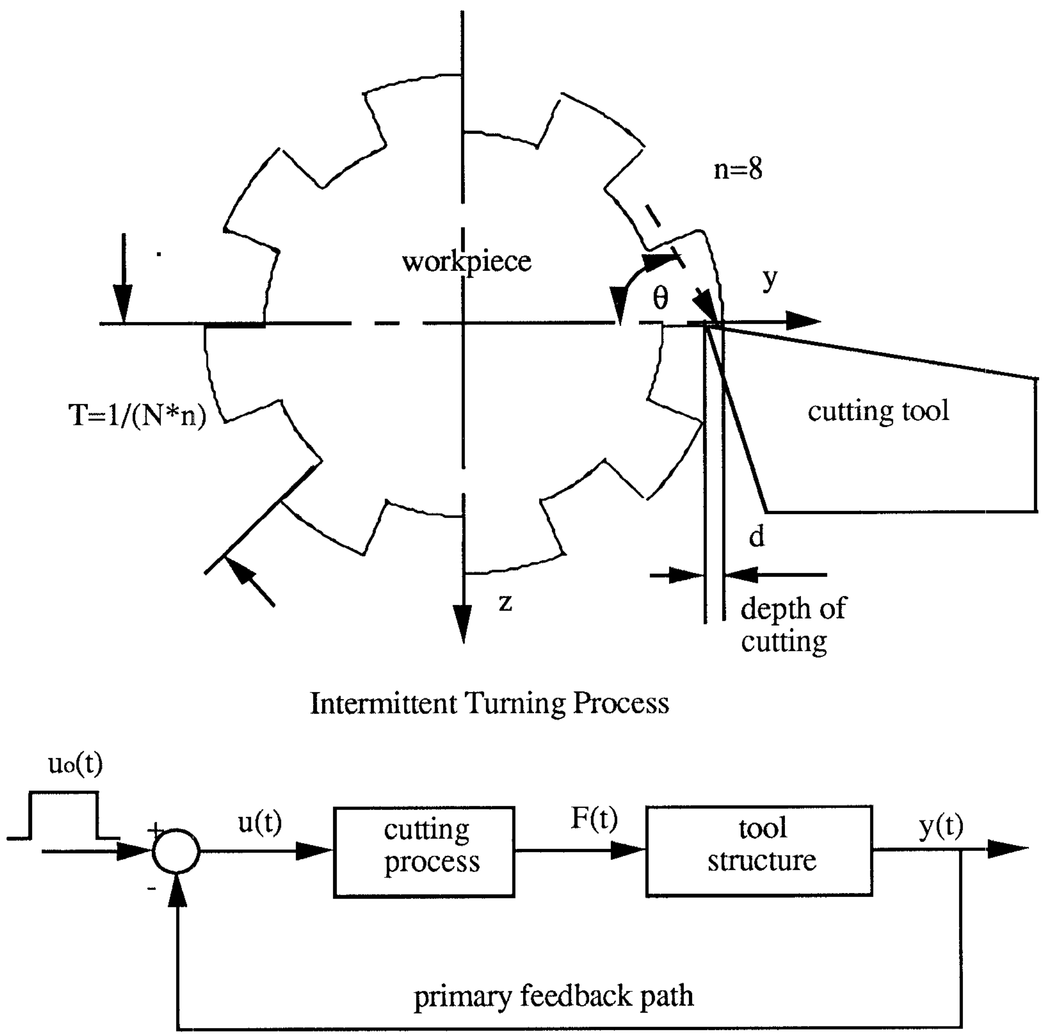

Fig. 3.2 General Machining System and Block Diagram for

Intermittent Turning Process

3.1.1 Basic Strategy and Assumptions

The mathematical representation of the system model developed in this thesis is built on the previous work. However, significant modifications have been made to characterize the feature of the intermittent turning process. Figure 3.2 presents the strategy of modeling the intermittent turning process. The workpiece geometry viewed in the cross section shows a hole located on the circumference. The discontinuous chip load during machining is expressed by a pulse string, or a rectangular wave form. The magnitude of the rectangular waves represents the nominal chip load. Parameters, T_1 and T_2, represent the time durations of the cutting and non-cutting periods. During the cutting period, the cutting force acts on the cutting tool with an angle, denoted as θ with respect to the Y direction, which is normal to the machined workpiece surface as illustrated in Fig. 3.2. The random excitation caused by the nonhomogeneous hardness distribution in the workpiece is treated as a disturbance during the cutting period. The whole cutting tool is treated as a lumped mass vibration system with two-degree-of-freedom. Parameters, k_1 and k_2, c_1 and c_2, represent the static stiffness and the damping factors of the cutting tool in the two principle directions. The positive direction of the Z axis is chosen to be downward in accordance with the direction of cutting speed. In this way, it will be easier to deal with the acceleration of the cutting tool in modeling the machining system. In the formulation of the system model, the following assumptions are made.

(1) The rigidity of the workpiece is assumed much greater then the rigidity of the tool. Therefore, the static deflection of the workpiece subjected to the cutting force is not accounted.

(2) The mass distribution of tool is considered as lumped system in the cutting and non-cutting periods. The tool mass is treated as a discrete lumped mass positioning at the contact point between the tool and workpiece.

(3) All disturbance forces in the cutting period are of random nature with an exception of the disturbance force due to the regenerative mechanism, which is dealt with a feedback loop.

(4) The impact period is a transient process between the non-cutting period and cutting period. The end conditions of a non-cutting period are the initial conditions of the impact period immediately followed. The end conditions of the impact period are the initial conditions of the cutting period immediately followed.

3.1.2 Dynamic Equations of Machine Tool Structure

Fig.3.3 is presents the configuration of modeling the machine tool structure. As the assumptions made in section 3.1.1, the machine tool structure is treated as a discrete lumped mass system with two-degree-of freedom, each of which displays second-order dynamics. The following two dynamic equations of machine tool structure are used for the model representation. The dynamic cutting force vector acts on the cutting tool. The resulting tool motion is governed by the following system of two second order differential equation

$$\begin{cases} m_1\ddot{q}_1(t) + c_1\dot{q}_1(t) + k_1q_1(t) = p_1(q_1, \dot{q}_1, q_2, \dot{q}_2) \\ m_2\ddot{q}_2(t) + c_2\dot{q}_2(t) + k_2q_2(t) = p_2(q_1, \dot{q}_1, q_2, \dot{q}_2) \end{cases} \tag{3.1}$$

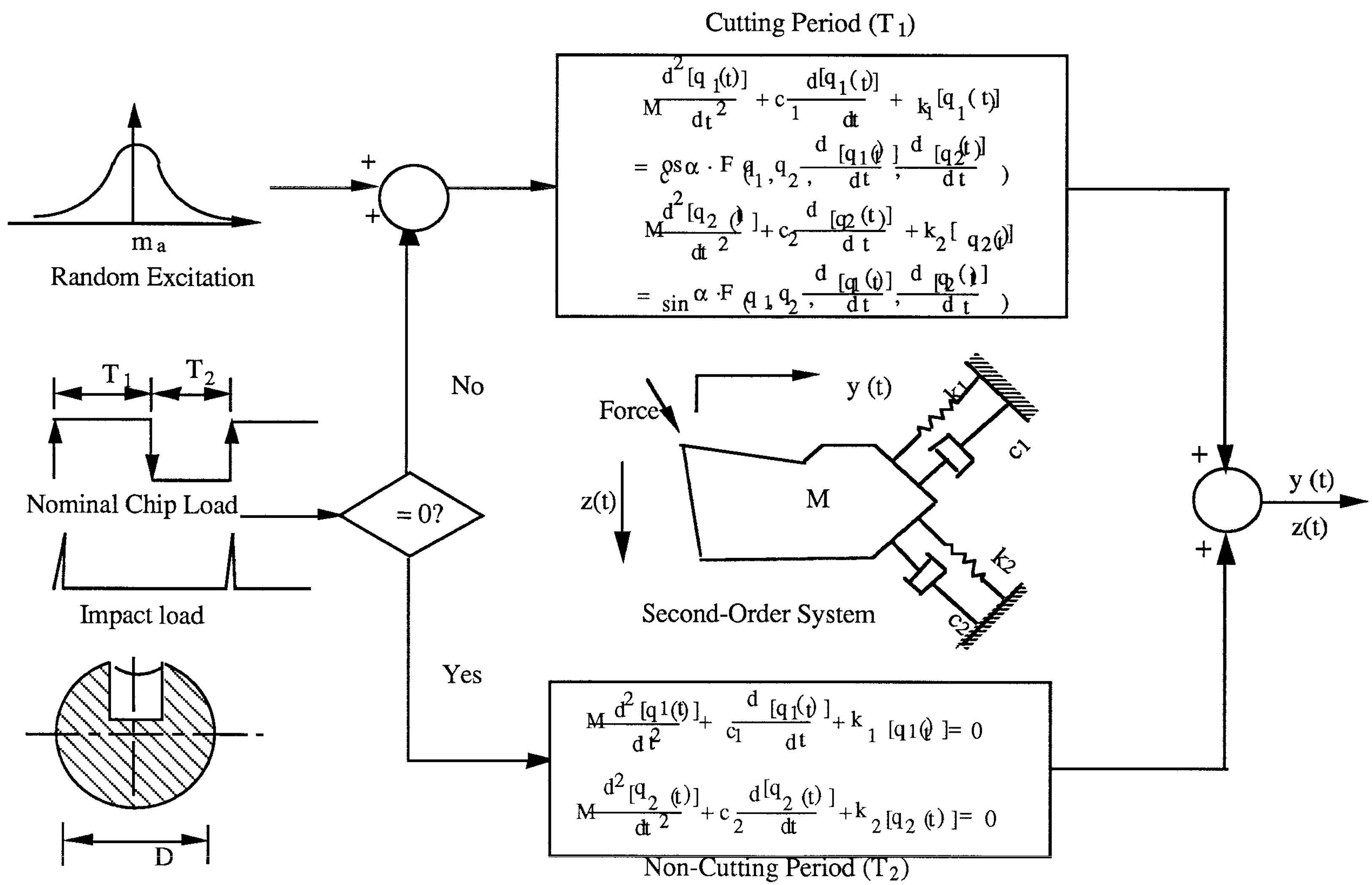

Fig. 3.3 Machining System Model of Intermittent Turning Process with Two Degree of Freedom

where $q_1(t)$ = displacement of mode 1

$\dot{q}_1(t)$ = velocity of mode 1

$q_2(t)$ = displacement of mode 2

$\dot{q}_2(t)$ = velocity of mode 2

Note that the terms on the right sides of Eq. (3.1) represent the cutting force acting on the machine tool structure. During the intermittent turning process, these terms are time variant. When the cutting tool is engaged in cutting, the generated cutting force is a function of the chip load and tool motion. These two terms drop to zero when the tool is flying over the discontinuous geometries. Mathematically speaking, these two terms are given by

Noncutting period: $p_1(t), p_2(t)=0$

Cutting period: $p_1(t), p_2(t)=p_1(q_1, \dot{q}_1, q_2, \dot{q}_2), p_2(q_1, \dot{q}_1, q_2, \dot{q}_2)$

The time duration of a cutting period can be determined by $t_1=T\bullet(l_1/l)$, where l is the length of workpiece circumference between two slots, the l_1 is the length of the continuous surface being machined. The time duration of a non-cutting period is given by $t_2=T\bullet(l_2/l)$, where l_2 is the length of non-cutting surface of workpiece between two continuous surface. In the case of continuous cutting, parameter T represents the time need for one revolution of the workpiece during machining. During an intermittent machining, the evaluation of parameter t_1, t_2 and T should be modified based on the characteristics of discontinuous geometries. In a special case of symmetry, parameter T can be determined by T=1/(NUM*N) where NUM represents number of slots which are uniformly distributed on the circumference shown in Fig. 3.2, and N is revolutions per second. It should be pointed out that a transient period exists between the noncutting period and the cutting period because of the impact between the cutting tool and the rotating workpiece. The effect of this impact force certainly plays an important role in the determination of the machining system performance. This effect should be included in the analysis of system dynamics. However, the time duration of this impact is rather small, comparing with the time durations of the cutting and noncutting periods. This thesis work will present an analytical method to evaluate the impact time duration.

3.1.3 Dynamic Cutting Force Equation

The cutting force generated during machining is a main concern affecting machining system performance such as surface finish and dimensional accuracy. The generation of the cutting force is also affected by two major factors, i.e., the chip load and tool motion. It has been said that the deeper we penetrated into this territory, the more problems were found [31]. In this thesis work, the cutting force model suggested by Tobias is used [47,54]. As stated in section 2.2, the cutting force is assumed to consist of the following three components.

$$\begin{aligned} F(t) &= F_1+F_2+F_3 \\ &= k_c u(t) + k_v \dot{z}(t) + k_p \dot{y}(t) \end{aligned} \tag{3.2}$$

The first cutting force component is due to the uncut chip thickness u(t). The proportionality coefficient can be evaluated by a product of the unit cutting force k_s and the width of cut, which is determined by the selected depth of cut and the tool geometry. In most of cases, numerical values of the unit cutting force can be found in machining handbooks.

The second cutting force component is due to the dynamic variation of cutting speed $\dot{z}(t)$ [63]. The proportionality coefficient, k_v, represents the effect of cutting speed variation on the cutting force variation. Numerical values of coefficient k_v may be experimentally identified from the relationship between the cutting force and cutting speed.

The third cutting force component refers to the effect of the tool motion in the direction normal to the machined surface, namely the penetration effect [1,47]. It has been observed that this motion causes the variation of the cutting force generated during machining. The proportionality coefficient, kp, can be found in literature [47].

How to determine the second and the third cutting force components have been studied by many researchers, and can been found in reference paper mentioned above. The selection of cutting parameter for the first cutting force component is much more different in the intermittent turning process than that in the continuous turning process. It is the major object in this thesis to determine the parameters of the first cutting force component which relate uncut chip load mentioned at previous section.

3.1.4 Dynamic Uncut Chip Thickness Equation

Fig. 3.4 shows the normal uncut chip thickness u(t) which is made of from three parts, i.e.,

$$u(t)=u_o-y(t)+y_{res}(t) \tag{3.3}$$

The first part u_o is called the normal uncut chip thickness, which is indeed determined by the machine operator. The second part, y(t), is related to tool vibration during machining. Assuming that no vibration is observed, then y(t) is set to zero. When vibration starts, the tool moves away from its set position. Such a relative movement between the tool and workpiece changes the chip load immediately. From mathematical modeling viewpoint, a negative feedback path exists between the tool vibratory motion and the chip load. Because this feedback path always exists, it is named as the primary feedback path. The third part, $y_{rest}(t)$, is related to the regenerative mechanism, a phenomenon commonly observed during the machining process. It is evident that the surface modulation, caused by tool vibration, produced during the current revolution of the workpiece will be transmitted to the chip load cut during the next revolution of the workpiece. From control theory, this part of chip load is called time delayed chip load. Some researchers model this transmission as a time delayed feedback path. The delayed time is equal to the time needed for one revolution of the workpiece. However, difficulties can be easily accounted because of the nonlinear nature of the time delay loop. A different approach was proposed in [63] to replace the regenerative feedback path by a residual chip load concept. Such a replacement maintains the linearity of the developed system model, facilitating the dynamic analysis of the machining system. The residual chip load is mathematically represented by

$$\Delta A_{res}(t) = \mu \cdot w \cdot [a_0 + \sum_{k=1}^{\infty} (a_k \cdot \cos \frac{2k\pi}{T} \cdot t + b_k \cdot \sin \frac{2k\pi}{T} \cdot t)]$$

or

$$y_{res}(t) = \mu[a_0 + \sum_{k=1}^{\infty} [(a_k \cdot \cos \frac{2k\pi}{T} \cdot t + b_k \cdot \sin \frac{2k\pi}{T} \cdot t)] \qquad (3.4)$$

where

w=width of cut

a_o, a_k, b_k=Fourier coefficients

μ=overlap factor $1>\mu>0$

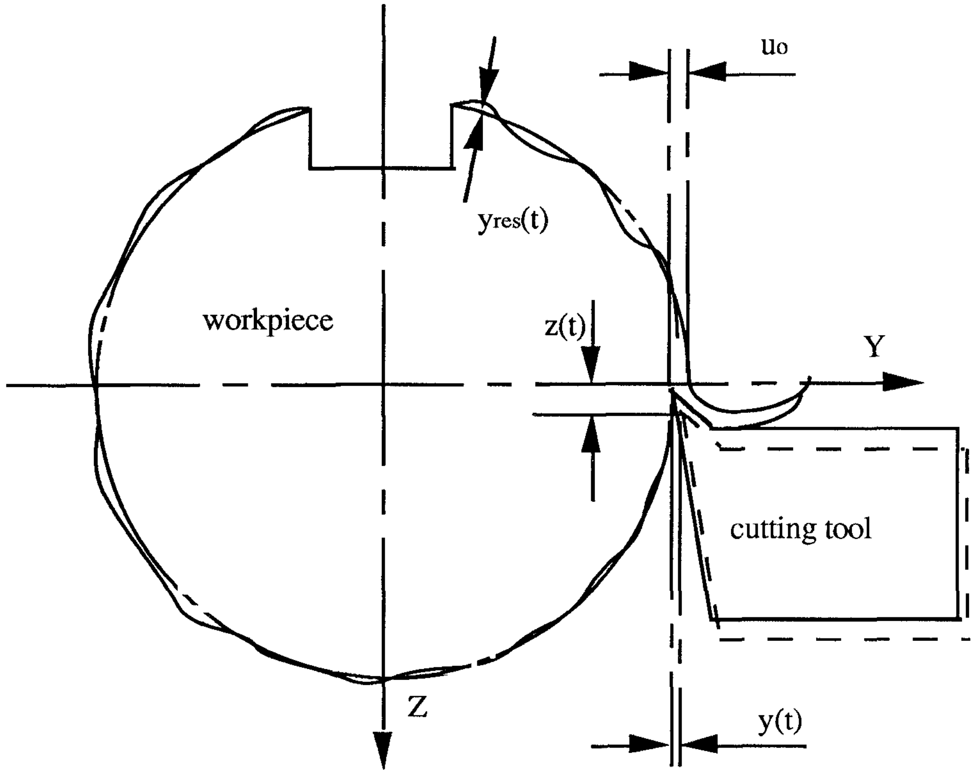

Fig. 3.4 Chip Load Components in The Cutting Period

3.1.5 State Variable System Model Formulation

In order to effectively use the linear control theory to perform system analysis, analysis techniques in the state space are applied to represent the model proposed in this thesis. The state variables are selected as follows:

$X_1(t)$=displacement of mode 1 $=q_1(t)$

$X_2(t)$=velocity of mode 1 $= \dot{q}_1(t)$

$X_3(t)$=displacement of mode 2 $=q_2(t)$

$X_4(t)$=velocity of mode 2 $= \dot{q}_2(t)$

Substituting the state variables into equation (3.1), results is written in the following four state equations.

$$
\begin{aligned}
\dot{x}_1(t) &= x_2(t) \\
\dot{x}_2(t) &= -\frac{c_1}{m}x_2(t) - \frac{k_1}{m}x_1(t) + \frac{1}{m}p_1[x_1(t),x_2(t),x_3(t),x_4(t)] \\
\dot{x}_3(t) &= x_4(t) \\
\dot{x}_4(t) &= -\frac{c_2}{m}x_4(t) - \frac{k_2}{m}x_3(t) + \frac{1}{m}p_2[x_1(t),x_2(t),x_3(t),x_4(t)]
\end{aligned}
\tag{3.5}
$$

In the cutting period

$$
\begin{aligned}
& p_1[x_1(t),x_2(t),x_3(t),x_4(t)] \\
&= k_c[u_0(t) - q_1\cos\alpha_1 - q_2\sin\alpha_1]\cdot\cos(\alpha_1+\theta_c) \\
&+ k_v(\dot{q}_2\cos\alpha_1 - \dot{q}_1\sin\alpha_1)\cdot\sin(\alpha_1+\theta_v) \\
&+ k_p(\dot{q}_1\cos\alpha_1 + \dot{q}_2\sin\alpha_1)\cdot\cos(\alpha_1+\theta_p) \\
&= k_c[u(t)\cos(\alpha_1+\theta_c) - q_1c_{11} - q_2c_{12}] + k_v[\dot{q}_2v_{21} - \dot{q}_1v_{22}] \\
&+ k_p[\dot{q}_1p_{11} + \dot{q}_2p_{12}]
\end{aligned}
\tag{3.6}
$$

and

$$
\begin{aligned}
& p_2[x_1(t),x_2(t),x_3(t),x_4(t)] \\
&= k_c[u_0(t) - q_1\cos\alpha_1 - q_2\sin\alpha_1]\cdot\sin(\alpha_1+\theta_c) \\
&+ k_v(\dot{q}_2\cos\alpha_1 - \dot{q}_1\sin\alpha_1)\cdot\cos(\alpha_1+\theta_v) \\
&+ k_p(\dot{q}_1\cos\alpha_1 + \dot{q}_2\sin\alpha_1)\cdot\sin(\alpha_1+\theta_p) \\
&= k_c[u(t)\cos(\alpha_1+\theta_c) - q_1c_{21} - q_2c_{22}] + k_v[\dot{q}_2v_{11} - \dot{q}_1v_{12}] \\
&+ k_p[\dot{q}_1p_{21} + \dot{q}_2p_{22}]
\end{aligned}
\tag{3.7}
$$

Arranging the four state equation in a matrix form and defining the output variable, the following dynamic equations of the machining system in a matrix form can be derived as follows.

$$\underline{\dot{x}}(t) = [A]\underline{x}(t) + [B]\underline{u}(t)$$

$$y(t) = [C]\underline{x}(t) \tag{3.8}$$

where

y(t) is the output variable, the displacement in the normal direction

$\dot{z}(t)$ is the velocity of cutting tool in the tangential direction

$[A]=$

$$\begin{bmatrix} 0 & 1 & 0 & 0 \\ \frac{-k_1-k_c c_{11}}{m} & \frac{-c_1+k_p p_{11}-k_v v_{22}}{m} & \frac{-k_c c_{12}}{m} & \frac{k_v v_{21}+k_p p_{21}}{m} \\ 0 & 0 & 0 & 1 \\ \frac{-k_c c_{21}}{m} & \frac{k_p p_{21}-k_v v_{12}}{m} & \frac{-k_2-k_c c_{22}}{m} & \frac{k_v v_{11}+k_p p_{22}-c_2}{m} \end{bmatrix}$$

$$\underline{u} = \begin{bmatrix} u(t) \\ y_{res}(t) \end{bmatrix}$$

$$[B] = \begin{bmatrix} 0 & 0 \\ \frac{k_c \cos(\alpha_1+\theta_c)}{m} & \frac{k_c \sin(\alpha_1+\theta_v)}{m} \\ 0 & 0 \\ \frac{k_c \sin(\alpha_1+\theta_c)}{m} & \frac{k_c \cos(\alpha_1+\theta_v)}{m} \end{bmatrix}$$

$$[C] = [\ \cos\alpha_1 \quad 0 \quad \sin\alpha_1 \quad 0\ ]$$

$$c_{11} = \cos(\alpha_1+\theta_c)\cdot\cos\alpha_1 \qquad v_{11} = \cos(\alpha_1+\theta_v)\cdot\cos\alpha_1$$

$$c_{12} = \cos(\alpha_1+\theta_c)\cdot\sin\alpha_1 \qquad v_{12} = \cos(\alpha_1+\theta_v)\cdot\sin\alpha_1$$

$$c_{21} = \sin(\alpha_1+\theta_c)\cdot\cos\alpha_1 \qquad v_{21} = \sin(\alpha_1+\theta_v)\cdot\cos\alpha_1$$

$$c_{22} = \sin(\alpha_1+\theta_c)\cdot\sin\alpha_1 \qquad v_{22} = \sin(\alpha_1+\theta_v)\cdot\sin\alpha_1$$

$$p_{11} = \cos(\alpha_1 + \theta_p) \cdot \cos\alpha_1$$
$$p_{12} = \cos(\alpha_1 + \theta_p) \cdot \sin\alpha_1$$
$$p_{21} = \sin(\alpha_1 + \theta_p) \cdot \cos\alpha_1$$
$$p_{22} = \sin(\alpha_1 + \theta_p) \cdot \sin\alpha_1$$

A block diagram of the machining system for the cutting period is shown in Fig. 3.5. For the non-cutting period, the cutting force is zero, and its block diagram is shown in Fig. 3.6. In addition to these two system models, a third model is also used for the representation of the impact between the cutting tool and the rotating workpiece at the beginning of every cutting period. The impact duration is treated as a transient period because its time duration is so limited if compared with the time durations of the cutting period and non-cutting period.

The new model processes two distinguishing feature. First, the impact can be studied separately. Second, the model include all factors which would affect the cutting tool motion in the intermittent turning process.

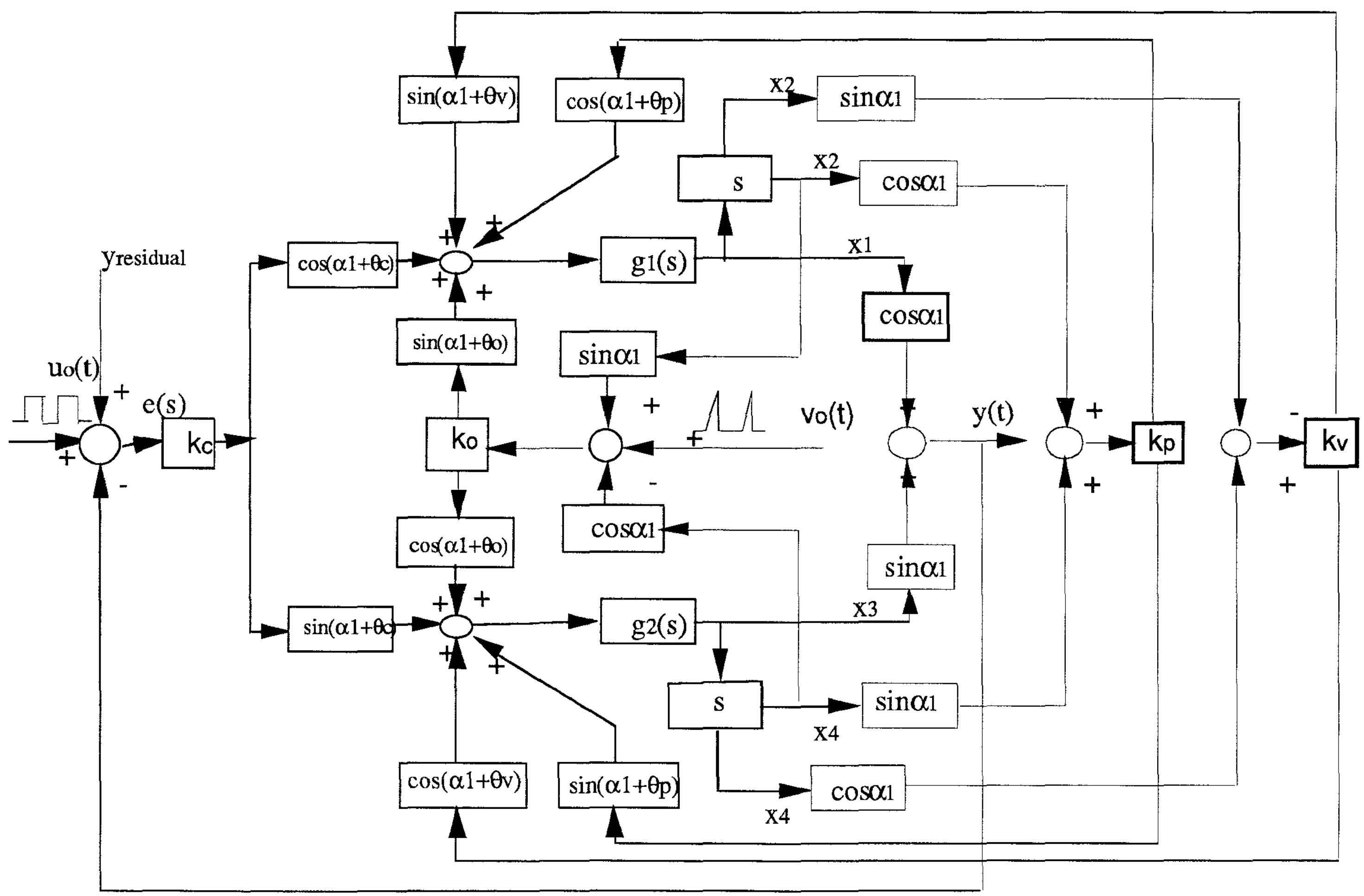

Fig. 3.5 Block Diagram for Intermittent Turning Process During Cutting Period

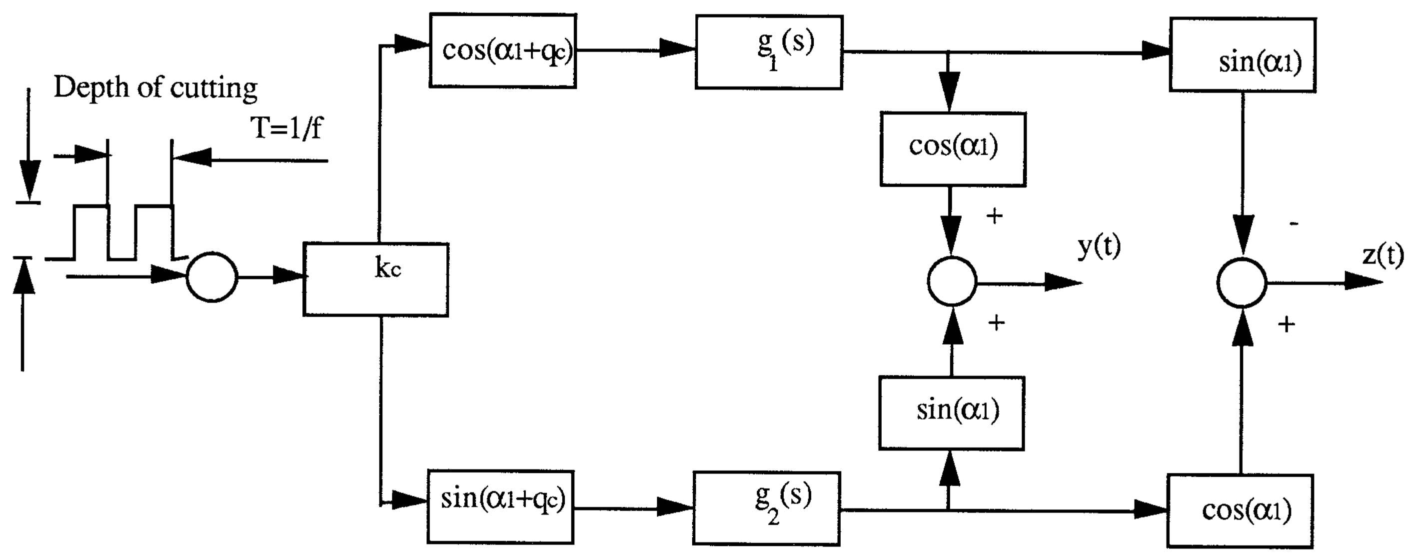

Fig. 3.6 Block Digram for Intermittent Turning Process during Non-cutting Period

3.2 Wave propagation theory

Conventionally, the impulsive force is replaced by an equivalent initial velocity in analyzing system dynamics. Such a replacement is based on an assumption that the impact duration is so small that the magnitude of the impulsive force is virtually infinite. In the present work, the magnitude of the impulsive force is finite according to the theory of colliding solids [70]. This indicates that it would not be valid to simply replace the impulsive force by an equivalent initial velocity, implying the elimination of the impact process, which is not appropriate. Therefore, estimating the impact force and impact duration in the intermittent turning process is necessary.

The response of materials and structures to intense impulsive loading is quite complex. In the process involving elastic-plastic flow, the force and the behavior of the material varies dramatically. For conceptual clarity, the behavior of impacted solids may roughly be divided into three regimes. For loading conditions that result in stress below the yield point, materials behave elastically. The Hooke's law can be applicable. As the intensity of the applied load is increased, the material is driven into the plastic range. The behavior in plastic range involves large deformation heating, and failure of the colliding solids through a variety of mechanism. With still further increases in loading intensity, pressure is generated that exceeds the strength of the colliding solids by several orders of magnitude, which, in effect, behave hydrodynamically [70].

To use the wave propagation for studying the effect of the impact in the intermittent turning process, the following assumptions are emphasized. 1) The impact force is the dominant force with its magnitude significantly larger than other cutting force, and the tool motion during the impact period is solely determined by the impulsive force; 2) the direction of the impulsive force is along the direction of the cutting speed; 3) before the tool breakage, the deformation of the cutting tool mass is in the elastic range, the material behaviors obey the linear principle.

3.2.1 Basic Formulation

Classical theory of elasticity provides the basis for wave analysis in elastic solids. The equations of wave propagation are derived by a combination of three-dimensional stress-strain relations, compatibility conditions, and the equations of motion. Generally, the elastic solid is regarded as a linear spring with stress proportional to strain, or

$$\sigma_q = E\varepsilon_q = E\frac{\partial u_q}{\partial q} \tag{3.9}$$

where σ is stress, E is Young's modulus, ε is strain, and q is the direction which the force acts on. The displacement equations of motion in rectangular coordinate system are expressed as

$$\begin{aligned}
\rho\frac{\partial^2 u_x}{\partial t^2} &= (\lambda + G)\frac{\partial \Delta}{\partial x} + G\nabla^2 u_x \\
\rho\frac{\partial^2 u_y}{\partial t^2} &= (\lambda + G)\frac{\partial \Delta}{\partial y} + G\nabla^2 u_y \\
\rho\frac{\partial^2 u_z}{\partial t^2} &= (\lambda + G)\frac{\partial \Delta}{\partial z} + G\nabla^2 u_z
\end{aligned} \tag{3.10}$$

where

$$\nabla^2 \equiv (\frac{\partial^2}{\partial x^2} + \frac{\partial^2}{\partial y^2} + \frac{\partial^2}{\partial z^2})$$

λ and G are called the Lamė constants with $\lambda = \frac{\mu E}{[1+\mu][1-2\mu]}$; u_x, u_y, u_z are the deformations of the mass in the three directions; ρ is the density of the material; and μ is the Poisson's ratio. With suitable manipulation [33], Eq. (3.9) may be expressed in the form which represents the standard form of the wave equation [18].

$$\rho\frac{\partial^2\Delta}{\partial t^2} = (\lambda + 2G)\nabla^2\Delta$$

$$\text{or} \quad \frac{\partial^2\Delta}{\partial t^2} = c_D{}^2\nabla^2\Delta \qquad \text{with} \quad c_D = \frac{\lambda + 2G}{\rho} \tag{3.11}$$

thus Δ is propagated with dilatational velocity c_D.

The basic force equation for the impact is based on Hert's Law of contact between two free bodies,

$$F = n\alpha^{3/2} \tag{3.12}$$

where F is the impact force, n is a function of parameters of the material property and the radius of a spherical impactor. The term α, called the approach, represents the maximum relative compression of the body [18]. Equation (3.12) describes the impact force between a spherical impactor and an isotropic plane target. The impact duration between these two bodies is

$$t=\frac{2\alpha 1}{v}\int_0^x \frac{dx}{(1-x^{5/2})^{1/2}} \tag{3.13}$$

where $x=(\alpha/\alpha_1)$. α_1 is the maximum value of α, and v is the impact speed. With different combinations of impactors and targets, the impact force and impact duration are different. In the intermittent turning process, the impact between the workpiece and the cutting tool is imitated as an impact between a free body and a cantilever beam. In additional, a special model describing the impact force in the intermittent turning process is proposed.

3.2.2 Impact Force

This specific characteristic of the intermittent cutting process is newly introduced in this thesis. The necessity of introducing the impact force comes from a phenomenon that intermittent cutting process is much easier to break cutting tools than any kind of continuous cutting process. The phenomenon implies that the impact force which occurs between the cutting tool and workpiece at every start of cutting period, plays a very important role in tool breakage during the intermittent cutting process. The impact force is associated with the the chip load, the material property of the workpiece and the relative speed between the cutting tool and workpiece at that instant. Although the rotational speed of workpiece is a constant during machining, the relative speed between the cutting tool and workpiece varies with respect to time. It is equal to the sum of two vectors, cutting speed and tool velocity. The relative speed is determined by both the direction and magnitude of the motion of cutting tool at the end of free-vibration period. Therefore, a unique description of the dynamic cutting force produced during intermittent cutting requires a functional relation between the cutting force and the relative speed between the cutting tool and workpiece. A proportionality coefficient, or a gain factor, called k_o

are introduced. In this thesis, the magnitude of the impact force component is assumed to be proportional to the relative speed which is described as

$$F_{impact}=k_o v_z(t)=k_o(v_o - \dot{z}(t)) \tag{3.14}$$

where v_o is the nominal cutting speed and acts on the tangential direction at the cutting point, $\dot{z}(t)$ is the velocity of the cutting tool at the tangential direction, and k_o is defined as impact coefficient.

The reason for such an assumption can be derived from the principle of impact. For a flexible, plate-type target, the surface pressure, area of contact and impact duration will be functions of the parameters of the material property, the velocity of impactor as well as beam bending stiffness and boundary conditions. From a view point of energy balance in the system, it can be written as:

$$\frac{1}{2} m_1 v_{re}^2 = \int_0^{\delta_{Max}} p_p \, d\delta_p + \int_0^{\alpha_1} p_c \, d\alpha \tag{3.15}$$

where α is the deformation of the mass, and d is the displacement of the beam (toolpost); the p_p is the force causing the displacement of the beam; the p_c is the force causing the mass deformation of the cutting tool at the contact area. Here $F=p_p=p_c=F_o \sin\xi t$, which is an identical force causing both the mass deformation and beam displacement. The $F=F_o \sin\xi t$ is based on the impact theory that the impact force behaves like a sine wave pulse in most impact cases [70]. This is shown in Fig. 3.7. Therefore

$$F_o = \frac{\frac{1}{2} m_1 v_{re}^2}{\int_0^{\delta_{Max}} \sin \xi t \, d\delta_p + \int_0^{\alpha_1} \sin \xi t \, d\alpha} = k_o v_{re} \tag{3.16}$$

where the ξ is a constant. It can be observed that the k_o is also a function of the relative velocity. This is because most of the cutting force parameters are the function of cutting speed.

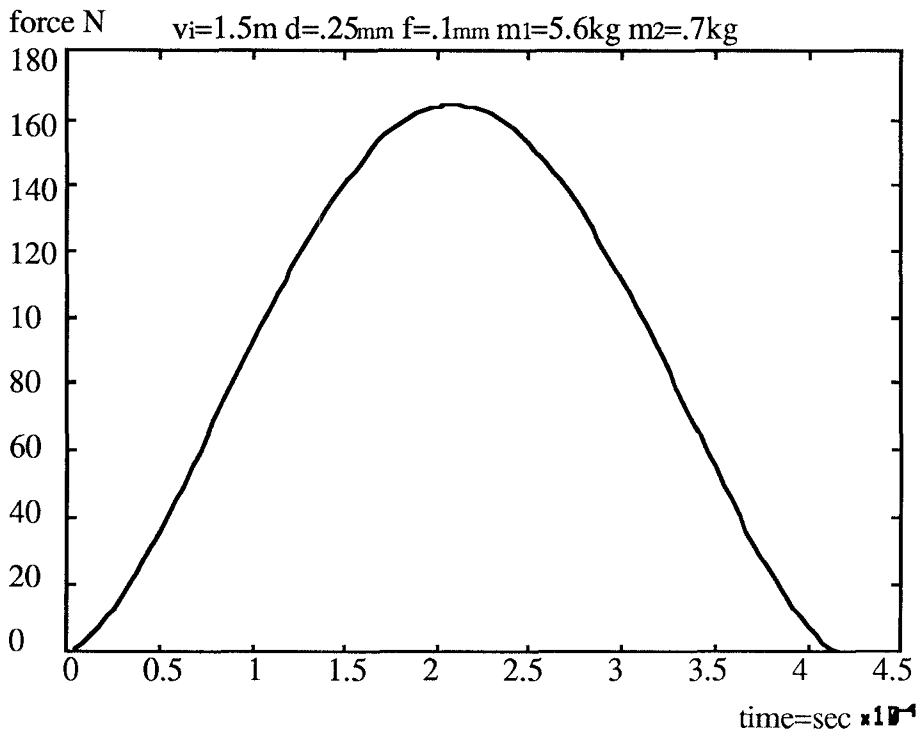

Fig. 3.7 The Impact Force during the Impact Duration

In order to correctly predict the tool vibration instability or tool breakage, the numerical value of k_o should be properly determined. Based on the low velocity impact theory, the relationship between the impact force and velocity in the impact between a free fall and cantilever beam can be derived as follows:

$$F=F_o \sin\xi t \tag{3.17}$$

$$F_o \approx \frac{v_0 m\rho AL\xi(\xi^2 - \omega_1^2)}{(cm + \rho AL)\xi^2 - \rho AL\omega_1^2} = k_o v_o \tag{3.18}$$

and

$$k_o = \frac{m\rho AL\xi(\xi^2 - \omega_1^2)}{(cm + \rho AL)\xi^2 - \rho AL\omega_1^2} \tag{3.19}$$

where m is the mass of the impactor; v_o is the velocity of the impactor; A is the cross section of the cantilever beam,or tool holder; ρ is the dentist of the beam; ω_1 is the first mode of the beam; L is the length of the beam; ξ is a constant, which is function of R, E, and ν. R is the radius of spherical impactor, E is the Young's modulus, and ν is poisson's ratio of the both impactor and target. The ξ is determined by following equation.

$$\xi^5 = \frac{v_0 K_2^2}{A^{-3}\; m^2 (\frac{\rho AL}{c})^2} \left[\frac{(m + \frac{\rho AL}{c})\xi^2 - \frac{\rho AL}{c}\omega_1^2}{\xi^2 - \omega_1^2} \right] \tag{3.20}$$

The detailed derivation of Eqs. (3.17), (3.18) and (3.20) is presented in Appendix A. The v_o is the impact speed which represents the relative velocity, v_{re}, between the workpiece and cutting tool in the intermittent turning process. The problem rises here that in the equation (3.1), the mass of an impactor is a free fall. In the intermittent cutting process, the workpiece is clamped on the lathe. Thus, the equivalent mass should be used to instant m. It is known that the nominal cutting force during a continuous cutting process is a constant. If only the uncut chip load is considered, it is assumed that uncut chip load is equal to the weight of the equivalent mass, i.e

$$W = m'_1 g = k_s A \tag{3.21}$$

where k_s is the unit cutting force in continuous cutting, which can be found in machining hand books. Then the equivalent mass in Eq (3.18) can be written as

$$m'_1 = \frac{k_s A}{g} \tag{3.22}$$

with this equivalency , the proportionality coefficient of the impact force, k_o, is presented as follow:

$$k_o = C\ V^a\ M^b\ K_2^c \tag{3.23}$$

The theoretical formula, Eq. (3.18), is used to calculate the impulsive force by substituting the equivalent mass, the material property and the area of the crosss section of the tool holder. Based on the theoretical calculation, C, a, b, c in Eq. (3.23) are determined by the method of linear regression analysis. The reason for this substitution is that Eq (3.18) is too complicated to be accepted in the practical application. For example, the function to determine ξ is a ninth order polynomial as shown in Eq. (3.20). Table 3.1 lists the calculated values based on a two-level design of experimentation. Figure 3.8 shows the graphical representation of the two-level design of experimentation.

$$k_o = 3.217E\text{-}6\ V^{0.4195}\ M^{0.0228}\ K_2^{0.8069}$$

Vrelative	Meq	K2	ξ	Tsec	ko	Fo=N
1.5m/s	5kg	8.4E8	44883	0.000070	63.3	95.0
3m/s	5kg	8.4E8	46500	0.000066	84.1	254
1.5m/s	9kg	1.0E9	45641	0.000069	73.5	110.3
3m/s	9kg	1.0E9	47500	0.000065	97.9	293.8
1.5m/s	5kg	1.27E9	46859	0.000067	86.6	134.4
3m/s	5kg	1.27E9	49093	0.000063	118.2	354.6
1.5m/s	9kg	1.46E9	47714	0.000066	100.6	151.04
3m/s	9kg	1.46E9	50200	0.000062	131.9	395.92

Table 3.1 The Relation between the Impact Coefficient and Cutting Conditions

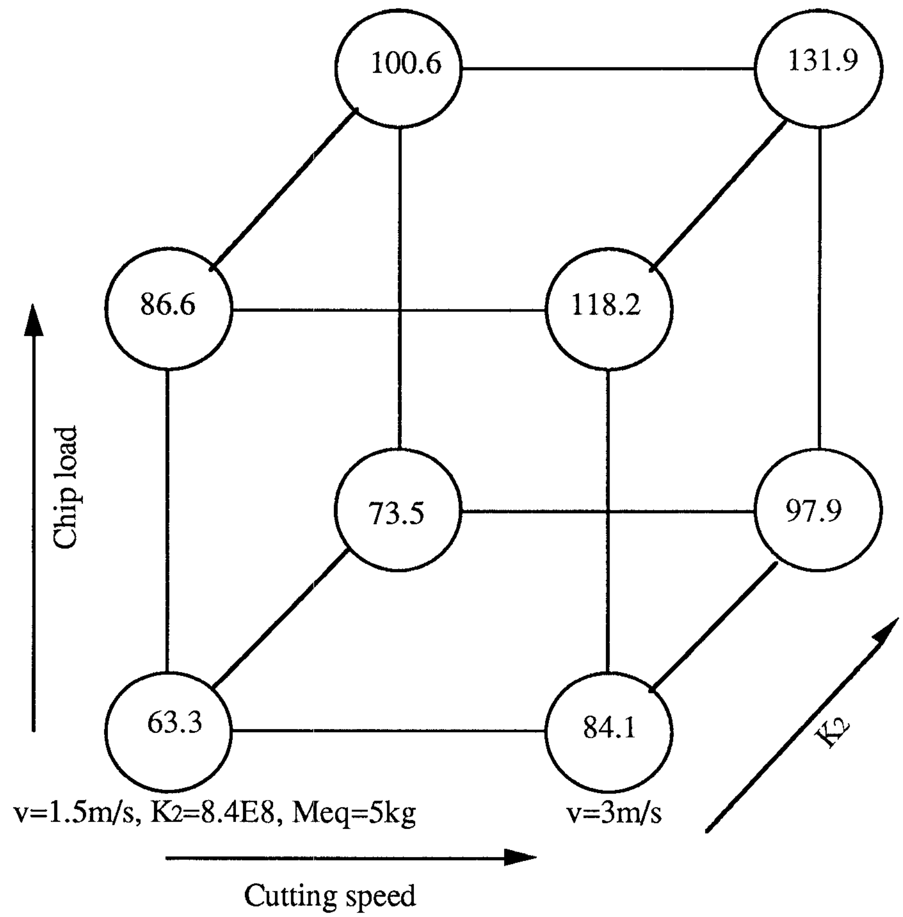

Fig. 3.8 Two - Level Design of Experimentation

The impact is a very complicated problem, the surface being machined undergoes from an elasticity compliance to a plasticity deformation during the impact period. The impact force and the strain and stress distribution in the cutting tool vary dramatically in a very short time period. Therefore, it is difficult to describe and calculate these variations theoretically. The above equation only represents the maximum value of the impact force occurring on the contact point. For an entire stress and strain distribution history in the cutting tool during the impact period, finite element method can be used for this complicated calculation.

3.2.3 Impact Duration

Since the impact process is treated as a separate process in this thesis, it is necessary to estimate the impact duration. In fact, Eq. (3.17) has already formed a basis for estimating the impact time duration. The period of a sine wave is $t=\frac{\pi}{\xi}$.

In the impact process, the maximum impact force occurs at the middle of the impact duration. During the intermittent turning process, when the impact force gets its maximum value, the process is considered to enter the cutting period. The reason for this consideration is based on the finite element calculation (presented in Chapter 5), in which the meshes of the workpiece at the contact area show severe distortion when the maximum stress reaches. Therefore, the impact duration for the intermittent cutting process is half of that in the free body impact process. The time duration of the impact for intermittent turning process can be described as

$$t_o = \frac{\pi}{2\xi} \tag{3.24}$$

where ξ is a constant as expressed in Eq. (3.20). The key element in the determination of the impact duration is the material property K_2, equivalent mass and the impact speed. The effect of these parameters has been shown in Table 3.1.

CHAPTER 4

SYSTEM STABILITY ANALYSIS

In this chapter, the system dynamics during the impact period is analyzed based on the mathematical model developed in Chapter 3. In this chapter, a detailed impact process is described, and the effect of the impact process on the performance of intermittent turning process is studied. This study forms a basis for the establishment of criterion to determine the occurrence of tool breakage during machining. The state space approach is applied to define the boundary condition for the finite element analysis. By correlating the distortion energy during the impact process to the cutting speed and cutting area, a criterion to determine the stability boundary condition is found. A map is constructed to direct the selection of cutting speed for avoiding tool breakage under given cutting conditions.

4.1 System Response Analysis

The impact force dominates the characteristics of the transition from the impact period to the cutting period. It is known that the instability of the intermittent turning process is related to the impact force. Basically, there are two types of instability phenomenon, which are tool breakage and chatter. While some attention is paid to the chatter occurrence, more attention should be paid to the tool breakage. This is because the occurrence of tool breakage seems more appearing during the impact process. The occurrence of tool breakage is related to the cutting speed, chip load and the maximum stress in the cutting tool. The relationship between the tool breakage and the cutting parameters has to be studied. In addition, the system stability during the cutting period and noncutting period is studied within the stable region of the impact period.

4.1.1 Transient Process Analysis

The calculation of the stress and strain in the cutting tool is complicated. The calculation can be simplified if only the maximum stresses need to be calculated. This is because the maximum stresses occur along the z direction and depend on the impact force according to the impact theory [70]. It can be assumed that the cutting speed and cutting load are in the stable region for the impact period if the maximum deformation in the contact area of the cutting tool is within the elastic range. In other words, the maximum stress in the cutting tool can be assumed to be less than the maximum allowed stress. Under this assumption, the relationships between the maximum stresses and cutting parameters are derived.

During the impact process, the total applied force, F, must equal the total resisting force supplied by the vertical component of the pressure within the contact area, i.e.,

$$F = \int\int q\,dxdy. \tag{4.1}$$

where q is the pressure in the z direction. if the contact area is (f • d), the impact force F is equal to q•(f •d), and maximum force F_0 is equal to q_o•(f •d). The q_o is the maximum pressure. The principal stress values can be expressed in terms of q_o [44].

$$\sigma_x = \sigma_y = \{(1+\nu)[\frac{z}{a}\cot^{-1}(\frac{1}{z/a}) - 1] + \frac{1}{2(1+\frac{z^2}{a^2})}\}q_o(t) \tag{4.2}$$

$$\sigma_z = \frac{1}{(1+\frac{z^2}{a^2})}q_o(t) \tag{4.3}$$

where

$$q_o = \frac{F_o}{f\,d}$$

The equations for the stress and strain state become more complicated when stress states off the z axis are to be determined, because in this case, the x and y coordinates must also be included. For the failure criteria, only the maximum stresses on the z direction are needed. The location of the maximum tensile, compressive and shear stresses in the target or in the cutting tool during the impact period is shown in Fig. 4.1 where a is radius of the circular area during the contact.

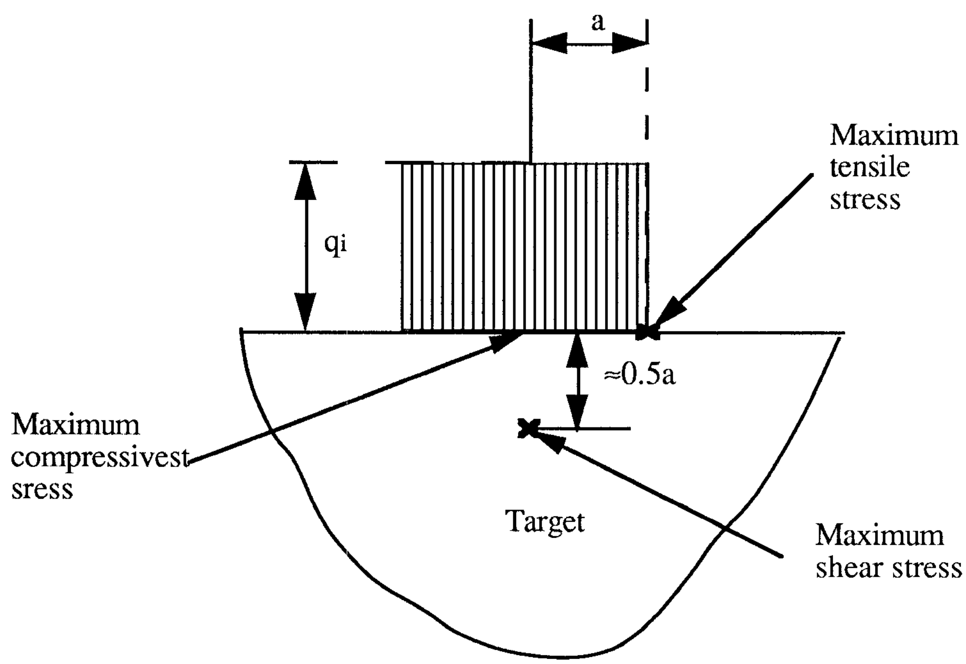

Fig. 4.1 Locations of Maximum Tensile, Compressive, and Shear Stresses in an Elasticity Space under Surface Loading

In the wave propagation theory, the failure of the tool material is based on the distortion energy theory. The conditions for failure is that $\sigma_e \geq 1$ [70]

$$\sigma_e = \frac{\sigma_{11}^2}{S_{11}^2} + \frac{\sigma_{22}^2}{S_{22}^2} + \frac{\sigma_{33}^2}{S_{33}^2} + \frac{\sigma_{12}^2}{S_{12}^2} + \frac{\sigma_{13}^2}{S_{13}^2} + \frac{\sigma_{23}^2}{S_{23}^2}$$
$$- (\frac{\sigma_{11}^2}{S_{11}^2})(\frac{\sigma_{22}^2}{S_{22}^2})\left[\frac{(1+2\nu_{21}-\nu_{23})E_1 + (1+2\nu_{12}-\nu_{13})E_2}{\{(2+\nu_{12}+\nu_{13})(2+\nu_{21}+\nu_{23})E_1E_2\}^{\frac{1}{2}}}\right]$$
$$- (\frac{\sigma_{11}^2}{S_{11}^2})(\frac{\sigma_{33}^2}{S_{33}^2})\left[\frac{(1+2\nu_{31}-\nu_{32})E_1 + (1+2\nu_{13}-\nu_{12})E_3}{\{(2+\nu_{12}+\nu_{13})(2+\nu_{31}+\nu_{23}32)E_1E_2\}^{\frac{1}{2}}}\right]$$
$$- (\frac{\sigma_{22}^2}{S_{22}^2})(\frac{\sigma_{33}^2}{S_{33}^2})\left[\frac{(1+2\nu_{23}-\nu_{21})E_3 + (1+2\nu_{32}-\nu_{31})E_2}{\{(2+\nu_{21}+\nu_{22})(2+\nu_{31}+\nu_{32})E_1 2E_3\}^{\frac{1}{2}}}\right] \quad (4.4)$$

where σ_e is an equivalent stress as defined above, σ_{ii} are principal stress in the impact-induced direction and σ_{ij} are shear stresses, S's are the allowable stresses associated with the three orthogonal directions, E's is the Young's moduli, and ν's is Poisson's ratios associated with directions 1, 2, and 3. In the present study, the maximum value is only considered since the occurrence of tool breakage is concerned.

In general, cutting tool materials are considered to be homogeneous. Therefore, Young's modulus E's and Poisson's ratio ν's are same in the cutting tool, S_x, S_y and S_z are equal to each other, and $\sigma_{ij} = \frac{\sigma_{ii}-\sigma_{jj}}{2}$. At the contact area of the tool surface as shown in Fig. 4.1, $\sigma_x = \sigma_{11}$, $\sigma_y = \sigma_{22}$, and $\sigma_z = \sigma_{33}$. Substituting Eqs. (4.2) and (4.3) into Eq. (4.4). the condition for failure, Eq. (4.4), can be rewritten as follow:

$$\sigma_e = 2\frac{\sigma_x^2}{S_x^2} + \frac{\sigma_z^2}{S_z^2} + \frac{(\sigma_x - \sigma_z)^2}{2S_{xz}^2} - (\frac{\sigma_x^2}{S_x^2})\left[(\frac{\sigma_y^2}{S_y^2}) - 2(\frac{\sigma_z^2}{S_z^2})\right]\left[\frac{(1+2\nu)}{(1+\nu)}\right] \quad (4.5)$$

Let $\sigma_x = \sigma_y = aF_o$, and $\sigma_z = bF_o$, and substitute Eqs. (4.1-4.3) into Eq. (4.5), the following equation can be obtained:

$$\sigma_e = (2a^2 + b^2)\frac{F_o^2}{S_x^2} + \frac{(a+b)^2}{2}\frac{F_o^2}{S_{xy}^2} - [a^2 - 2b^2]\frac{a^2}{S_x^4}F_o^4 \quad (4.6)$$

It can be seen from Eq. (4.6) that the equivalent stress σ_e is the function of the impact force. The cutting tool breaks from contact area where z equals to zero, at z=0, $a=\frac{(\upsilon-1/2)}{f\ d}$ and $b=\frac{1}{f\ d}$. It is noted that the impact force, F_o, is function of the cutting speed and chip load. With the requirement of $\sigma_e<1$, the Eq. (4.6) represents the relationship between the failure condition and cutting parameters. In Fig. 4.2, the impact force is plotted versus cutting speed under certain chip loads, and the stable boundary line is determined by the Eq. (4.6). In this figure, f=.0001 represents that both feed and cutting depth are equal to .0001m. For this map, k_c =900,000 * d is assumed and the material of cutting tool is assumed to be tool steel.

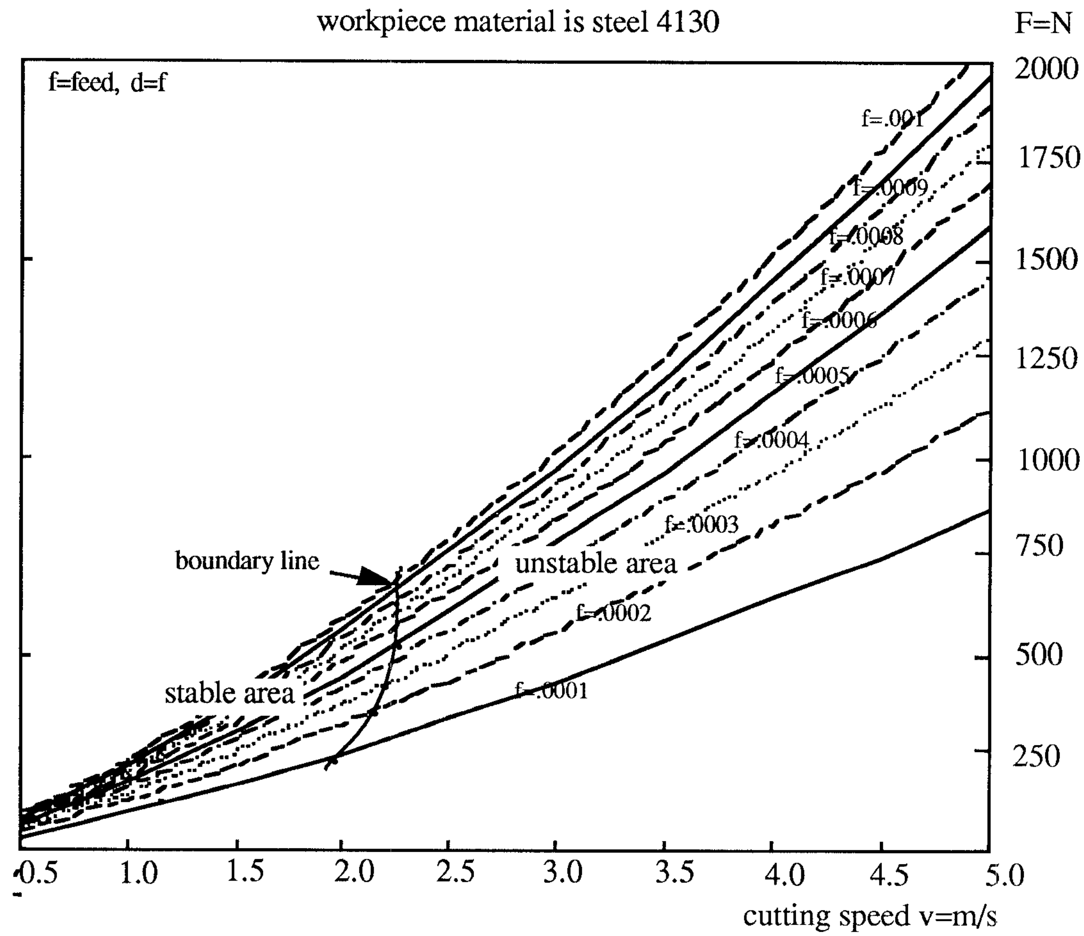

Fig. 4.2 Impact Force under Different Cutting Speeds and Chip Loads

4.1.2 Cutting Period Analysis

Since the time-varying parameter method is applied in the system analysis, the system can be considered as a continuous cutting process during the cutting period. Therefore, it is possible to apply the methods used in the continuous turning process to the cutting period of the intermitting turning process for stability analysis. In the cutting period, there are two kinds of instability form, system instability and regenerative instability. The system instability with out overlap cutting is caused by the variation of the system parameter, and the regenerative instability is caused by the regenerative mechanism as presented in Chapter 3.

Under non-overlapping cutting conditions, the input to the system model of the cutting period is the normal chip thickness. The system response in an analytical form can be obtained by a linear transformation $\underline{x}(t)=[p]Q(t)$ [63]. As a result, the system dynamic equations Eq. 3.8, can be decoupled in its eigenvector space.

$$\dot{\underline{Q}}(t) = [p]^{-1}[A][p]\underline{Q}(t) + [p]^{-1}[B][u] = [M]\underline{Q}(t) + [B'][u] \tag{4.7}$$

where

$$[M] = \begin{bmatrix} -\sigma_1 & \omega_{n1} & 0 & 0 \\ -\omega_{n1} & -\sigma_1 & 0 & 0 \\ 0 & 0 & -\sigma_2 & \omega_{n2} \\ 0 & 0 & -\omega_{n2} & -\sigma_2 \end{bmatrix} \tag{4.8}$$

Note that ($-\sigma_1$ and ω_1) and ($-\sigma_2$ and ω_2) are the real and imaginary parts of the eigenvalues of the system matrix [A] and the associated eigenvectors form the transformation matrix [p]. For the system stability boundary conditions, the Routh - Hurwitz criteria should be met, that the real parts of the eigenvalues of the system matrix should be negative. It is known that the elements contained in the matrix [M] are functions of the cutting force parameters, k_c, k_p, and k_v as discussed in Chapter 3. The relationships between the cutting force parameters are expressed as follows:

$$k_p = \frac{0.117 \times k_c}{N} \tag{4.9}$$

$$k_v = \begin{cases} 120 & N \le 500\,\text{rpm} \\ 60 & 500\,\text{rpm} < N \le 1000\,\text{rpm} \\ 0 & 1000\,\text{rpm} < N \end{cases}$$

where k_c and N are selected cutting parameters. When k_c and N get the critical value, the system will become instable. Therefore, the stability boundary for the cutting period without overlapping can be obtained.

When the overlap factor $0 < \mu < 1$, the system stability analysis has to include the effect of the regenerative mechanism. The regenerative input y_{rest} is caused by the previous revaluation, and is presented in Eq. (3.4). As a linear system, the superposition principle can be applied, and the relationship between this second input and the system output in the frequency domain is $y(j\omega) = \mu y_{rest}(j\omega)M\,(j\omega)$, where M $(j\omega)$ is the complex form of the system transfer function M (s). It can be seen that the system will be instable if the second input spectrum falls in the region $|\mu M\,(j\omega)| >1$. As shown in Eq. 3.4, the second input spectrum is a discrete power spectrum, and the frequency increment is determined by $\Delta\omega = 2\pi/T = 2\pi N/60$. It is the function of N. With known bandwidth of $|\mu M\,(j\omega)| >1$, a set of critical spindle speed, N_{cri}, can be determined to avoid the second input spectrum falling in the critical frequency bandwidth [63].

A stable boundary includes the both system instability and regenerative instability for the cutting period (or for the continuous turning process) is shown in Fig. 4.3. However, it is natural to think that the stability analysis for the intermittent turning process should be carried out within the stable region of the impact period. Therefor, these cutting force parameters have to be confined within the stable boundary determined in the impact period, as shown in Fig. 4.2. This stable boundary of cutting force parameters for the impact period reflected in the cutting period stable boundary is shown in Fig. 4.3 as a dark shadow area. It needs to be point out that there is a significant difference in the stable region between the impact period and cutting period as shown in Fig. 4.3. This means that the cutting period in the intermittent turning process is always stable because these cutting parameters have to selected according to the impact period.

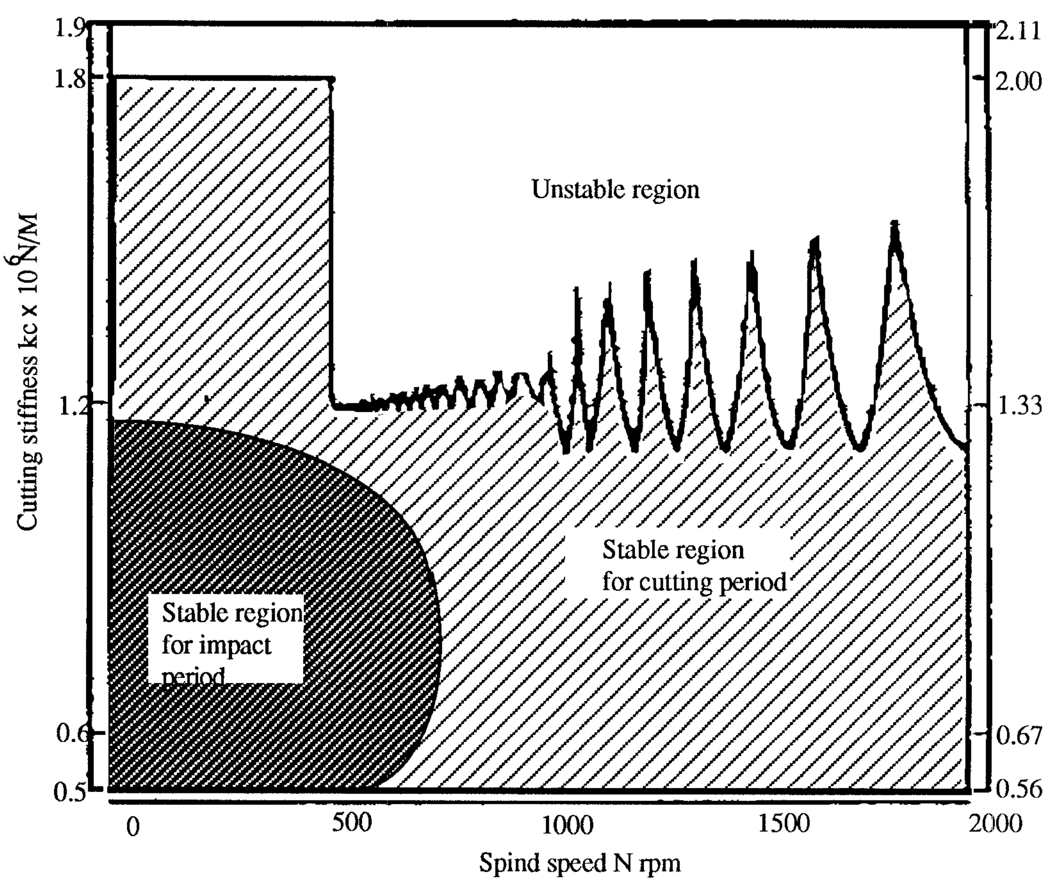

Fig 4.3 System Stable Border Curve for Impact Period and Cutting Period in (N, kc) Plane (kc =900,000 * d Assumed)

4.1.3 Noncutting Period Analysis

In the non-cutting period, the force function is equal to zero, and the two-degree-of-freedom system is two uncoupled second order difference equations, as presented by Eq. (3.1). The noncutting period is a free vibration problem with the end conditions of the cutting period serving as the initial conditions of the noncutting period. The system stability is determined by the system parameters which are material properties of the toolpost. For a system to be stable, it requires that $k_1*k_2>0$. The k_1 and k_2 are the stiffness of the cutting tool material, and are always positive. Therefor, the stable requirement for the noncutting period is always met. The system for the noncutting period always stays in a stable state.

4.2 Summary

Using a time -varying parameter model, the boundary of the system stability for the intermittent cutting process have been developed for the three individual periods. In the impact period, the equivalent stress should be less than 1. In the cutting period, both the system parameters and cutting parameters should be in the allowed area which is obtained in the above sections. In the non-cutting period, the system parameters determine the system stability. Since the system stable boundary for the impact period is much conservative as discussed in this chapter, the first requirement for the system stability is that the selection of the cutting force parameters should based on the stable boundary of the impact period. In other words, if the cutting parameters selected according to the impact stable boundary, the system instability will not occur in the cutting period and noncutting period during the intermittent turning process. Otherwise, if the cutting parameters selected out of the impact stable boundary but within the stable boundary of the cutting period, the cutting tool will break at the beginning of the cutting, and no machining process can be carried out further. This is much closer to the phenomenon observed in the actual machining. Since the impact force is the dominate factor for the system stability during the intermittent turning process, Fig. 4.2 provides a preliminary reference for the selection of the cutting parameters in the intermittent turning process.

CHAPTER 5

SIMULATION AND EXPERIMENT

This chapter consists of three parts. The first part discusses numerical simulation of the intermittent turning process. The developed system model is implemented on computer through programming. Characteristics of the cutting dynamics during the intermittent turning process are studied through computer simulation. The second part discusses the results obtained from the conducted experiments. A comparison is made between the simulation and experimental results. Good agreements, which confirm the validity of the analytical approach proposed in this thesis work, have been observed. In the third part, computer simulation using finite element method to study the impact process is presented. The simulation results offer a vivid picture of the tool deformation process during the impact, providing a strong evidence to support the occurrence of tool breakage.

5.1 Numerical Simulation

In this section, the main focus is to implement the developed system model on a computer system. A computer program written in FORTRAN is used to simulate the tool vibratory motion. Combining the tool vibratory motion with the tool geometric motion and tool geometry, topography of the machined surface generated during the intermittent turning process is constructed. This information will be useful for quality control of machined surfaces.

A unique feature has been built in developing the simulation program. During the cutting period, the damping effect on the system dynamics has been distinguished between the tool motion toward the workpiece and the tool motion away from the workpiece. It is evident that the resistance due to the workpiece presence when the tool moves toward it consumes more system energy than the energy loss when the tool moves away from the workpiece. In order to model this phenomenon, the system damping coefficient has been implemented as a time-varying parameter for the evaluation of the tool motion during the cutting period.

5.1.1 Simulation Model

The mathematical formulation of the system model has been discussed in Chapter 3. In general, the two coupled differential equations, Eq. (3.1) are used for the purpose of evaluating the tool vibratory motion. To implement this system model through programming, the following two assumptions have been used for the evaluation of the tool motion during the cutting period.

1. Two cutting force components are considered. These two components are contributed by the chip load and the random excitation due to the nonhomogeneous hardness distribution in the workpiece. Specifically, the cutting force is evaluated by the following two formulas:

Cutting force component related to the chip load = kc w [a - y(t)], and

Cutting force component related to the random excitation = $kc\ w\ a\ \{[\frac{\mu_s(t)}{\mu a}]^m - 1\}$

A sum of these two components is given by

$$F = k_c \cdot w \cdot \cos\theta \cdot \{a \cdot ([\frac{\mu_s(t)}{\mu}]^m - y\} \qquad (5.1)$$

2. Values of the stiffness and damping in the two principal directions are equal, i.e., $k_1=k_2=k$ and $c_1=c_2=c$. Making this assumption will certainly narrow the coverage of the system model. However, this assumption allows the derivation of an analytical solution, which can be used as the reference for checking the results from computer simulation.

Based on these two assumptions, Eq. (3.1) can be written as follows:

$$m_1\ddot{q}_1(t) + c\dot{q}_1(t) + kq_1(t) = F\bar{\alpha}_1 \tag{5.2}$$

$$m_2\ddot{q}_2(t) + c\dot{q}_2(t) + kq_2(t) = F\bar{\alpha}_2 \tag{5.3}$$

where

$$\bar{\alpha}_1 = \cos(\alpha_1 + \theta_c)$$
$$\bar{\alpha}_2 = \sin(\alpha_1 + \theta_c)$$

Recalling the study of the impact process in Chapters 3 and 4, the initial conditions of the tool motion during the cutting period is determined by the end conditions of the tool motion during the impact period. In this thesis, the assumption was been made that when the tool motion reaches the maximum tool displacement, this time instant represents the very beginning of the cutting period. Therefore, the initial displacement of the tool motion for the cutting period is given by $z_o=(F_o l^3)/(3EI)$, and the initial velocity is equal to zero.

Equations (5.2) and (5.3) should be decoupled in order to obtain an analytical solution. By substituting Eq. (5.1) into Eqs. (5.2) and (5.3), the following equation is obtained:

$$m(\ddot{q}_1\mathrm{con}\alpha_1 + \ddot{q}_2\sin\alpha_1) + c(\dot{q}_1\mathrm{con}\alpha_1 + \dot{q}_2\sin\alpha_1) + k(q_1\mathrm{con}\alpha_1 + q_2\sin\alpha_1)$$
$$= \{k_c \cdot w \cdot \cos\theta \cdot (a \cdot [\frac{\mu_s(t)}{\mu_a}]^m - y)\} \cdot (\bar{\alpha}_1 \cdot \cos\alpha_1 + \bar{\alpha}_2 \cdot \sin\alpha_1) \tag{5.4}$$

It is worth noting that in Eq. (5.4)

$$q_1 \cos\alpha_1 + q_1 \sin\alpha_1 = y$$
$$\dot{q}_1 \cos\alpha_1 + \dot{q}_2 \sin\alpha_1 = \dot{y}$$
$$\ddot{q}_1 \cos\alpha_1 + \ddot{q}_2 \sin\alpha_1 = \ddot{y}$$

By substituting these relations into Eq. (5.4), we have

$$m\ddot{y} + c\dot{y} + y[k + k_c \cdot w \cdot \cos\theta \cdot (\bar{\alpha}_1 \cdot \cos\alpha_1 + \bar{\alpha}_2 \cdot \sin\alpha_1)]$$
$$= \{k_c \cdot w \cdot \cos\theta \cdot a \cdot [\frac{\mu_s(t)}{\mu_a}]^m\} \cdot (\bar{\alpha}_1 \cdot \cos\alpha_1 + \bar{\alpha}_2 \cdot \sin\alpha_1) \tag{5.5}$$

Equation (5.5) is the governing equation in the y direction. Similarly, the governing equation in the z direction can be written as:

$$m(\ddot{q}_2 \cos\alpha_1 - \ddot{q}_1 \sin\alpha_1) + c(\dot{q}_2 \cos\alpha_1 - \dot{q}_1 \sin\alpha_1) + k(q_2 \cos\alpha_1 - q_1 \sin\alpha_1)$$
$$= \{k_c \cdot w \cdot \cos\theta \cdot a \cdot ([\frac{\mu_s(t)}{\mu_a}]^m - y)\} \cdot (\bar{\alpha}_2 \cos\alpha_1 - \bar{\alpha}_1 \sin\alpha_1) \tag{5.6}$$

In a similar manner, we first identify the following relations:

$$q_2 \cos\alpha_1 - q_1 \sin\alpha_1 = z$$
$$\dot{q}_2 \cos\alpha_1 - \dot{q}_1 \sin\alpha_1 = \dot{z}$$
$$\ddot{q}_2 \cos\alpha_1 - \ddot{q}_1 \sin\alpha_1 = \ddot{z}$$

By substituting these relations into Eq. (5.6), we have

$$m\ddot{z} + c\dot{z} + kz$$
$$= \{k_a \cdot w \cdot \cos\theta \cdot (a \cdot [\frac{\mu_s(t)}{\mu_a}]^m - y\} \cdot (\bar{\alpha}_2 \cdot \cos\alpha_1 - \bar{\alpha}_1 \cdot \sin\alpha_1) \tag{5.7}$$

From Eqs. (5.5) and (5.7), it can be observed that Eqs. (5.2) and (5.3) have been decoupled. The two uncoupled, principal modes are along the y and the z directions, respectively. The natural frequency in the y direction is given by

$$\omega_{n1} = \sqrt{\frac{k'}{m}} \tag{5.8}$$

where

$$k' = k + k_c \cdot w \cdot \cos(\bar{\alpha}_1 \cos\alpha_1 + \bar{\alpha}_2 \sin\alpha_1)$$

and its associated damping ratio is given by

$$\xi_1 = \frac{c(t)}{2\sqrt{k'm}} \tag{5.9}$$

where c(t) is the system damping coefficient, and a function of time. Usually, in the simulation studies of the cutting process, the damping coefficient of the tool was considered as the total damping coefficient of the system, and therefore the damping coefficient of the system was treated as a constant. In fact, in the cutting process, both the tool damping coefficient and the material damping coefficient of the workpiece will affect the tool motion. Therefore, the system damping coefficient, c(t), should be a function of time. In this thesis, both of these damping coefficients have been included. However, it is considered that these two damping coefficients can play an important role only when the cutting tool is moving toward the workpiece. In other words, only the tool damping coefficient needs to be taken into account when the cutting tool is moving away from the workpiece. The system damping ratio thus varies with the moving direction of the cutting tool during the cutting period.

By introducing

$$\frac{k_c \cdot w \cdot a \cdot \cos\theta \cdot [\frac{\mu_s(t)}{\mu_a}]^m}{m}$$
$$= \frac{\omega_{n1}^2 \cdot k_c \cdot w \cdot a \cdot \cos\theta \cdot (\bar{\alpha}_1 \cos\alpha_1 + \bar{\alpha}_2 \sin\alpha_1)}{k + k_c \cdot w \cdot \cos(\bar{\alpha}_1 \cos\alpha_1 + \bar{\alpha}_2 \sin\alpha_1)} \cdot [\frac{\mu_s(t)}{\mu_a}]^m$$
$$= \omega_{n1}^2 \cdot k_{m1} \cdot [\frac{\mu_s(t)}{\mu_a}]^m \tag{5.10}$$

where

$$k_{m1} = \frac{k_c \cdot w \cdot a \cdot \cos\theta \cdot (\bar{\alpha}_1 \cos\alpha_1 + \bar{\alpha}_2 \sin\alpha_1)}{k + k_c \cdot w \cdot \cos(\bar{\alpha}_1 \cos\alpha_1 + \bar{\alpha}_2 \sin\alpha_1)} \tag{5.11}$$

the solution of Eq. (5.5) can be written as

$$y(t) = k_{m1}\{1 + \frac{1}{\sqrt{1-\xi^2}} e^{-\xi_1 \omega_{n1} t} \sin(\omega_{n1}\sqrt{1-\xi^2} - \arctan\frac{\sqrt{1-\xi^2}}{-\xi_2})\}$$
$$+ \frac{[2\xi_2 \omega_n y(0) + \dot{y}(0)}{\omega_n \sqrt{1-\xi^2}} e^{-\xi_1 \omega_{n1} t} \sin(\omega_{n1}\sqrt{1-\xi^2})$$
$$+ \{\frac{y(0)}{\sqrt{1-\xi^2}} e^{-\xi_1 \omega_{n1} t} \sin(\omega_{n1}\sqrt{1-\xi^2} \cdot t + \arctan\frac{\sqrt{1-\xi^2}}{-\xi_2}\} \tag{5.12}$$

where

$$\omega_{n2} = \sqrt{\frac{k}{m}} \tag{5.13}$$

$$\xi_2 = \frac{c(t)}{2\sqrt{k M}} \tag{5.14}$$

Similarly, by letting

$$\frac{k_c \cdot w \cdot \cos\theta \cdot a \cdot (\bar{\alpha}_2 \cos\alpha_1 - \bar{\alpha}_1 \sin\alpha_1) \cdot}{m} \cdot \left(\left[\frac{\mu_s(t)}{\mu_a}\right]^m - y \right) \cdot$$

$$= \omega_{n2}^2 \cdot \frac{k_c \cdot w \cdot \cos\theta \cdot a \cdot (\bar{\alpha}_2 \cos\alpha_1 - \bar{\alpha}_1 \sin\alpha_1) \cdot}{k} \cdot \left(\left[\frac{\mu_s(t)}{\mu_a}\right]^m - y \right)$$

$$= \omega_{n2}^2 \cdot k_{m2} \cdot \left(\left[\frac{\mu_s(t)}{\mu_a}\right]^m - y \right) \tag{5.15}$$

where

$$k_{m2} = \frac{k_c \cdot w \cdot \cos\theta \cdot a \cdot (\bar{\alpha}_2 \cos\alpha_1 - \bar{\alpha}_1 \sin\alpha_1) \cdot}{k} \tag{5.16}$$

the solution of Eq. (5.7) can be expressed as

$$z(t) = k_m \{1 + \frac{1}{\sqrt{1-\xi^2}} e^{-\xi_1 \omega_n t} \sin\left(\omega_n \sqrt{1-\xi^2} \cdot t + \arctan\frac{\sqrt{1-\xi^2}}{-\xi_1}\right)\}$$
$$+ \frac{[2\xi_1 \omega_n z(0) + \dot{z}(0)]}{\omega_n \sqrt{1-\xi^2}} e^{-\xi_1 \omega_n t} \sin\left(\omega_n \sqrt{1-\xi^2}\right)$$
$$+ \{\frac{z(0)}{\sqrt{1-\xi^2}} e^{-\xi_1 \omega_n t} \sin\left(\omega_n \sqrt{1-\xi^2} \cdot t + \arctan\frac{\sqrt{1-\xi^2}}{-\xi_1}\right)\} \tag{5.17}$$

Equations (5.13) and (5.17) are the analytical solutions of the two governing equations for the evaluation of the tool motion during the cutting period. These solutions can be used to study the cutting dynamics during the cutting period.

For the noncutting period, Eqs.(5.4) and (5.6) can be used by setting the right sides of these two equations equal to zero, indicating that the tool motion during the noncutting period is in the free-vibration mode. Therefore, during the noncutting period, the two governing equations are given by

$$M\ddot{y} + c\dot{y} + ky = 0$$
$$M\ddot{z} + c\dot{z} + kz = 0 \tag{5.18}$$

The initial conditions of the noncutting process are given by the end conditions of the tool motion during the cutting period. Therefore, the natural frequency of the system is

$$\omega_{n1} = \omega_{n2} = \sqrt{\frac{k}{m}} \tag{5.19}$$

and the damping ratio of the system is

$$\xi_1 = \xi_2 = \frac{c}{2\sqrt{kM}} \tag{5.20}$$

The solution of Eq. (5.18) can be written as

$$y(t) = \frac{[2\xi_2\omega_n y(0) + \dot{y}(0)}{\omega_n\sqrt{1-\xi^2}} e^{-\xi_2\omega_n t} \sin(\omega_n\sqrt{1-\xi^2})$$
$$+ \{\frac{y(0)}{\sqrt{1-\xi^2}} e^{-\xi_2\omega_n t} \sin(\omega_n\sqrt{1-\xi^2} \cdot t + \arctan\frac{\sqrt{1-\xi^2}}{-\xi_2}\} \tag{5.21}$$

and

$$z(t) = \frac{[2\xi_2\omega_n z(0) + \dot{z}(0)}{\omega_n\sqrt{1-\xi^2}} e^{-\xi_2\omega_n t} \sin(\omega_n\sqrt{1-\xi^2})$$
$$+ \{\frac{z(0)}{\sqrt{1-\xi^2}} e^{-\xi_2\omega_n t} \sin(\omega_n\sqrt{1-\xi^2} \cdot t + \arctan\frac{\sqrt{1-\xi^2}}{-\xi_2}\} \tag{5.22}$$

5.1.2 Simulation Results

The above derived governing equations for the intermittent process have been programmed in FORTRAN. During the cutting period, the z(t) and y(t) are positive always, but special attention is given to the setting of the system damping coefficient. It is set to $c=c_{tool}$ when $\dot{z}(t)$ and $\dot{y}(t)$ are positive, and it is set to $c=c_{tool}+c_{workpiece}$ when the $\dot{z}(t)$ and $\dot{y}(t)$ are negative. During the noncutting period, the system damping coefficient is set to $c = c_{tool}$. Figures. 5.1, 5.2, 5.3, and 5.4 show the typical results with and without the consideration of the damping effect of the workpiece material. It can be seen from Figs. 5.1, 5.2 5.3 and 5.4 that the system response decays faster with the effects of the material damping coefficient than that without the effects of the material damping coefficient. This indicates that with and without the consideration of the damping ratio of the workpiece, the prediction of the surface finish will be different. The simulation results of surface finish with and without the effects of the material damping coefficient are shown in Figs 5.5 and 5.6. The surface roughness is the average value of the heights of the surface profile about its mean line. Although the mean value has no evident difference in Figs 5.5 and 5.6, which are 10.06μm and 10.02μm respectively, the mean line of the profile at first five peck shift in different ratio, which are listed below:

mean line	$First_{peak}$	$Second_{peak}$	$Third_{peak}$	$Fourth_{peak}$	$Fifth_{peak}$
y_{wo}	132μm	127μm	123μm	118μm	114μm
y_w	137μm	129μm	123μm	117μm	112μm

It is seen that the consideration of the effects of the material damping coefficient on the tool motion is more meaningful for the surface quality prediction during the intermittent turning process.

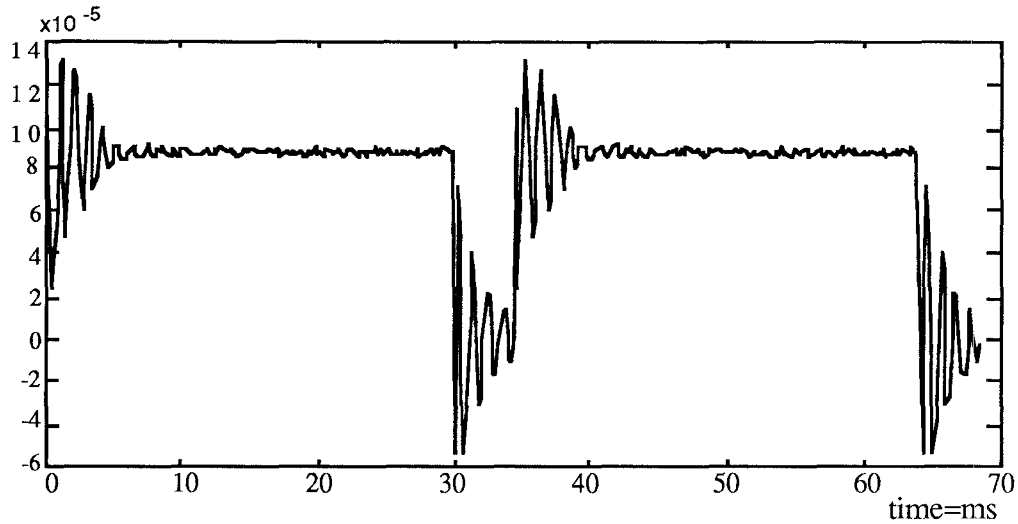

Fig. 5.1 Tool Vibration in Z Direction without Effect of Material Damping

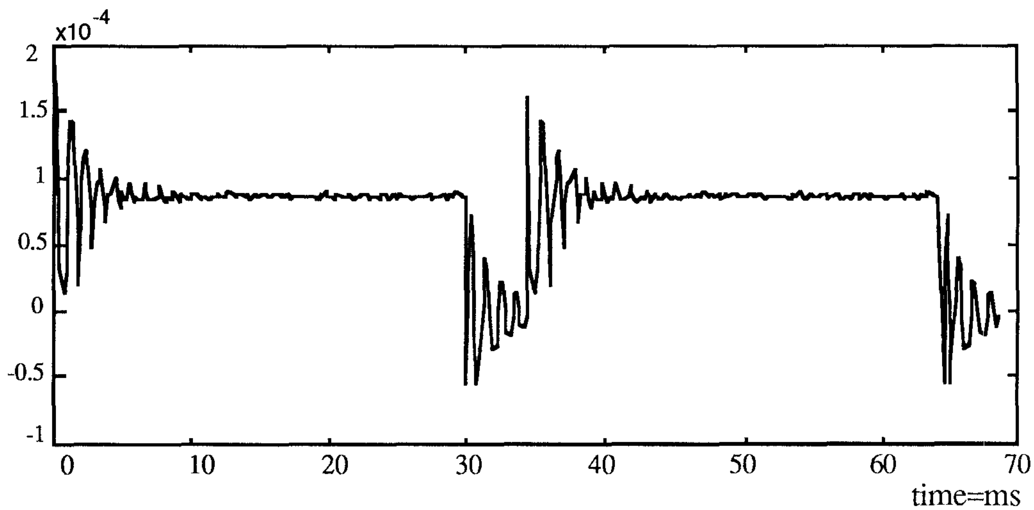

Fig. 5.2 Tool Vibration in Z Direction with Effect of Material Damping

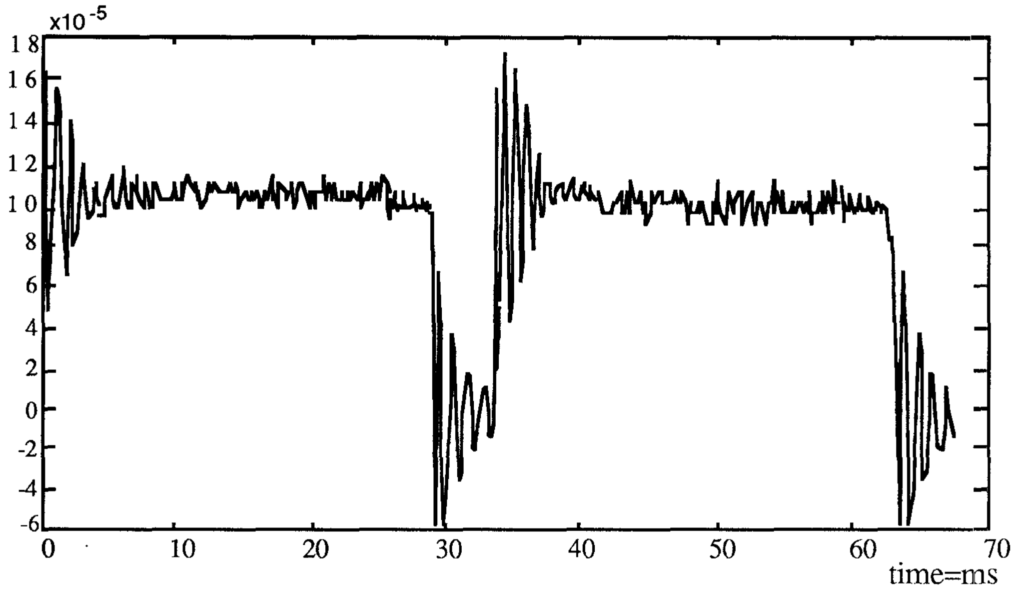

Fig. 5.3 Tool Vibration in Y Direction without Effect of Material Damping

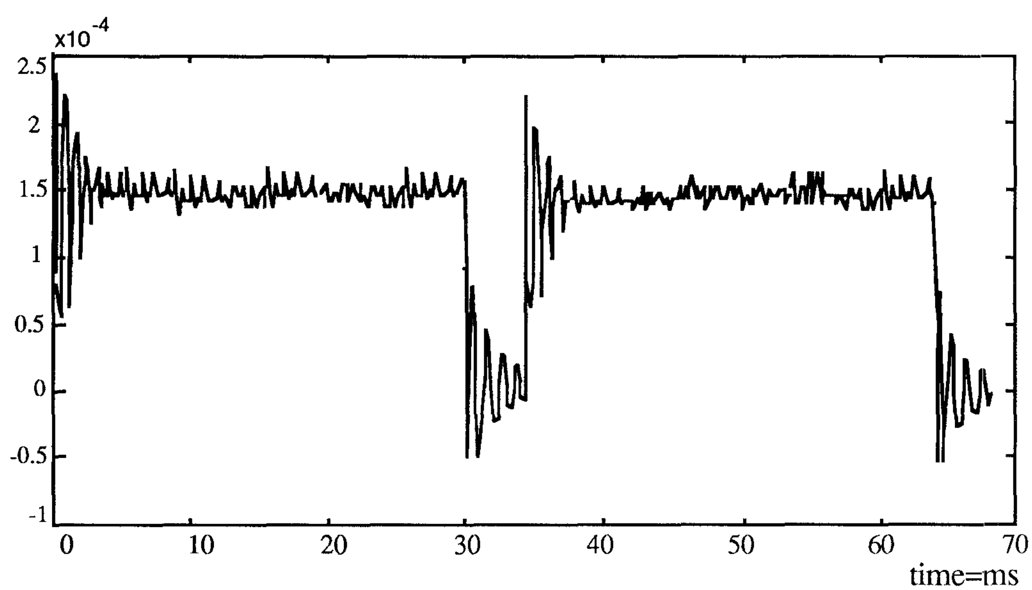

Fig. 5.4 Tool Vibration in Y Direction with Effect of Material Damping

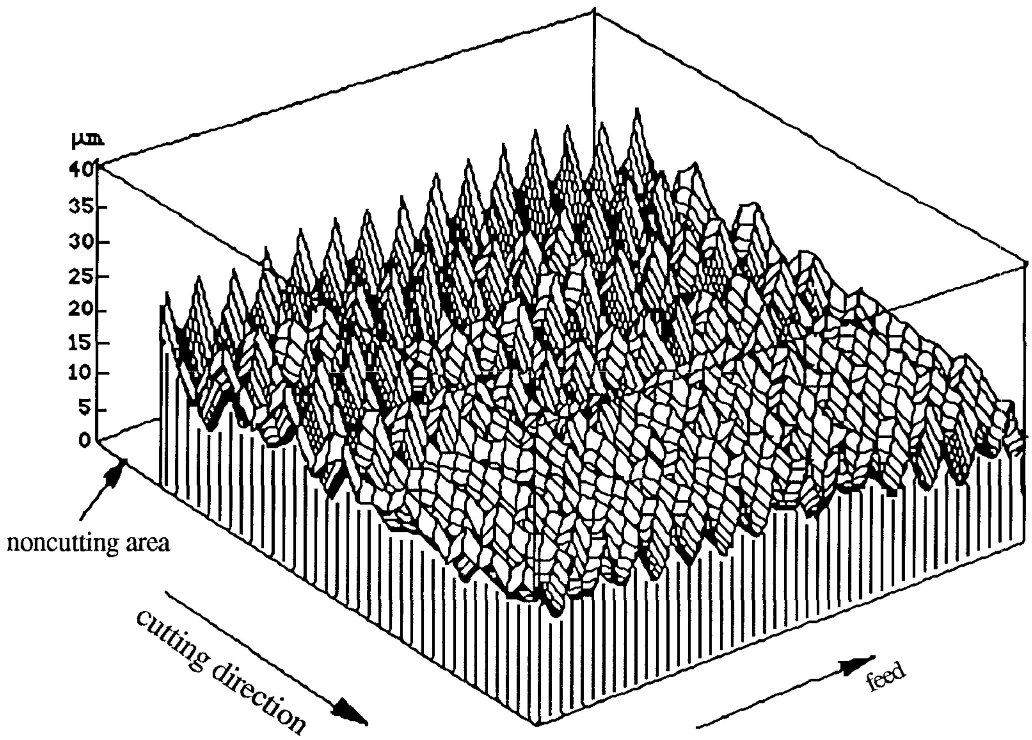

Fig. 5.5 Surface Finish without Effect of Material Damping

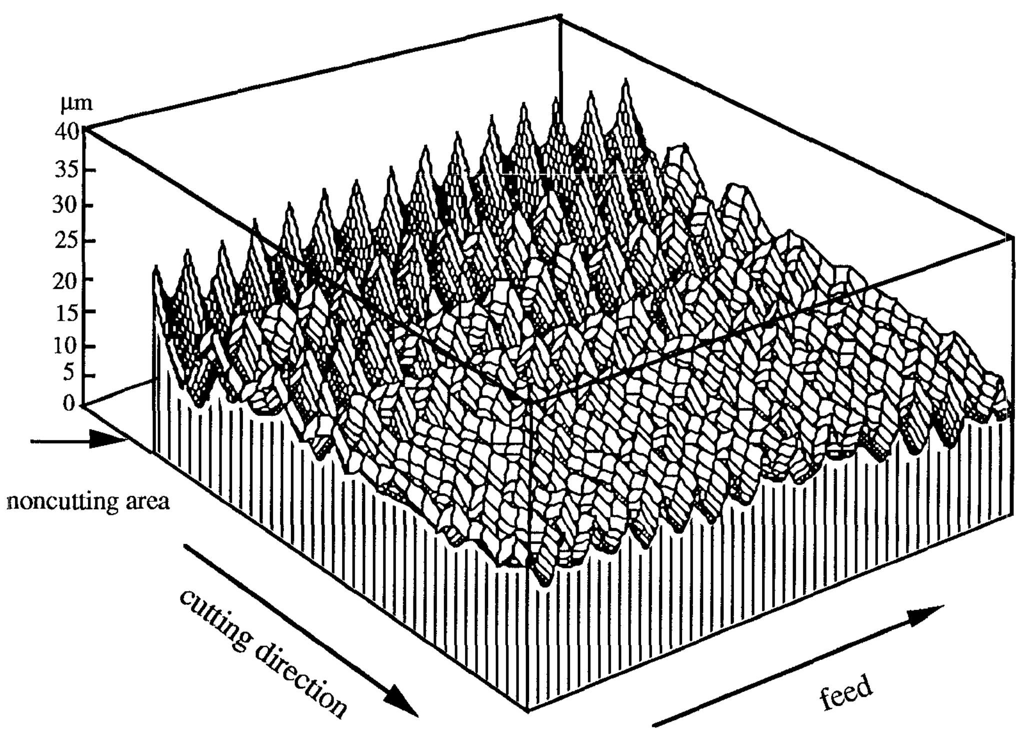

Fig. 5.6 Surface Finish With the Effect of Material Damping

5.2 Experimental Verification

Experiments were conducted to observe the phenomena which have been investigated during this thesis study. Data are collect during the experimental tests and used for the comparison with the results from the analytical study.

Experimental tests were performed in the machining shop of the Mechanical Engineering Department on the College Park campus. The workpiece material selected for the tests is an aluminium bar with 3 inches in diameter and 12 inches long, which is compatible for the conditions of the workpiece material used in the analytical study through computer simulation. The bar has four 10mm wide slots on its circumference. The experiments were conducted under the combination of different cutting speeds, depths of cut and feeds. For example, the time for one revolution of the workpiece is 60/N second. The time duration for the sum of a cutting and noncutting periods is equal to 60/4N second. The time duration of the noncutting period, T_2, is given by $40T/(3x25.4x\pi)$ second. Consequently, the time duration of the cutting period is equal to $T_1=T-T_2$.

5.2.1 Design of Dynamometer for Cutting Force Measurement

The experimental setup for measuring cutting force is shown in Figs. 5.7a and 5.7b. The instrumented cutting tool was rigidly held on the toolpost of the lathe. There are four foil strain gages mounted along the center line of the four surface of the tool holder, which are connected to two strain indicators. During machining, the signals measured by the strain gages are monitored through an oscilloscope and recorded onto an IBM 386 hard disc via an A/D convertor. Figure 5.8 shows the connections of the cutting tool, strain gages and the computer-based data acquisition system. Figure 5.9 is a typical plot of the measured voltage outputs during the cutting tests.

The strain gages were calibrated prior to the tests to establish the transfer function relation between the voltage signals and the cutting force generated during the machining process. The diagram of the strain gage calibration process is shown in Fig. 5.10. The relationship between the applied forces and the voltage outputs of the strain gage is shown in Table 5.1. The transfer function, Tr is defined as the relation between the input (applied force) and the output (oscilloscope readings).

$$\mathbf{Tr} = \frac{\text{Input}}{\text{Output}} = \frac{v_{out}}{F} \tag{5.23}$$

or in matrix form

$$[T_r] = \begin{bmatrix} \dfrac{\Delta v_y}{\Delta F_y} & \dfrac{\Delta v_y}{\Delta F_z} \\ \dfrac{\Delta v_z}{\Delta F_y} & \dfrac{\Delta v_z}{\Delta F_z} \end{bmatrix} = \begin{bmatrix} T_{11} & T_{12} \\ T_{21} & T_{22} \end{bmatrix} = \begin{bmatrix} 2.402 & 0.5072 \\ 0.030 & 9.939 \end{bmatrix} \tag{5.24}$$

Each element of [Tr] is the transfer function of the i^{th} oscilloscope voltage output and the j^{th} cutting force component. The force matrix is calculated as $[F] = [Tr]^{-1}[V]$, or

$$\begin{bmatrix} F_z \\ F_y \end{bmatrix} = \begin{bmatrix} +0.4166 & -0.0213 \\ -0.0013 & +0.1007 \end{bmatrix} \begin{bmatrix} V_z \\ V_y \end{bmatrix} \tag{5.25}$$

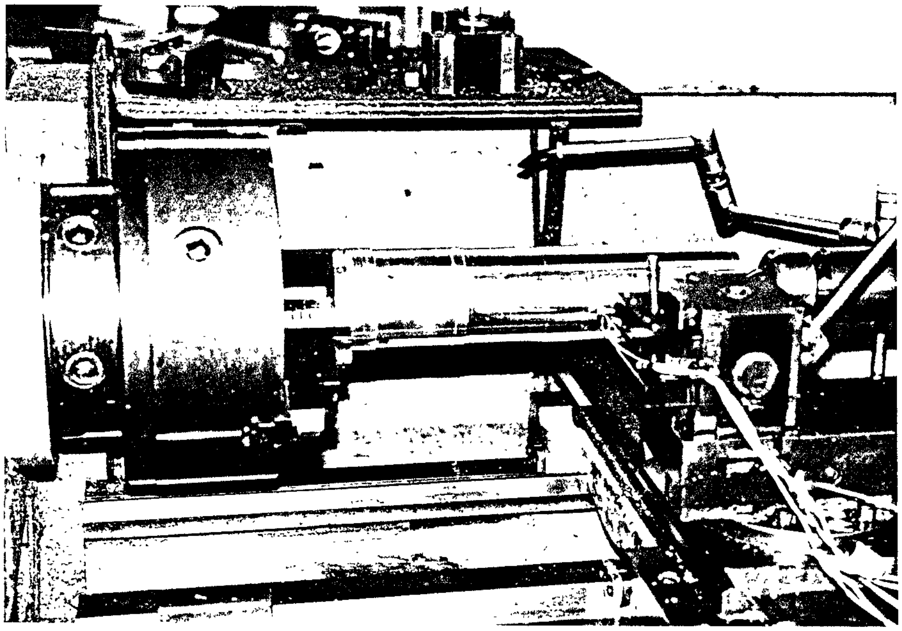

Fig. 5.7a Experimental Setup for the Cutting Force Measurement

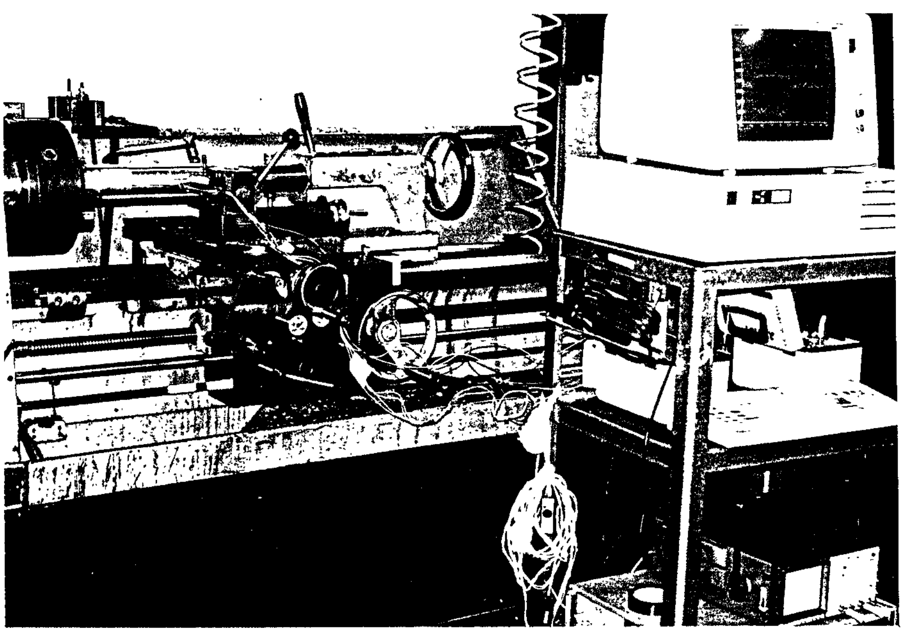

Fig. 5.7b Experimental Setup for the Cutting Force Measurement

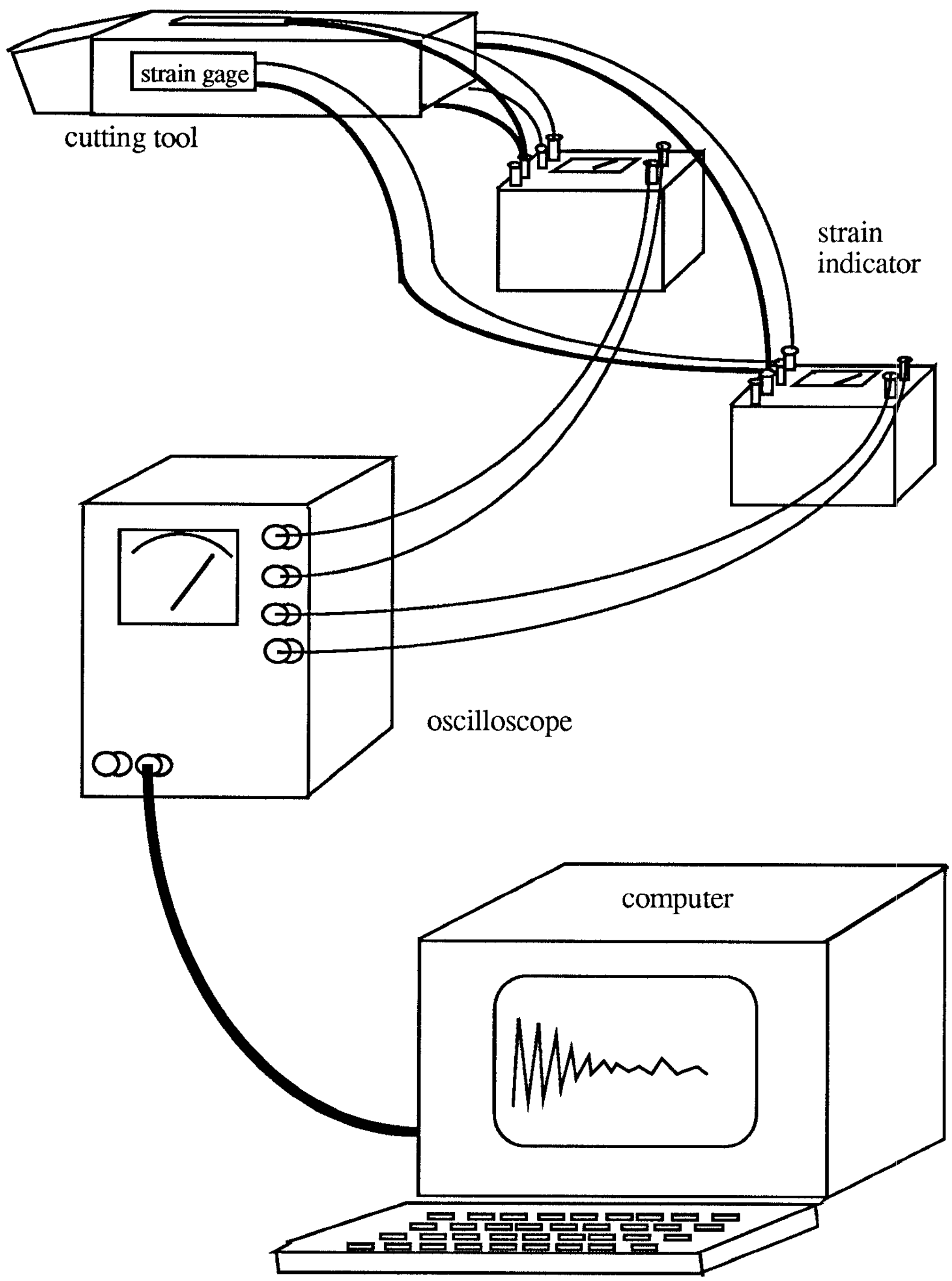

Fig. 5.8 Connection of the Experimental Test

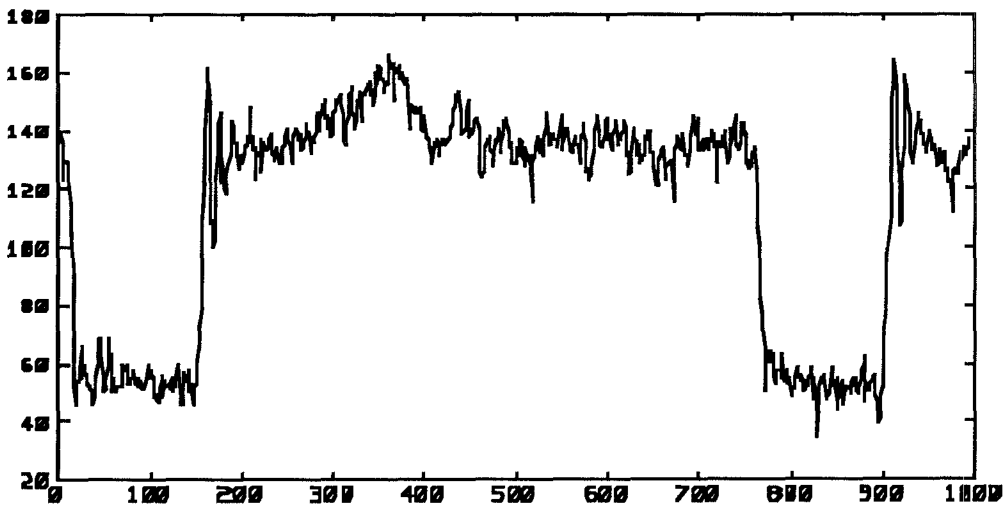

Fig. 5.9 Plot of Measured voltage Outputs (f = 0.15 mm/rev, d= 1.016 mm, and v = 3.24 m/s, workpiece is aluminium)

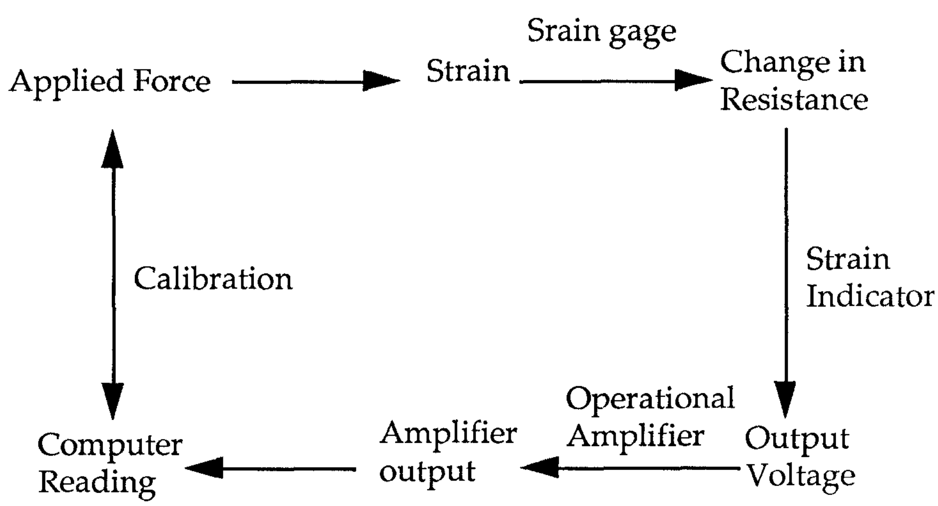

Fig. 5.10 Diagram for strain gage calibration

Force in Tangential Direction (Fz)

Weight(kg)	με1	με2	μv1	μv2
0.000	0.0	0.0	0.0	0.0
0.355	3.0	0.0	0.8	0.0
4.895	31.0	2.0	12.0	2.4
9.435	58.0	4.0	24.0	4.8
13.975	84.0	5.0	34.4	7.2
17.153	102.0	6.0	42.4	9.6
20.331	120.0	7.0	48.8	10.4
23.509	138.0	8.0	56.0	11.2

Force in Normal Direction (Fy)

Weight(kg)	με1	με2	μv1	μv2
0.000	0.0	0.0	0.0	0.0
0.170	0.0	2.0	0.0	4.0
4.170	0.5	27.0	0.0	47.2
9.250	1.0	57.0	0.0	96.0
13.790	1.5	85.0	0.0	117.0
16.968	2.0	103.0	0.0	174.0
20.146	2.5	121.0	0.8	205.0
23.324	3.0	139.0	0.8	236.0

Table 5.1 Calibration Voltage and Applied Weights

5.2.2 Experimental Results

There are four sets of experiment being conducted. The results of these four sets are shown in Fig. 5.11 - Fig. 5.14. respectively.

Test 1............... Fig. 5.11

Test 2............... Fig. 5.12

Test 3............... Fig. 5.13

Test 4............... Fig. 5.14

The relationship among the cutting condition, measured force and calculated force for each test is list in Table 5.2 By comparing test results (Figs. 5.11 - 5.14) with simulation results (Figs. 5.1 - 5.4), it can be seen that the response of the cutting tool from the test results is in a good agreement with the simulation results when the damping ratio of the workpiece is considered. The test results show that the system response decays faster when the cutting tool moves toward workpiece than that when the cutting tool moves away from the workpiece. It is also shown that in the prediction of the surface finish, the workpiece damping needs to be taken into account in order to obtain a high accuracy.

From the results in Table 5.2, it has been found that when using low cutting speeds, the measured impact force is close to the calculated impact force with a relative error of 12%. However, when using high cutting speeds, a significant error between the measured response and the calculated response. The reason for this discrepancy could be quite complex. However, it could be mainly due to the measurement error and the range of the frequency response of the strain gages. Further study is, therefore, needed in order to understand this phenomenon.

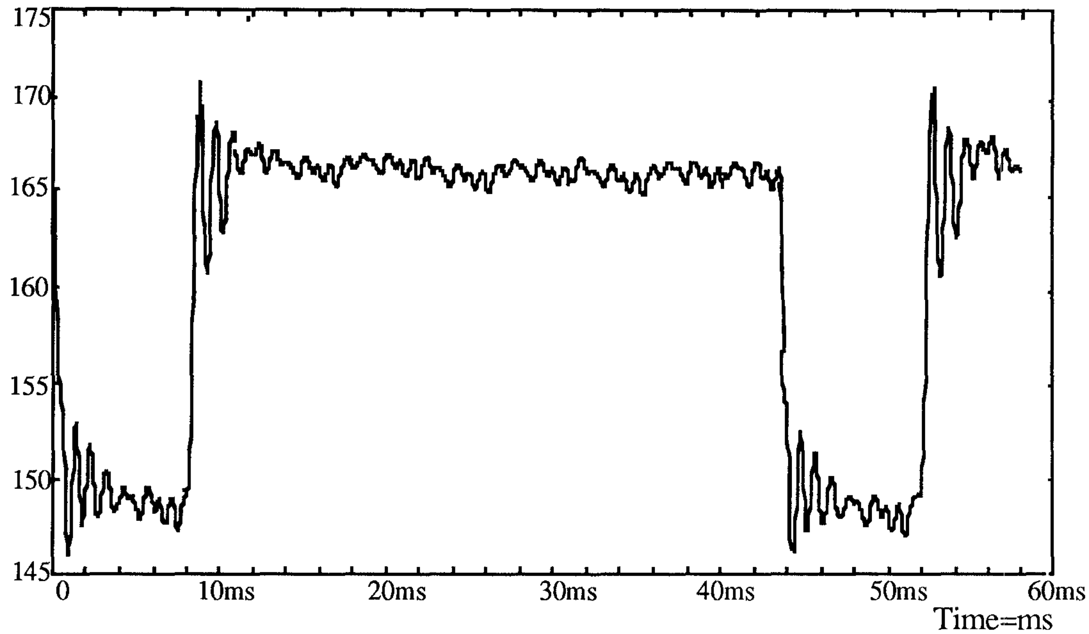

Fig 5.11 Test Result for Case One (A = 0.155mm^2 , v = 1.83 m/s)

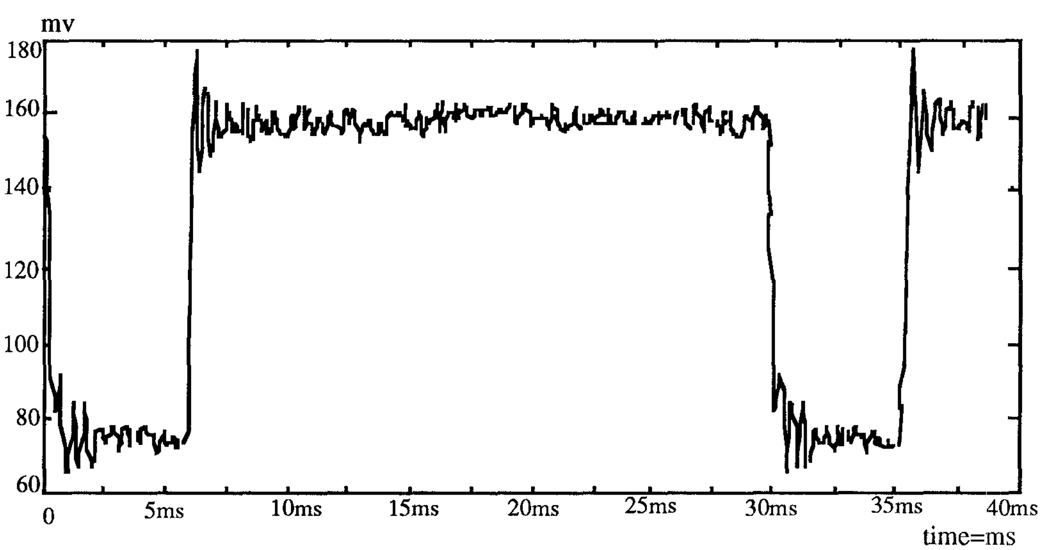

Fig. 5.12 Test result for Case Two (A = 0.155mm^2 , v = 3.24 m/s)

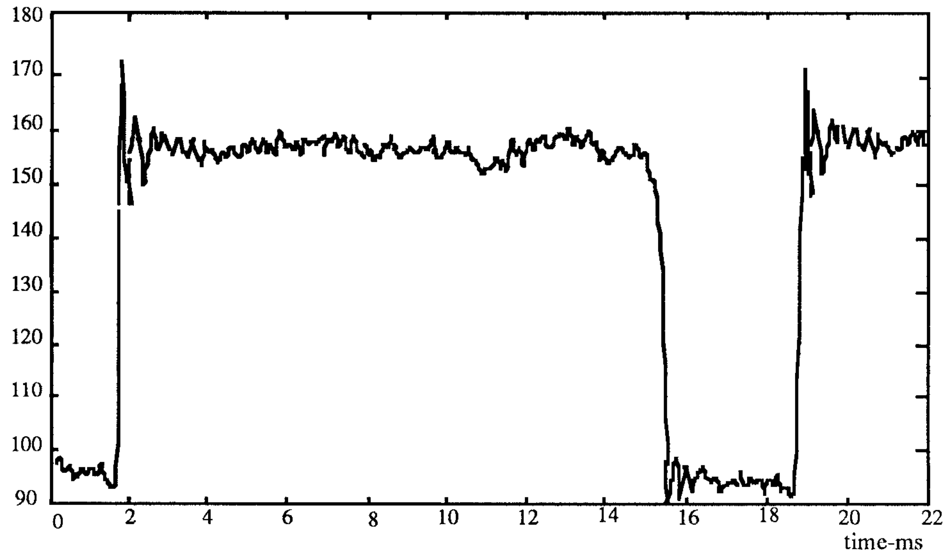

Fig. 5.13 Test Result for Case Three (A = $0.3mm^2$, v = 1.83m/s)

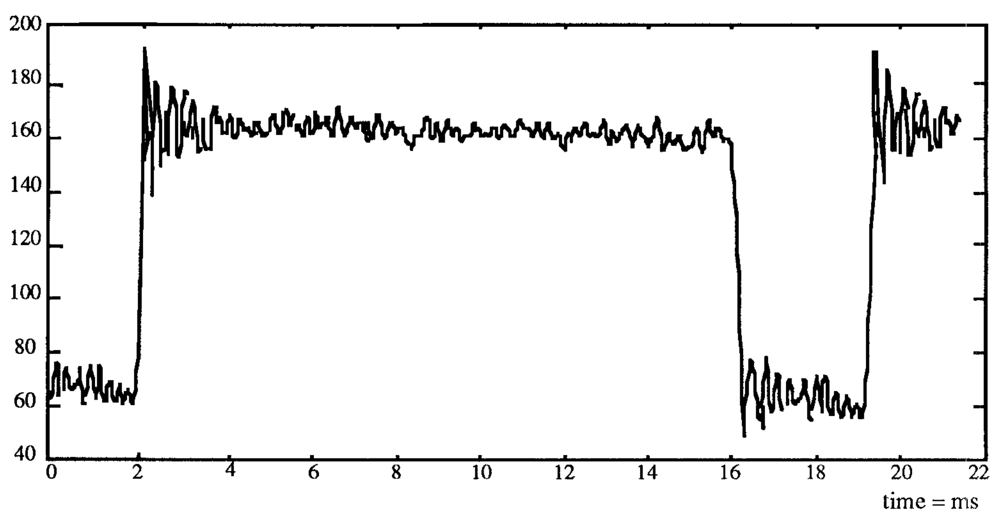

Fig. 5.14 Test Result for Case Four (A = $0.3mm^2$, v = 3.24m/s)

Number of test	Cutting chip-area	Cutting speed	Measured impact force	Calculated impact force
Test 1	$0.155mm^2$	1.83m/s	96.6	110
Test 2	$0.155mm^2$	3.24m/s	117	174
Test 3	$0.3mm^2$	1.83m/s	124	159
Test 4	$0.3mm^2$	3.24m/s	146	204

Table 5.2 The Relation between Cutting Condition, Measured Impact Force and Calculated Impact Force

5.3 Method of Finite Element Analysis (FEA)

Finite element method has been successfully used for analyzing structural dynamics for decades. It is also used in this thesis work to simulate the impact process. This is because the analytical formulation from the wave propagation theory results in a non-linear differential equations.

An FEA code named APIC2 is used in this thesis work. The software was developed based on the wave propagation theory discussed in Chapter 3. The required input consists of

1. Type of materials used. The software automatically retrieves the basic material properties such as Young's moduli, Poison ratios, and strength of materials from the database stored in it.
2. Selection of elements and geometrical configuration through mesh generation.

3. Boundary conditions applied, and initial conditions of the impact process.

The result of calculation, in which the behavior of workpiece during the impact period goes through elasticity regime to plasticity regime, shows good agreement with the observed phenomena in actual cutting processes. The stress distribution in the cutting tool also varies accordingly with the variation of the mass deformation in the workpiece during this period. The stress wave propagates radially, in a systematic manner, from contact area and throughout the tool. For a better understanding of the finite element simulation, the modeling and analysis process is discussed as follows.

5.3.1 Finite Element Calculation Steps

The predictable capability of current computer codes for impact studies is dependent on the theory of wave propagation solutions, which includes non-linear material properties and large displacements. A comprehensive description of the basic finite-element method is given in the text by Zienkiewicz [68]. A brief description of the finite-element method presented in this thesis are as follows.

1. Represent the geometry of the problem with elements of triangular cross section having specific material characteristics.
2. Lump the distributed mass at the nodes and assign initial velocities to represent the motion at impact.
3. Begin the numerical integration loop.
   (a) Determine the strains and strain rates in the elements.
   (b) Determine the stresses in the elements. The stresses consist of elastic stresses, plastic deviator stresses, hydrostatic pressure, and artificial viscosity.

(c) Determine equivalent concentrated forces to act on the nodal masses.

(d) Determine the integration time increment.

(e) Apply the equations of motion to the nodes for the integration time increment.

4. Repeat the numerical integration loop until the time of interest is elapsed.

In the above calculation steps, the strains are determined from the initial geometry of the element and the displacements of the nodes. The stresses in the elements are determined from the strains, strain rates, internal energies, and material properties. If the strains are within the elastic range, the elastic stresses can be obtained in a straight forward manner. For larger strains, involving plastic flow, the stresses are obtained by combining plastic deviator stresses with the hydrostatic pressure. In order to maintain a numerically stable solution for dynamics problems, the numerical integration time increment should be sufficiently smaller than the lowest period of vibration of the system.

5.3.2 Finite Element Mesh Generation

It is emphasized that with the impact condition, the whole system during the intermittent cutting process behaviors like a dynamic impact system with a free fall impactor hitting a clamped flexible target. The free impactor is the workpiece, and the clamped target is the cutting tool which is a cantilever beam model clamped at one end. The velocity of the impactor is equal to the relative tangential velocity between the cutting tool and workpiece. The mass of the impactor is the equivalent mass of the chip load. The finite element model for the intermittent turning process is shown in Fig. 5.15. The cutting tool clamped at the right side is hit by the impactor with a equivalent mass at the top of the left side. There are different kinds of elements available for calculating the dynamic response due to impact. The element used in this model is the triangular element. The reason for this selection is that in the impact problem involving severe distortions, the triangular element formulation is better suited to represent the severe distortions than the traditional quadrilateral finite-difference method [23]. The mesh size is so determined that both workpiece and cutting tool have a node at the contact point to avoid mesh overlap during the calculating process. The time increment is chosen as 10^{-8} second to guarantee the numerical stability and that the time for the elastic wave to propagate between two nodes is greater than the time increment used in the computer evaluation. To reduce the calculation time, the density of the meshes is reduced from contact area to the other side. Figure 5.15. shows the impactor (workpiece) hitting the target (cutting tool) with relative speed on the tangential direction at the instant of contact.

5.3.3 Simulation of Impact Process

Two examples of the finite element simulation with relative speed v=1.5 m/s and v=6m/s are presented to demonstrate the effect of the cutting speed during the impact. The workpiece material is steel 4020. The Young's module is 2.03×10^9. The yield strength, S_s, is 1.6×10^9 pa, and ultimate stress, S_r, is 1.8×10^9 pa.

The first example shows the impact process under cutting speed of 1.5m/s. The stress and displacement variation vs time are shown in Fig 5.16. The maximum stress occurs at 15 μs. The maximum displacement occurs at 50 μs which is 35 μs delay comparing with occurrence of the maximum stress. In appendix B, a detailed displacement process of the cutting tool and the stress distribution process in the cutting tool are visiblely described by a set of figures. After the maximum stress occurs, the mesh of the workpiece at the contact area shows severe distortion. At that instant, the process is considered entering the cutting process. The stresses in both of the cutting tool and workpiece increase rapidly at the beginning of the impact, and fall down after severe distortion occurs in the workpiece. In the entire impact process, the meshes of the cutting tool have no evident collapse. It means that the cutting tool is working in the elasticity region. This example shows that the stress wave radially propagates from the contact area throughout the cutting tool and workpiece during the impact period. Fig. 5.17 shows a glimpse of stress distribution in the cutting tool, and the meshes collapse in the workpiece.

The second example shows the impact process occurring when using a higher machining speed. The meshes of both workpiece and cutting tool at the contact area show severe distortion 10 μs after impact. However, there is no evident displacement of the cutting tool at that moment. Figure 5.18 shows the statue of the stress, deformation, and displacement of the cutting tool and workpiece at that moment. A set of figures in appendix B represent the whole dynamic process of this impact. The stress variation in the cutting tool in the impact period under the high machining speed is shown in Fig. 5.19.

In addition to the aforementioned examples of steel, another example of aluminium impactor (workpiece) with a velocity of 1.5 m/s and equivalence mass of 5kg is also included. This example shows the effect of the material property on the impact force. The maximum stress variation is shown in Fig. 5.20. The compression of the maximum stress variation in the cutting tool due to the aluminium workpiece and steel workpiece (example 1) is also shown in Fig 5.20. The difference shows that the impact force not only relates to the cutting speed, but also is the function of the workpiece material.

The finite element simulation presents the entire dynamic impact process. It shows that the impact process is a stress wave propagation process. Virtually, there are no model can deal with such complex impact process. The simulations shows that the stress in the cutting tool caused by the impact varies with the the machining speed and material of the workpiece, which has good agreement with the analytical model. In addition, the simulation shows that the maximum displacement of the cutting tool has a time delay comparing with the maximum stress. The explanation of this phenomena is far more involved and thus beyond the scope of this research work.

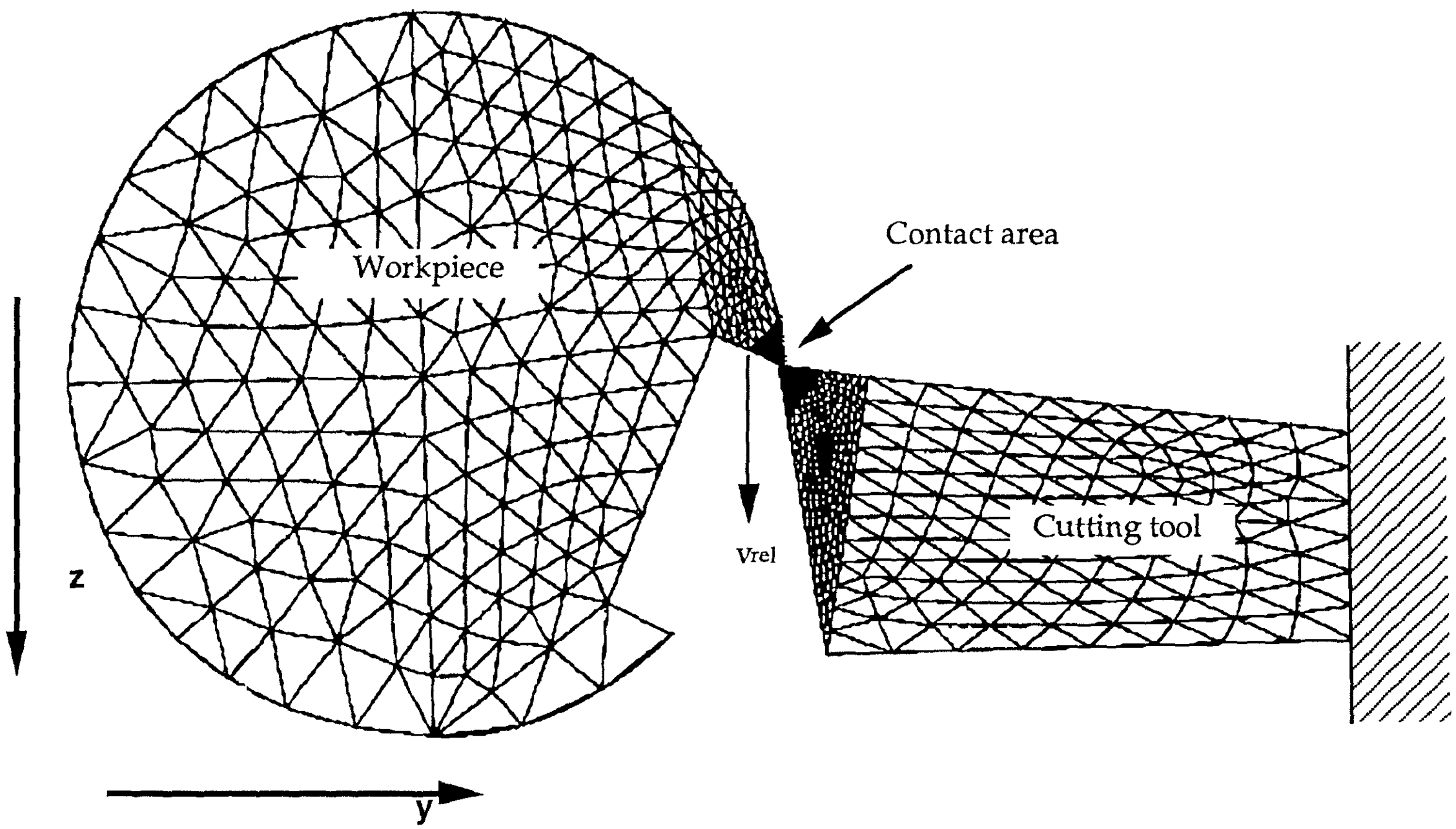

Fig. 5.15 Finite Element Model of the Cutting Tool during the Impact in the Intermittent Turning Process

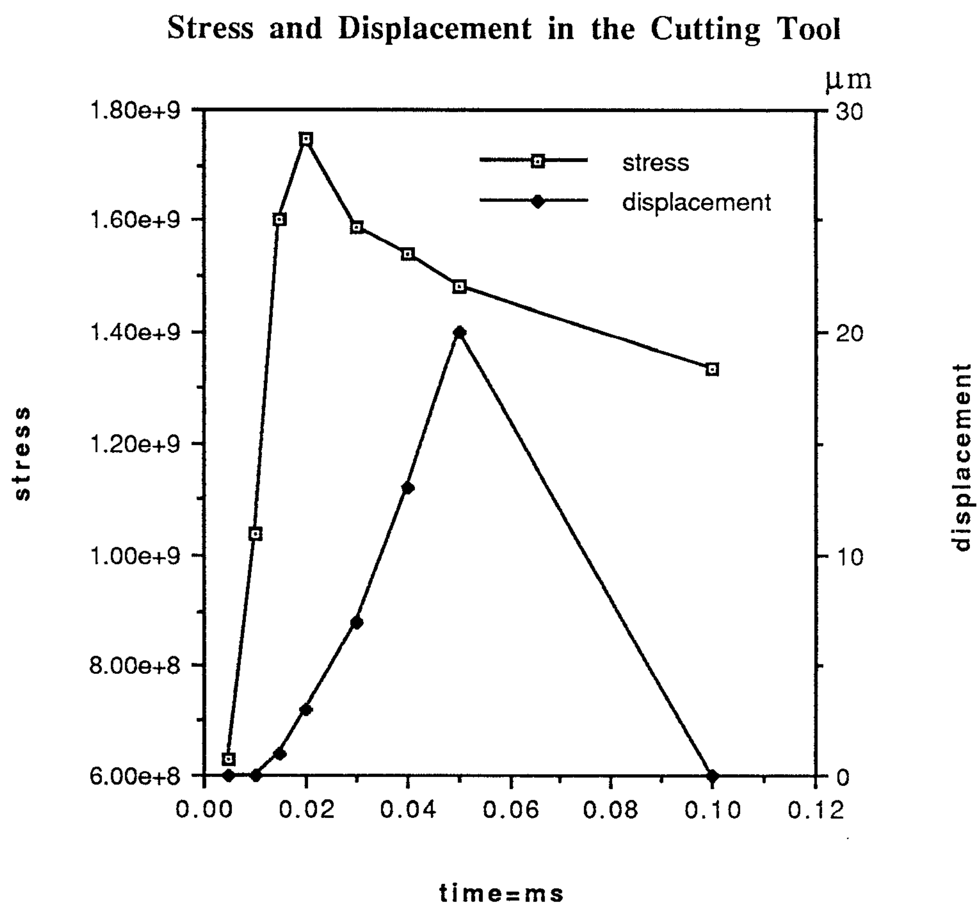

Fig. 5.16 Stress and displacement in the Cutting Tool

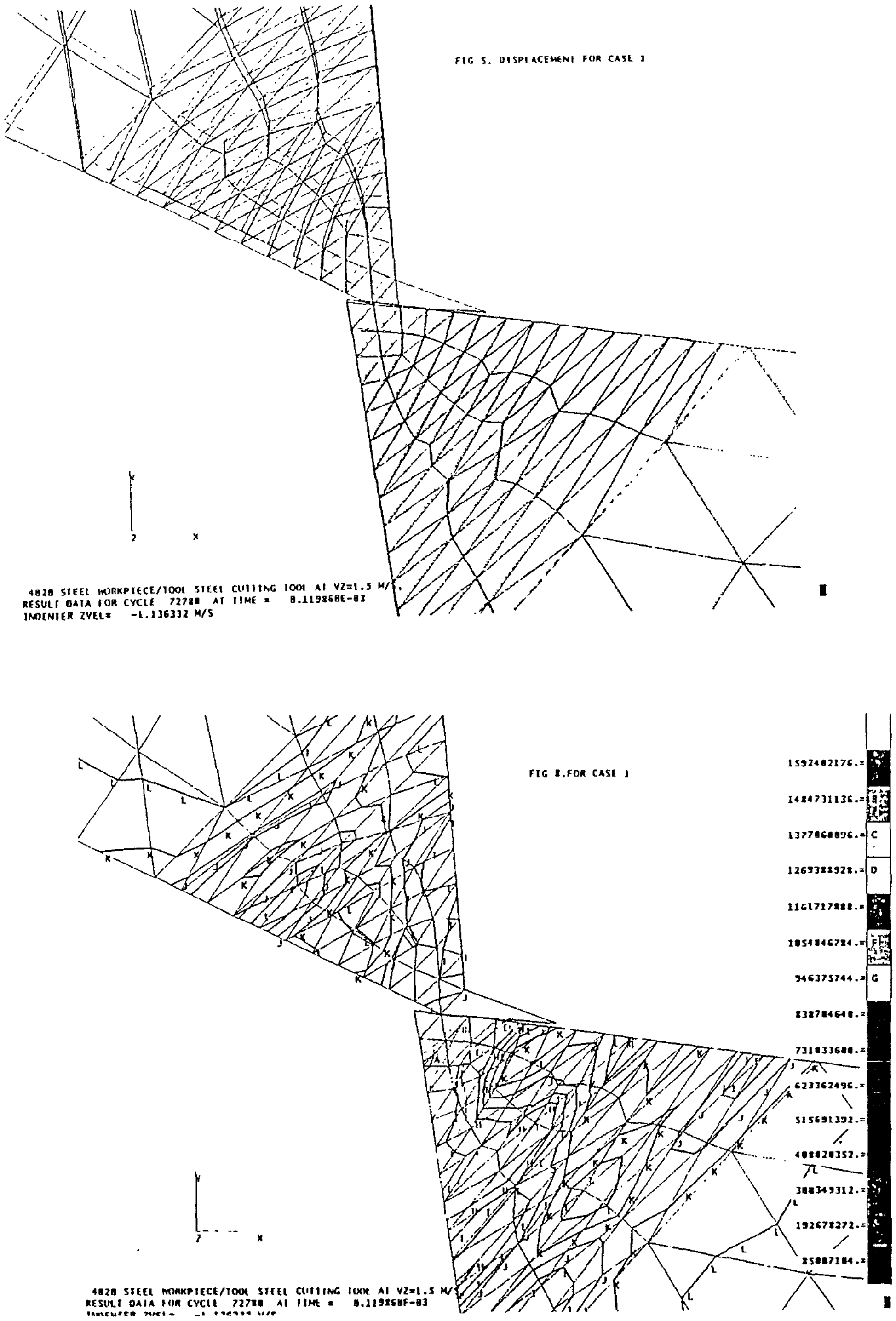

Fig. 5.17 Stress Distribution in the Cutting Tool and Mesh Collapse in the Workpiece during the Impact

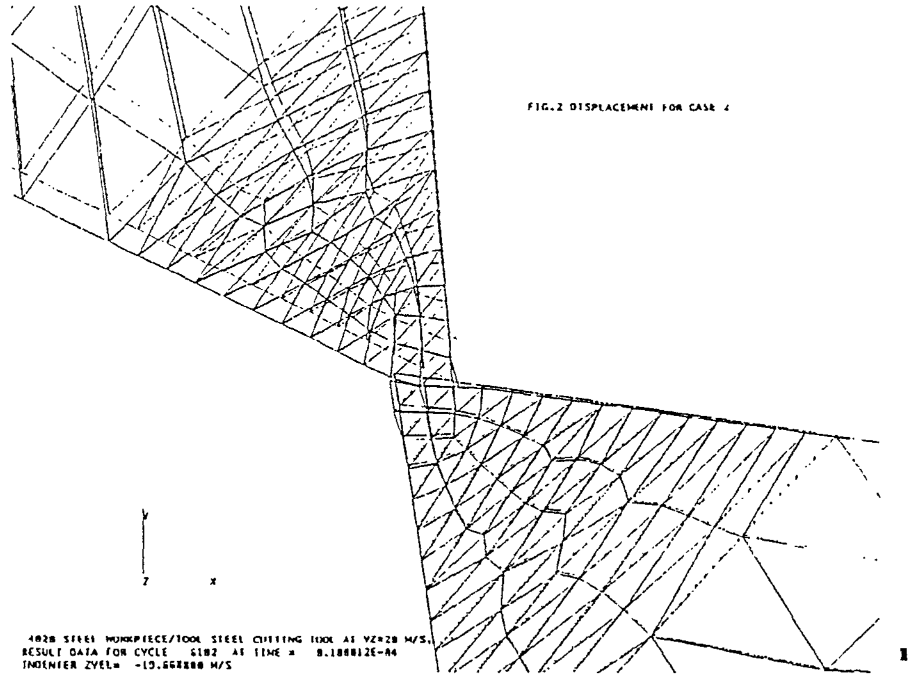

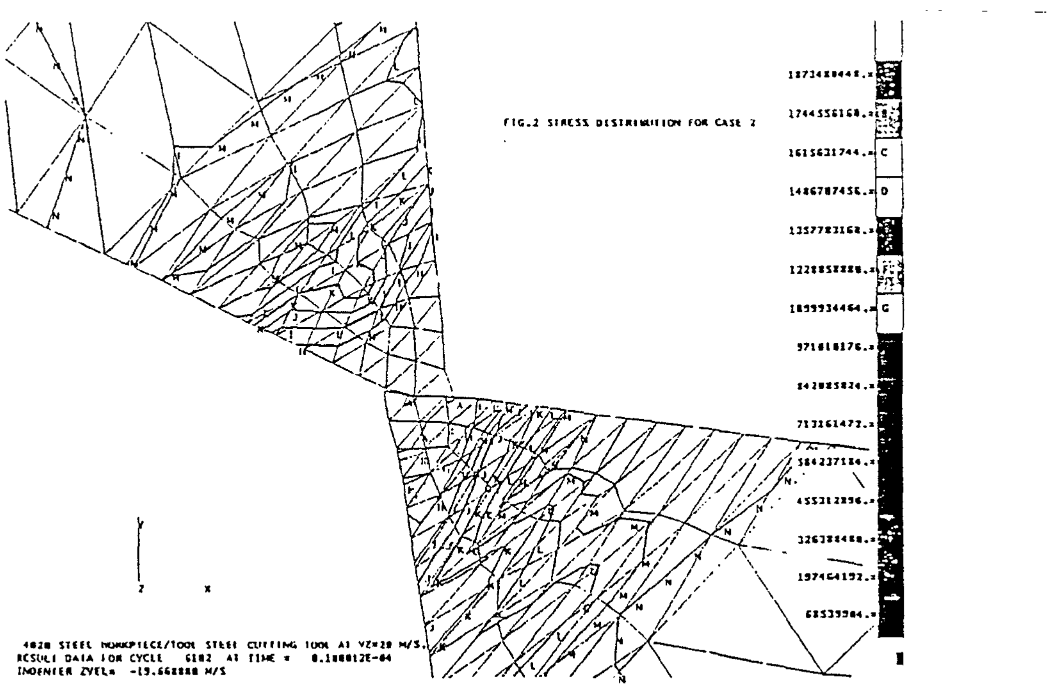

Fig. 5.18 Stress, Deformation, Displacement in the both Cutting Tool and Workpiece in the Beginning of the Impact during high Cutting Speed

Stress in the Cutting Tool in the Impact during High Cutting Speed

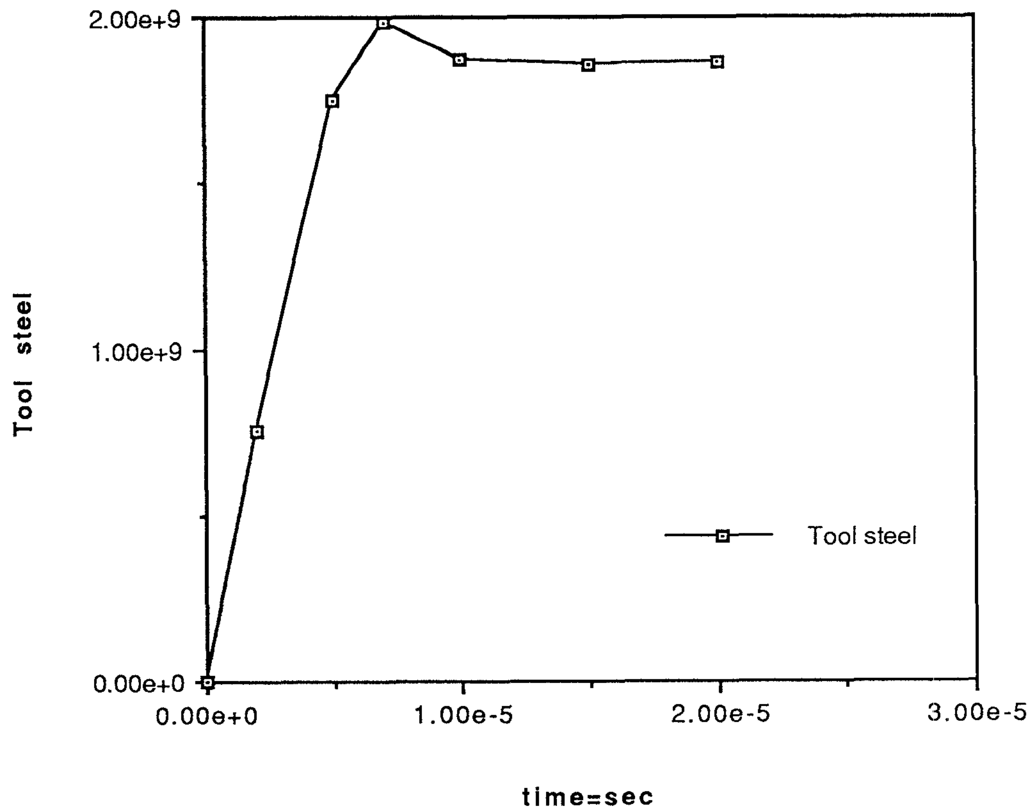

Fig. 5.19 Maximum Stress Variation in the Cutting Tool in the Impact under High Machining Speed

Stress in the Cutting Tool With Different Workpiece

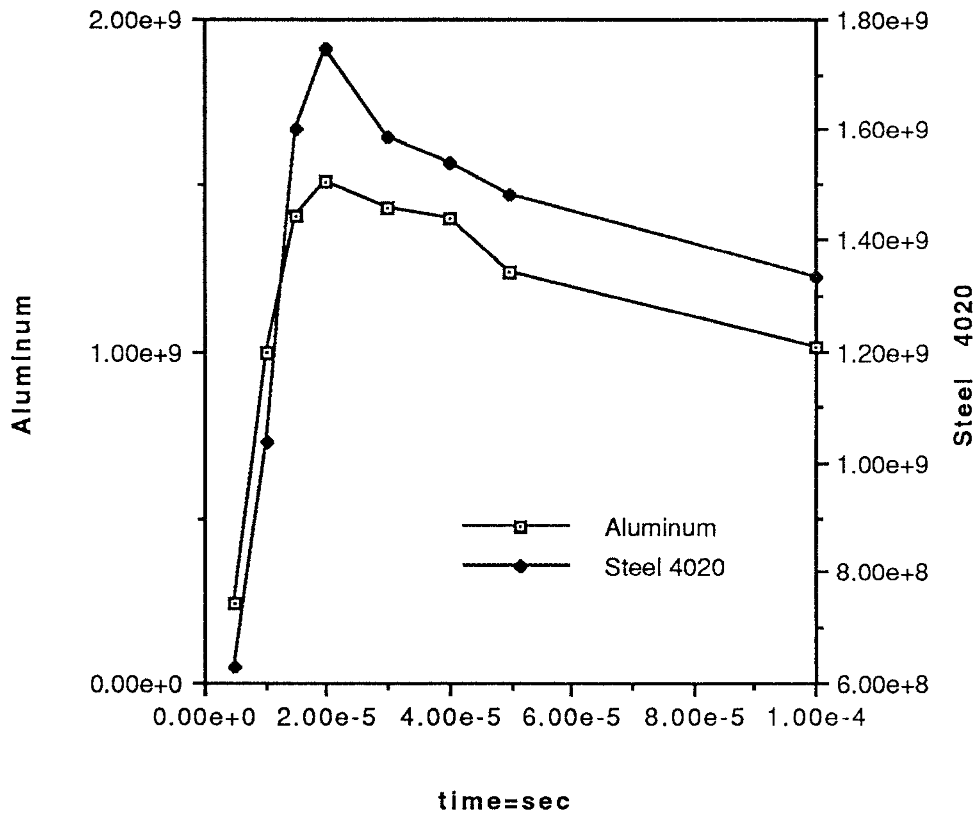

Fig. 5.20 Stress Variation in the Cutting Tool during Impact period

CHAPTER 6

CONCLUTIONS AND RECOMMENDATIONS

In this chapter, the main conclusions from the present study are first summarized, and followed by the recommendations for the future work.

6.1 Conclusions

In the present study, the intermittent turning process has been examined in the following four aspects: 1) a dynamic model including the impact force during the intermittent turning process, 2) the fundamental phenomena of the impact in the intermittent turning process, 3) an experimental study to confirm the analytical approach, and 4) applications of this thesis study to the prediction of tool breakage and surface quality.

The following detailed conclusions have been drawn from the present study:

(1) The system model developed has shown that the impact is the main source for the system instability during the intermittent turning process. Therefore, system model in the intermittent turning process should include the impact process in order to analyze the system stability, a phenomenon being neglected in most of the previous studies.

(2) The wave propagation theory has been used to study the impact force. A dynamic impact force equation for the intermittent turning process relating the cutting parameters has been explicitly established. It has been found that the impact force is a function of the cutting speed, chip load and the property of the workpiece material. Therefore, special attention should be

paid to the selection of cutting speed and cutting load for a stable cutting in the intermittent turning process. The stable boundary for the intermittent turning process obtained using the wave propagation theory can provide a preliminary reference in the selection of the cutting parameters. With the consideration of the impact, the stability boundary found in this thesis work seems more condensed than that found in the previous studies.

(3) The three periods in the intermittent turning process have been successfully modeled in the analysis of cutting dynamics. The effects of the damping of the workpiece on the tool motion have been included in the study of the tool motion during the intermittent turning process. It has been found that the inclusion of the workpiece damping gives a better prediction of the surface quality.

(4) Finite element method has been successfully used to simulate the impact process. The results predicted using FEM are in good agreement with the experimental data. It has been found that the impact process is actually a type of the strain and stress propagation process and therefore, can't be treated as an initial conditions.

6.2 Recommendations

Based on the present study, the following two recommendations with respect to the future work in this area are made.

(1) Tool geometry plays a significant role in determining characteristics of the impact process. It is evident that a negative rake angle or a large lead angle

can reverse the impact force direction, avoiding the occurrence of tool breakage. Therefore, the effects of tool geometry on the impact force should be further investigated in order to obtain a more comprehensive system model to describe the intermittent turning process.

(2) The system modeling should consider effect of the flexibility of the workpiece on the cutting generation. The assumption made in this thesis work that the workpiece is ideally rigid should be relaxed in order to obtain a more comprehensive system model to describe the intermittent turning process.

References

1. American Society of Mechanical Engineering, "Manual on Matel Cutting", Second Edition, 1952.
2. Ahn, T.Y. Eman, K.F.and Wu, S.M., "Cutting Dynamics Identification by Dynamic Data System (DDS) Modeling Approach," Journal of Engineering for Industry, ASME, Vol. 107, May 1985, pp. 159-166.
   3. pp. 31-38.
4. Alberti, N., Diego, S. and Passannanti, A., "Interdependence between Tool Fracture and Wear," Annals of the CIRP, Vol. 34, No. 1, 1985, pp. 61-63.
5. American National Standards Institute - "Dimensioning and Tolerancing" ANSI Y14.5M - 1982.
6. Bolz, R.G., "Production Process", Conquest Publications, 1974, pp. 181.
7. Braun, S. Lenz, E. Wu, C. L. "Signature Analysis Applied to Drilling," Journal of Mechanical Design, ASME, Vol. 104, April 1982.
8. Cook, N.H. and Subarmanian, K., "Micro-Isotope Tool Wear Sensor," Annals of the CIRP, Vol. 27, 1978, pp. 73-78.
9. De Filippi, A. and Ippolito, R., "Adaptive Control in Turning: Cutting Forces and Tool Wear Relationships for P10, P20, P30 Carbides," Annals of the CIRP, Vol. 17, 1969, pp. 377-379.
10. Danai, K., and Ulsoy, A. G., "An Adaptive Observer for On-Line Tool Wear Estimation in Turning, Part I and II," Mechanical System and Signal Processing, 1987, pp. 211-240.
11. EI Gomayel, J. I. and Bregger, K. D., "On-Line Tool Wear Sensing for Turning Operations," Journal of Engineering for Industry, Trans. ASME, Vol. 108, February, pp. 44-47.
12. Fiegenbaum, A. V., "Total Quality Control," McGraw-Hill Book Company, New York, 1965.
13. Foster, L. W., "Geo-Metrics: The Metric Application of Geometric Tolerancing Techniques," Addison-Wesley Publishing Company, Inc., 1986.
14. Fujii, H. Marui, H. and Ema, S., "Whirling Vibration in Drilling, Part 1: Cause of Vibration and Role of Chisel Edge," Journal of Engineering for Industry, ASME, Vol. 108 August 1986, pp. 157-162.

15. Fujii, H. Marui, H. and Ema, S., "Whirling Vibration in Drilling, Part 2: Influence of Drill Geometries, Particularly of the Drill Frank, on the Initiation of Vibration,"Journal of Engineering for Industry, ASME, Vol. 108 August 1986, pp. 163-168.
16. Giusti, F., Santochi, M., Tantussi, G., "On-Line Sensing of Flank and Crater Wear of Cutting Tools," Annals of the CIRP, Vol. 36, No. 1, 1987, pp. 41-44.
17. Glaser, D. L. and Nachtigal, C. L. "Development oa a Hydrautic Chambered, Actively controlled Boring Bar" J. fof Engr. for Industry, Trans. ASME. Vol. 101. Nov. 1979, pp. 362-368
18. Goldsmith, Werner "Impact The Theory and Physical Behaviour of Colliding Solids," London, Edward Arnold(publishers) Ltd, 1960
19. Grabec, I. and Leskovar, P., "Acoustic Emission of a Cutting Process," Ultrasonics, January 1977, pp. 17-20.
20. Hallam, R. A. and Allsopp R. S.,"The design, Development and Testing of a prototype Boring Dynamometer", Int. J. mach. Tool Des. Res., Vol. 24 No. 1, 1962, pp. 241-266.
21. Ham, I. H. and Yoshida, T. "Group Technology: Applications to Production Management," Kluwer-Nilhoff Publishing Co., Boston, Mass.
22. Ishikawa, T. and Yamada, Y. "Fracture Detection of Cutting Edge in Multi-Point Tools," Proceedings of the 16th North American Manufacturing Research Conference, May 1988, pp. 256-263.
23. Johnson, G. R. "Analysis of elastic-Plastic Impact Involoving Severe Distortions" Journal of Applied Mechanics, September 1976, pp. 439-444.
24. Kannatey, Jr. E., "Tool Failure Monitoring in Turning by Pattern Recognition Analysis of AE signals," Journal of Engineering for Industry, Trans. ASME, Vol. 110, May 1988, pp. 137-145.
25. Kegg, R. L., "Cutting Dynamics in Machine Tool Chatter," Journal of Engineering for Industry, ASME Trans., Vol. 87, 1965, pp. 464-470.
26. Kline, R. G., "Active Control of a Boring Bar Operation," Ph.D. Thesis, Purdue University, 1973.
27. Klin, R. G. and Nachtigal C. L., "The Application of Active Control to Improve Boring Bar Performance," Trans. ASME. Series G, Vol. 97, Nov. 1975 pp.179-183.

28. Klopstock, "Recent Investigation in Turning and Planing and a New Form of Cutting Tool," Werkstattstechnik, vol. 17,1923, Nos. 23 and 24. In English.
29. Koren, Y., "Dynamic and Static Optimization of the Cutting Processes," Proceedings of the First North American Manufacturing Research Conference, May 1973, pp. 67-94.
30. Ko, T. and Koren, Y., "Cutting Force Model for Tool Wear Estimation," Transactions of the North American Manufacturing Research Institution of SME, May 1989, pp. 166-169.
31. Kronenberg, M., "Machining Science and Application," Pergamon Press Inc., 1966.
32. Li-Pin, Yi., "Bending and Torsional Vibration in an Overhung Boring BAr During Boring," Irv. Vurov Mvo, USSR. Mashinostronie, No. 1, 1958.
33. Love, A. E. H. "A Treatise on the Mathematical Theory of Elasticity," 4th Edition. Hew Youk, Dover Publications. 1944.
34. Lovett, C.D., "Progress Report of the Quality in Automation Project for FY88," NISTIR 89-4045, National Institute of Standards and Technology, April 1989.
35. Lu, S. C-Y. and Zhang, G. M. "A Combined Inductive Learning and Experimental Design Approach to Manufacturing Operation Planning," Journal of Manufacturing Systems, Vol. 9, No. 2, 1990.
36. MacBain, J. C., Harding, K. G. and Tekinalp, O., "Vibration Modes and Frequencies of Twist Drills Using Laser Holographic Interferometry," PED-V0l. 18, WAM 1985, pp. 1-10.
37. Matthews, J. R., "Acoustic Emission," Gordon and Breach Science Publishers, 1983.
38. Merchant, M.E., "Mechanics of the Metal Cutting Process - Orthogonal Cutting and a Type - 2 Chip," Journal of Applied Physics, Vol. 16, No. 5, 1945, pp. 267-275.
39. Merritt, H. E., "Theory of Self-Excited Machine-Tool Chatter," Trans. ASME, Vol. 87, November 1965, pp. 447-454.
40. Nicolson, "Rapid Cutting Tool Steels," Engg., 1903, P. 598.
41. Nedess, C. and Himburg, T., "Drilling Dynamics - a Fundamental Base for Drill-Life Monitoring," Proceedings of the 16th North American Manufacturing Research Conference, May 1988, pp. 300-306.

42. Pandit, S.M. and Kashou, S., "A Data Dependent Systems Strategy of On-Line Tool Wear Sensing," Journal of Engineering for Industry, ASME Trans., Vol. 104, 1982, pp. 217-223.
43. Peklenik, J. "Investigation of the Surface Typology," Annals of the CIRP, Vol. 15, 1967, pp. 381-385.
44. Shigley, Joseph Edward and Mitchell, Larry D., "Mechanical Engineering Design" Mcgraw-Hill International Book Company, Fouth Edition, 1983.
45. Shaver, D. P. "Internal Report on Drill Wear Monitoring," The Speech and Image Understanding Laboratory, Texas Instruments Inc., 1989.
46. Shaw, M. C., "Metal Cutting Principles," Clarendon Press, Oxford, 1984.
47. Smith, J. D. and Tobis, S. T., "The Dynamic Cutting of Metals", Int. J. Mach. Tool Des. Res. , Vol. 1, No. 4, 1961, pp. 283-292.
48. Taguchi, G., and Wu, Y., "Introduction to Off-Line Quality Control," Central Japan Quality Control Association, Nagoya, Japan, 1980.
49. Taylor, F. W., "On the Art of Cutting Metals," Trans. ASME, Vol. 28, 1906, p. 240.
50. Timoshenko, S., Young, D. H. and Weaver, W., "Vibration Problems in Engineering," John Wiley and Sons, Inc., Fouth Edition,1974.
51. Tlusty, J., "Analysis of the State of Research in Cutting Dynamics," Annals of the CIRP, Vol. 27/2/1978, pp. 583-589.
52. Tlusty, J. and Andrews, G.C., "A Critical Review of Sensors for Unmanned Machining," Annals of the CIRP, Vol. 32/2/1983, pp. 563-572.
53. Tlusty, J. and Polacek, M., "The Stability of the Machine Tool Aganist Self-Excited Vibration in Machining," ASME Prod. Eng. Res. Conf., Pittsburgh, 1963, pp. 465-454
54. Tobias, S. T. and Fishwish, W., "Theory of Kegenerative Machine Tool Chatter", Engineer, London, Vol. 205, 1958, p. 199.
55. Weck, W. and Schmit, M., "A New Methods for Determining Geometric Accuracy in the Axis of Movement of Machine Tool," Precision Engineering, Vol. 8, No. 2, April, 1986, pp. 97-103.
56. Williams, R. V., "Acoustic Emission," British Steel Corporation (Overseas Services) Ltd., 1980.
57. Yen, D. W. and Wright, P. K., "Adaptive Control in Machining - a New Approach Based on the Physical Constraints of Too Wear"

58. Zhang, G. M. Yerramareddy, S. Lee, S. M. and Lu, S. Y-C. "Simulation of Intermittent Turning Processes," DSC-Vol. 18, 1989 ASME Winter Annual Meeting, pp. 1-9, San Francisco, CA, December 1989.
59. Zhang, G. M. and Lu, S. C-Y. "An Expert System Framework for Economic Evaluation of Machining Operation Planning," Journal of the Operational Research Society, Vol. 41, No. 5, 1990.
60. Zhang , G. M. and Hwang, T. W. "Analysis of the Cutting Dynamics in Microscale," Symposium on Automation of Manufacturing Processes, 1990 ASME Winter Annual Meeting, Dallas, Texas.
61. Zhang, G. M. and Hwang, T. W. "Analysis and Control of Geometric Tolerancing through Surface Topography Generation," Symposium on Fundamental Issues in Machining, 1990 ASME Annual Meeting, Dallas, Texas.
62. Zhang, G. M. and Kapoor, S. G., "Development of an Instrumented Boring Bar Transducer," Proceedings of the 14th North American Manufacturing Research Conference, May 1986, pp. 194-200.
63. Zhang, G.M., "Dynamic Modeling and Dynamic Analysis of the Boring Machining System," Ph.D. Thesis, University of Illinois at Urbana-Champaign, 1986.
64. Zhang, G.M., Hwang, T.W., and Harhalakis, G., "Control of Surface Topographies Formed during Machining," Proceedings of the Second International Conference on Computer Integrated Manufacturing, May 1990.
65. Zhang, G.M. and Hwang, "Analysis of the Cutting Dynamics in Microscale," submitted to the 1989 ASME Winter Annual Meeting for review.
66. Zhang, G. M., S. Yerramareddy, S., Lee, S. M., and Lu, S. C-Y., "Simulation of Intermittent Turning Processes," DSC-Vol. 18, 1989 ASME Winter Annual Meeting, pp. 1-9, December 1989.
67. Zhang, G. M., S. Yerramareddy, S., Lee, S. M., and Lu, S. C-Y., "Simulation of Surface Topography Formed during the Intermittent Turning Process," DSC-Vol. 18, 1989 ASME Winter Annual Meeting, pp. 11-18, December 1989.
68. Zienkiewicz, O. C., "The Finite-Element Method in Engineering Science," McCraw, Hill NewYouk 1971.
69. Zorev, N. N., "Metal Cutting Mechanics," Pergamon Press, Oxford, 1965.

70. Zukas, Junas A., Nicholass, T., Swift, Hallock F., and Curran, Donald R. "Impact Dynamics" A Wiley-Interscince Publication. John Wiley & Sons, 1982.

Appendix A

Derivation of Impact Force and Impact Duration

The approach a is the difference of the displacement of the mass, w_2, and the deflection of the beam at the contact point, w_1<c>.as shown in the Fig. A.1

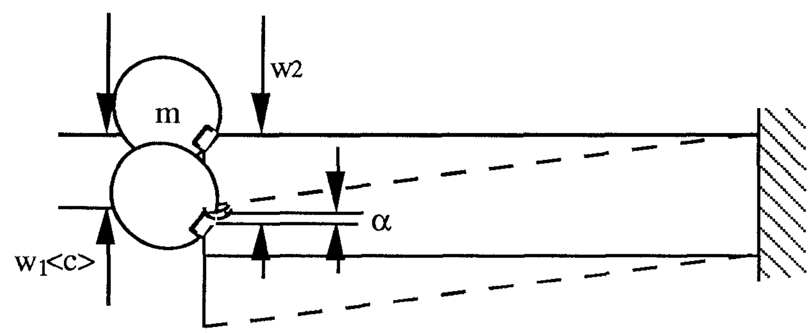

Fig. A.1 Impact between A Free Body and Cantilever Beam

$$\alpha = w_2 - w_1<c> = v_o t - \frac{1}{m}\int_0^t dt \int_0^t F dt - w_1<c> \tag{A.1}$$

where w_1<c> is given by the equation

$$w_1 < c > = \frac{1}{\rho A} \sum_{i=1}^{\infty} \frac{[X_i < c >]^2}{\omega_i \int_0^t X_i^2 dx} \int_0^t F < \bar{\tau} > \sin \omega_i (t - \bar{\tau}) d\bar{\tau} \tag{A.2}$$

The eigenfunctions X_i and frequency ω_i are determined from the equations of free vibration of the beam and depend upon the boundary conditions. For a cantilever beam, the frequency

$$\omega_i=\xi_i^2 a_i^2=\xi_i^2\sqrt{\frac{EI}{\rho A}} \tag{A.3}$$

for a number of boundary condition which involve only orthogonal eigenfunctions. and

$$x_i=\frac{\cosh \xi_i x-\cos \xi_i x}{\cosh \xi_i x+\cos \xi_i x}-\frac{\sinh \xi_i x-\sin \xi_i x}{\sinh \xi_i x+\sin \xi_i x} \tag{A.4}$$

$$\int_0^L X_i^2 dx=L\frac{\cos^2 \xi_i L}{\sin^4 \zeta_i L} \tag{A.5}$$

$$\cos \xi_i L \cosh \xi_i L=-1 \tag{A.6}$$

Also, according Hertz law

$$\alpha=\left[\frac{F}{K_2}\right]^{\frac{2}{3}} \tag{A.7}$$

where K_2 is the material property coefficient. For the toolpost x=L. The impact force is a function of the time and has been specified in the form

$$F=F_0 \sin \xi t \tag{A.8}$$

where $\bar{B}$ and x are constancies, corresponding to an impact duration $t=\frac{\pi}{\xi}$. When the motion of the beam is to be represented solely by its fundamental harmonic, it is possible to evaluate the resulting integrals by substituting Eqs. (A.2), (A.3), (A.4), (A.5), (A.6), (A.7) and (A.8) into Eq. (A.1). It can be rewritten as

$$[\frac{F_0 \sin \xi t}{K_2}]^{\frac{2}{3}} = v_0 t - \frac{1}{m}\int_0^t dt \int_0^t \bar{B} \sin \xi t dt - \frac{c}{\rho A L}\int_0^t \frac{\bar{B}}{\omega_1} \sin \xi \bar{\tau} \sin \omega_1 (t - \bar{\tau}) d\bar{\tau}$$

$$= v_0 t - \frac{F_0}{m}(\frac{t}{\xi} - \frac{1}{\xi^2} \sin \xi t) - \frac{cF_0}{\rho A L}[\frac{\xi \sin \omega_1 t - \omega_1 \sin \xi t}{\omega_1(\xi^2 - w_1^2)}] \tag{A.9}$$

where

$$c = \frac{[\frac{\cosh \xi_i x - \cos \xi_i x}{\cosh \xi_i x + \cos \xi_i x} - \frac{\sinh \xi_i x - \sin \xi_i x}{\sinh \xi_i x + \sin \xi_i x}]^2}{\frac{\cos^2 \xi_i L}{\sin^4 \zeta_i L}}$$

under the assumption of $\frac{\pi}{\xi} \ll \frac{2\pi}{\omega 1}$, the term $\sin \omega_1 t$ may now be replaced by $\omega_1 t$.

and

$$\sin^{\frac{2}{3}} \xi t \approx \bar{A} \sin \xi t \tag{A.10}$$

then

$$\alpha = K_2^{-\frac{2}{3}} \bar{A} \bar{B}^{-\frac{2}{3}} \sin \xi t \tag{A.11}$$

The quantity $\bar{A}$ is so chosen that the change of momentum of the striking mass is the the same whether Eq.(A.8) or (A.11) is applied. This requires that

$$\int_0^\pi \sin \xi d\xi = \bar{A}\int_0^\pi \sin \xi d\xi \tag{A.12}$$

so that $\bar{A}$=1.093

$$[\frac{F_o}{K_2}]^{\frac{2}{3}}\bar{A}\sin\xi t = v_0 t - \frac{\bar{B}}{m}(\frac{t}{\xi} - \frac{1}{\xi^2}\sin\xi t) - \frac{c\bar{B}}{\rho AL}[\frac{\xi t - \sin\xi t}{(\xi^2 - w_1^2)}] \qquad (A.13)$$

When the coefficients of the terms sinξt and t are now separately equated to zero, the constants ξ and $\bar{B}$ are determined by

$$\xi^5 = \frac{v_0 k_2^2}{\bar{A}^{-3} m^2 (\frac{\rho AL}{c})^2}\left[\frac{(m + \frac{\rho AL}{c})\xi^2 - \frac{\rho AL}{c}\omega_1^2}{\xi^2 - \omega_1^2}\right]$$

$$F_o \approx \frac{v_0 m\rho AL\xi(\xi^2 - \omega_1^2)}{(cm + \rho AL)\xi^2 - \rho AL\omega_1^2} \qquad (A.14)$$

where the quantity ξ may be evaluated by a numerical method. From the above equation, the time duration t and magnitude of impact force F_0 is obtained.

Appendix B

Finite Element Simulation of the Impact Process

There are two examples of the finite element simulation. The first example shows the impact process when machining at low cutting speed. Fig.B.1-B.3, show the displacement of the the cutting tool and the mass deformation processes in the cutting tool and workpiece. In this case, its displacement goes from zero to the maximum position and returns to origin position without any obvious collapse in the mashes. The maximum displacement occurs 50ms after impact take place, and the severe distortion appears on the workpiece. At that point, the cutting tool is engaging into the workpiece, and the system is considered to enter the normal cutting period. The Fig. B.4 to Fig B.7 show the stress wave propagation process in this period. The stresses in both of the cutting tool and workpiece increase rapidly at the beginning of the impact and slow down after severe distortion occurs in the workpiece. In the whole impact process, the cutting tool is working in the elasticity area since there is no obvious severe mass deformation occurring in the cutting tool. The maximum stress occurs at the time 15ms, which occurs earlier than the maximum displacement occurrence. The phenomenon shows that the displacement has a time delay compared to the stress wave propagation. It would be difficult to measure this impact force by mounting strain gages on the cutting tool. (In the high cutting speed, when the tool breakage takes place, the cutting tool even has no any obvious displacement, which is shown in next example.) This example shows that the stress wave radially propagates from the contact area throughout the cutting tool and workpiece during the impact period. during the whole impact process, the stress in the workpiece is lower than that in the cutting tool.

The second example shows the impact process occurring with high machining speed. A set of figures, i.e, Figs. B.8 -B.10, depict the simulated displacement of the cutting tool and the mass deformation in the cutting tool and workpiece. After 10ms from the beginning of the impact, which is shown in Fig. B.8, both meshes of the workpiece and cutting tool at the contact area demonstrate severe distortion and without obvious displacement of the cutting tool. In Fig.B.9 and B.10, the meshes collapse continues. In the actual case, it means the cutting tool is broken due to the impact force. A set of figures i.e. Fig. B.11 -B.12, gives the stress wave distribution in the cutting tool. When the maximum stress in the cutting tool exceed the allowed maximum stress of the cutting tool, the cutting tool breaks immediately along the maximum stress line, this is shown in Fig.B.11. When the cutting tool breakage takes place, the stress in the cutting tool keeps its value which is equal to the maximum allowed stress of the cutting tool material during the collapse period. This phenomenal could be found by looking at the deformation variation process (Fig. B.8 - B.10) and stress propagation process (Fig. B.11 - B.12) in the cutting tool simultaneously.

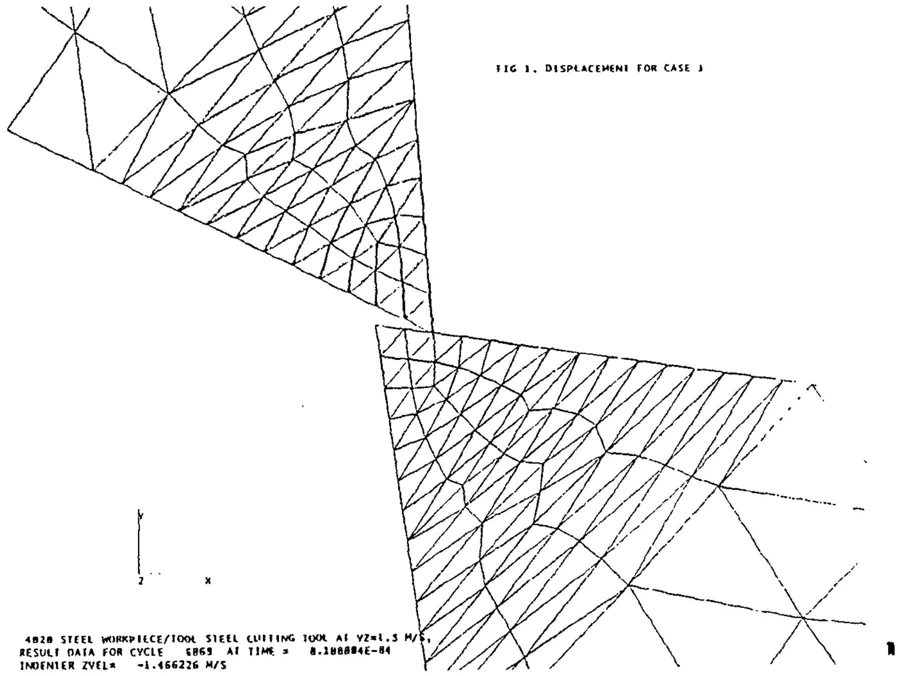

10 μs

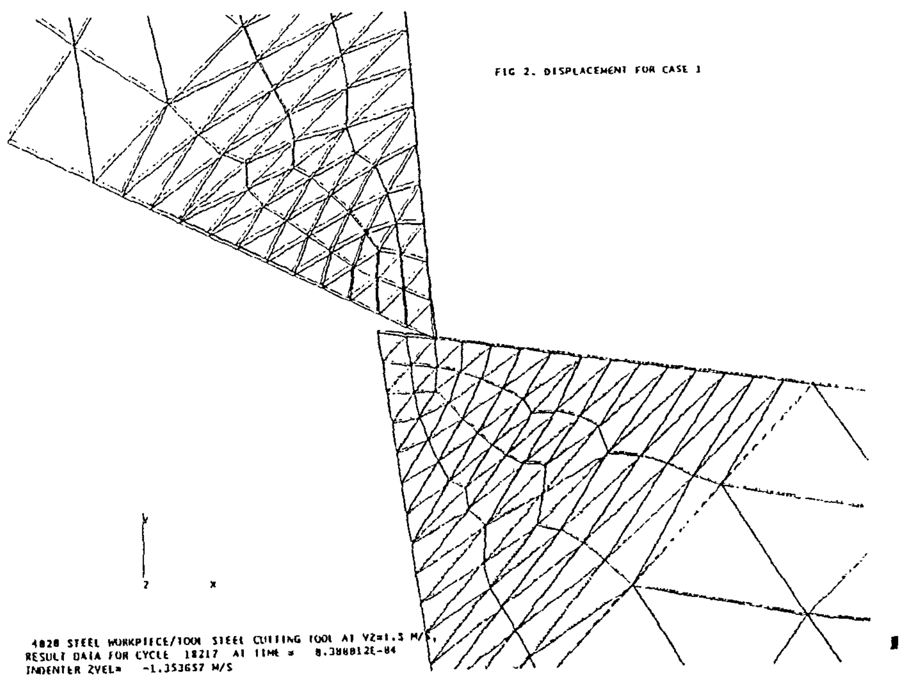

30 μs

Fig. B.1 Deformation Profiles of the Cutting Tool under Impact in the Intermittent Turning Process at 10 μs and 30 μs with 1.5m/s Cutting Speed

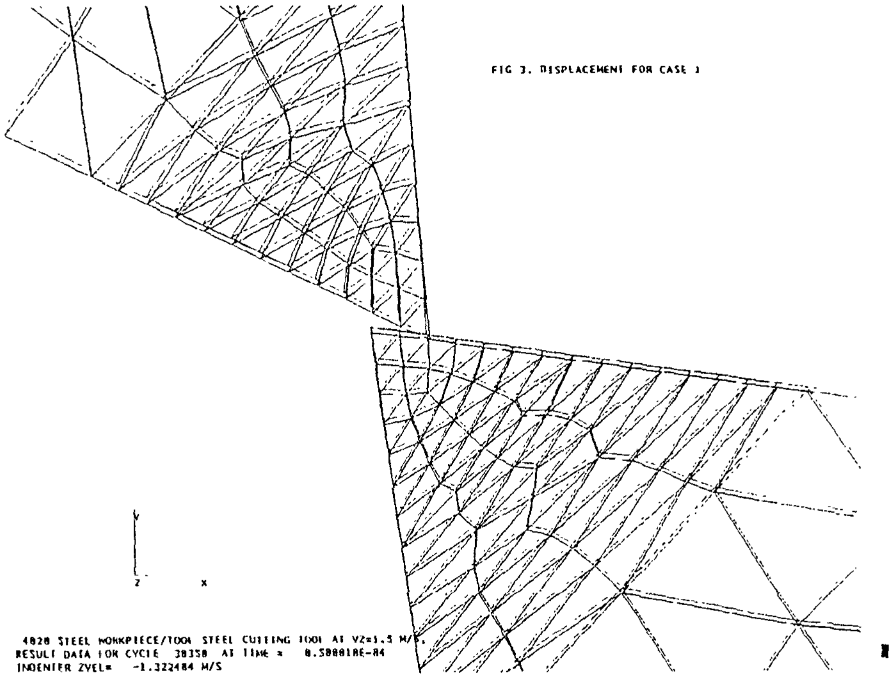

50 μs

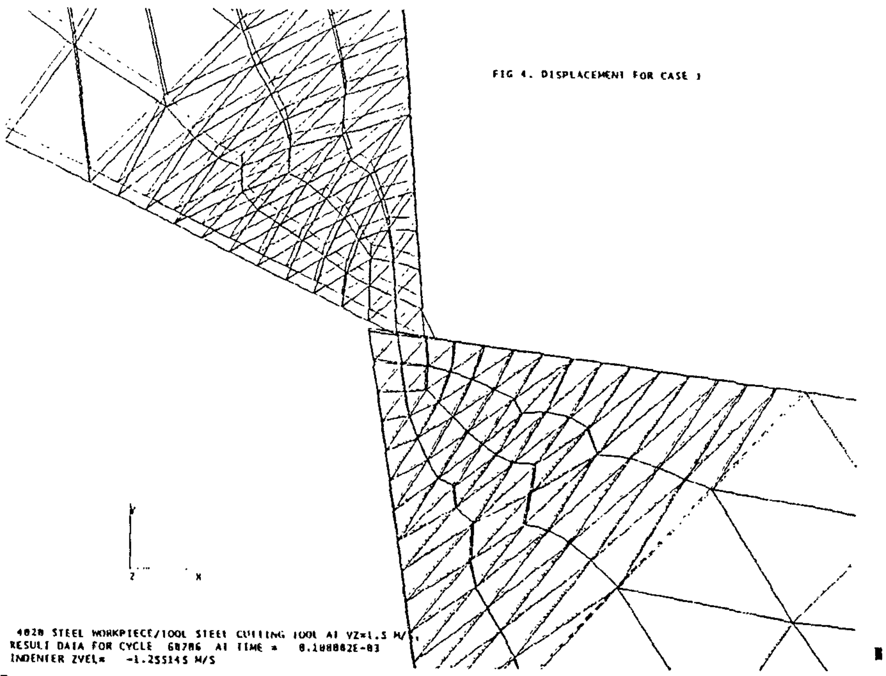

100μs

Fig. B.2 Deformation Profiles of the Cutting Tool under Impact in the Intermittent Turning Process at 50 μs and 100 μs with 1.5m/s Cutting Speed

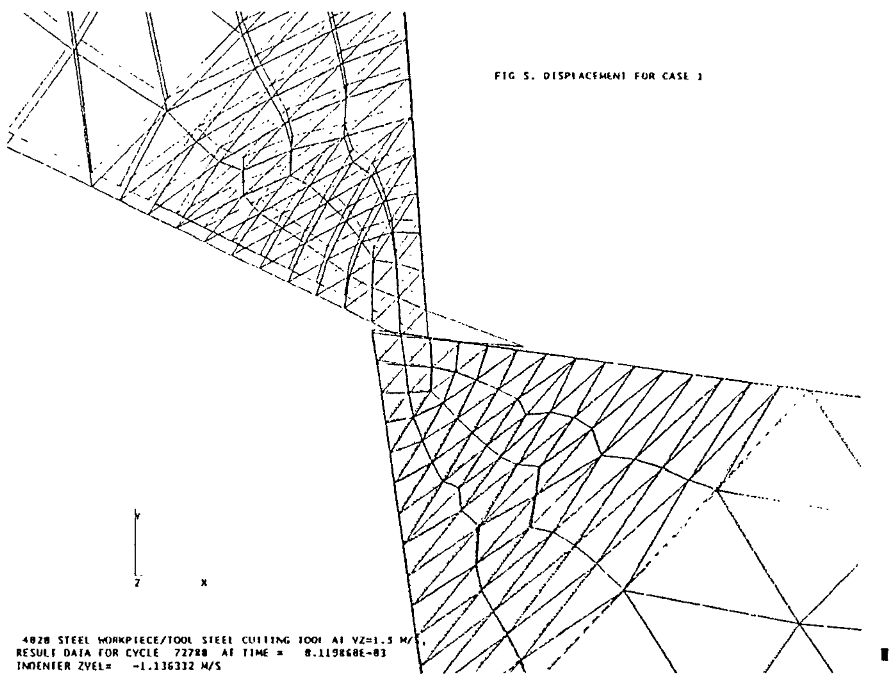

120µs

Fig. B.3 Deformation Profiles of the Cutting Tool under Impact in the Intermittent Turning Process at 120 µs with 1.5m/s Cutting Speed

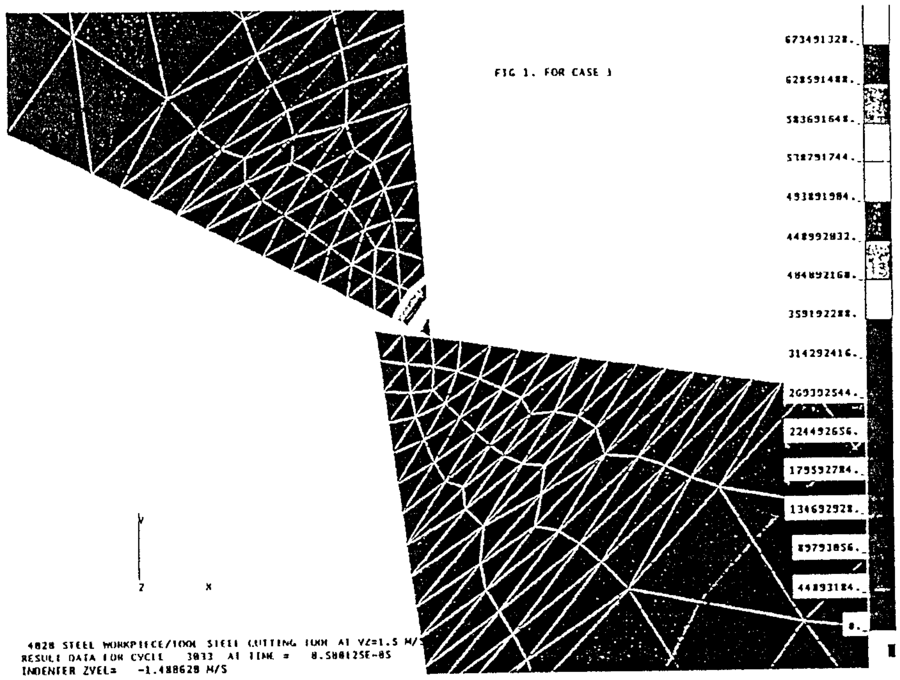

5 μs

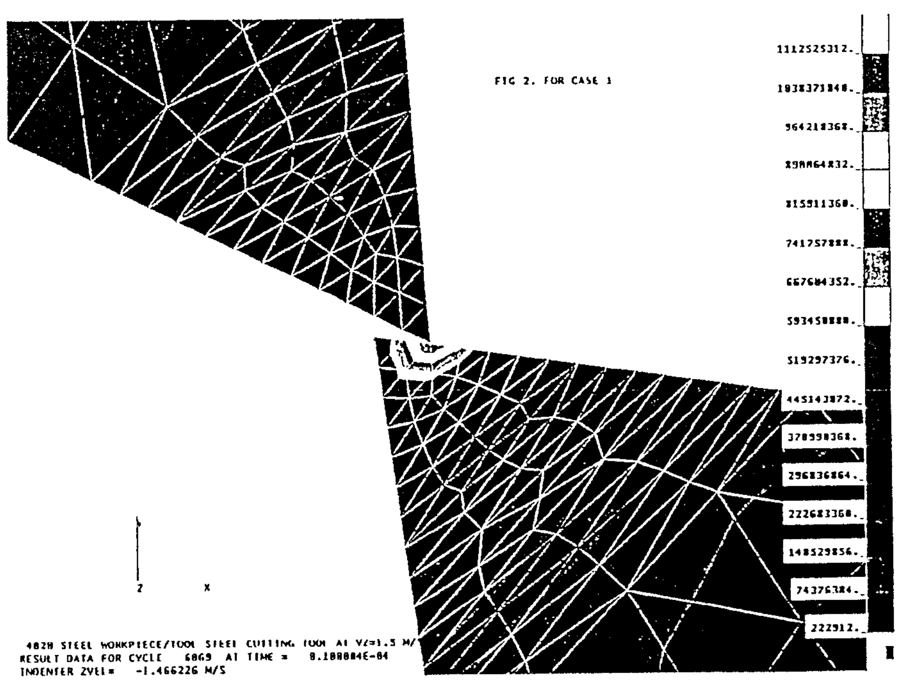

10 μs

Fig. B.4 Stress Distribution in the Cutting Tool under Impact in the Intermittent Turning Process at 5 μs and 10 μs with 1.5m/s Cutting Speed

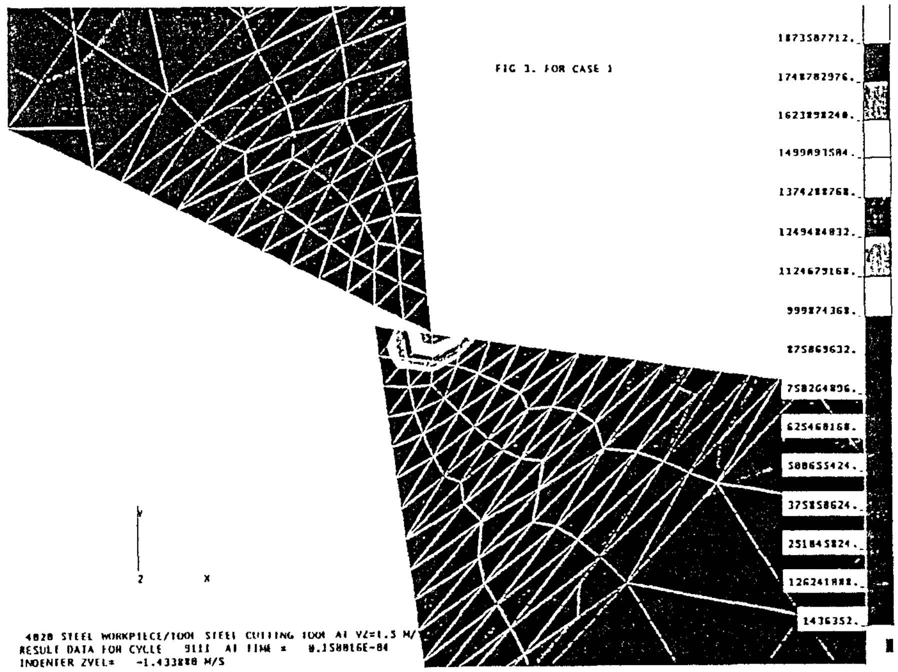

15 μs

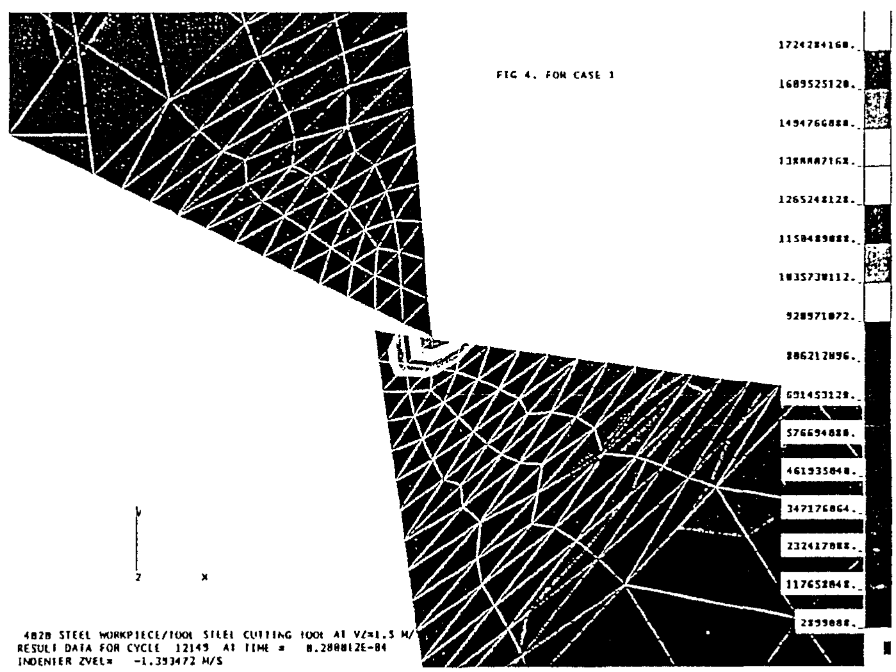

20μs

Fig. B.5 Stress Distribution in the Cutting Tool under Impact in the Intermittent Turning Process at 15 μs and 20 μs with 1.5m/s Cutting Speed

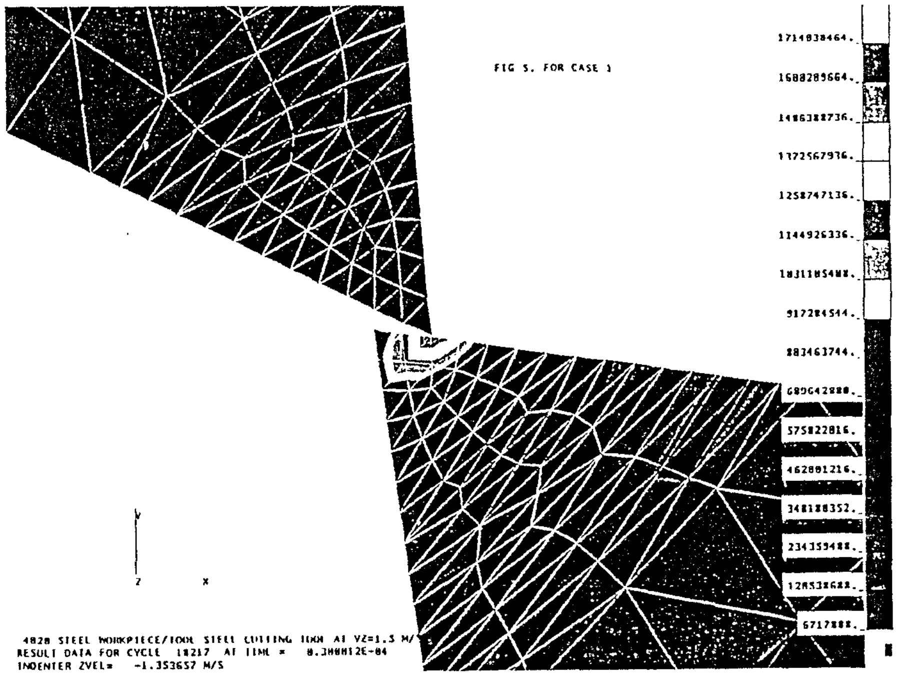

30 μs

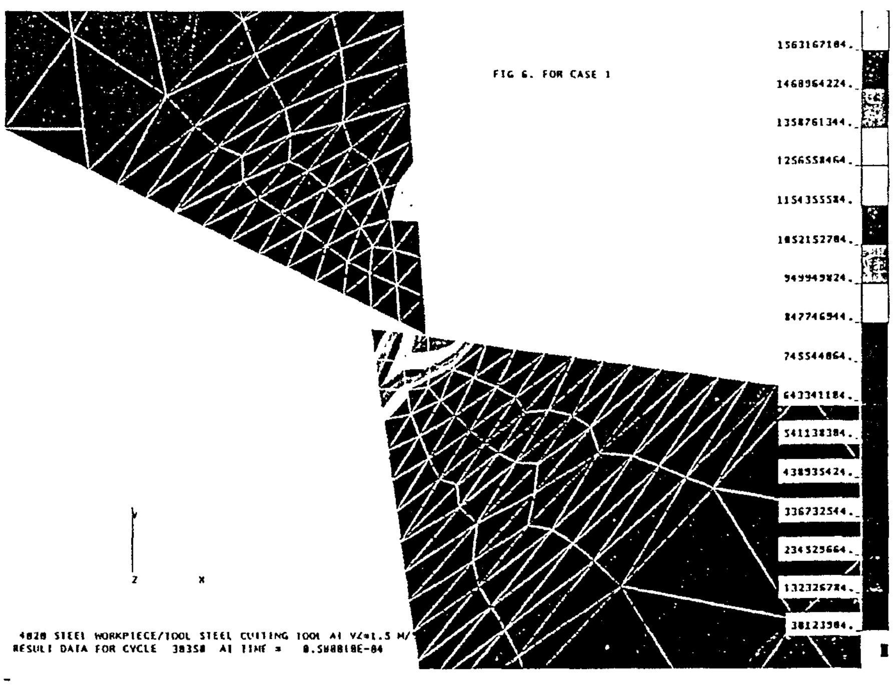

50 μs

Fig. B.6 Stress Distribution in the Cutting Tool under Impact in the Intermittent Turning Process at 30 μs and 50 μs with 1.5m/s Cutting Speed

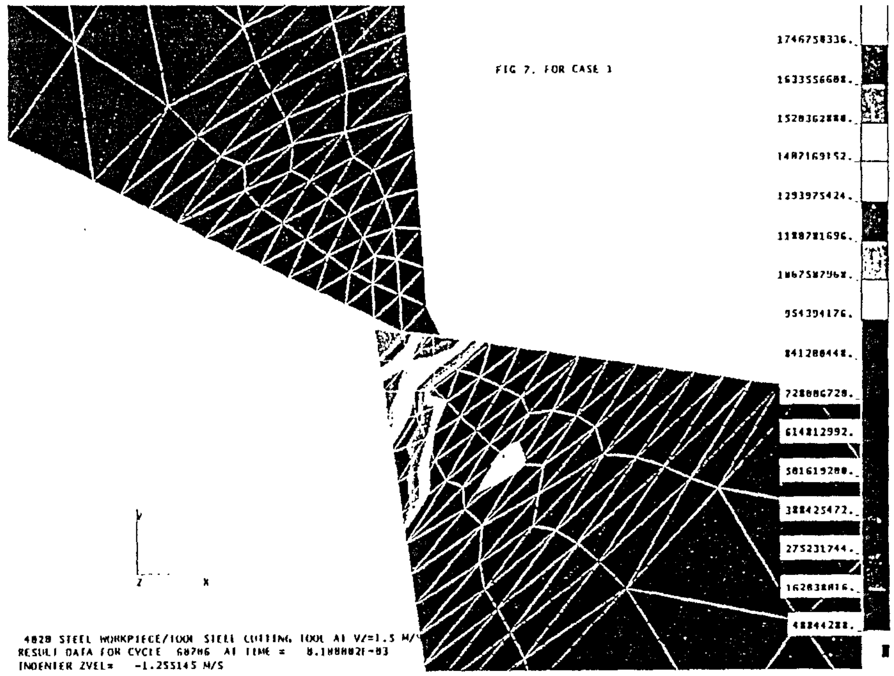

100μs

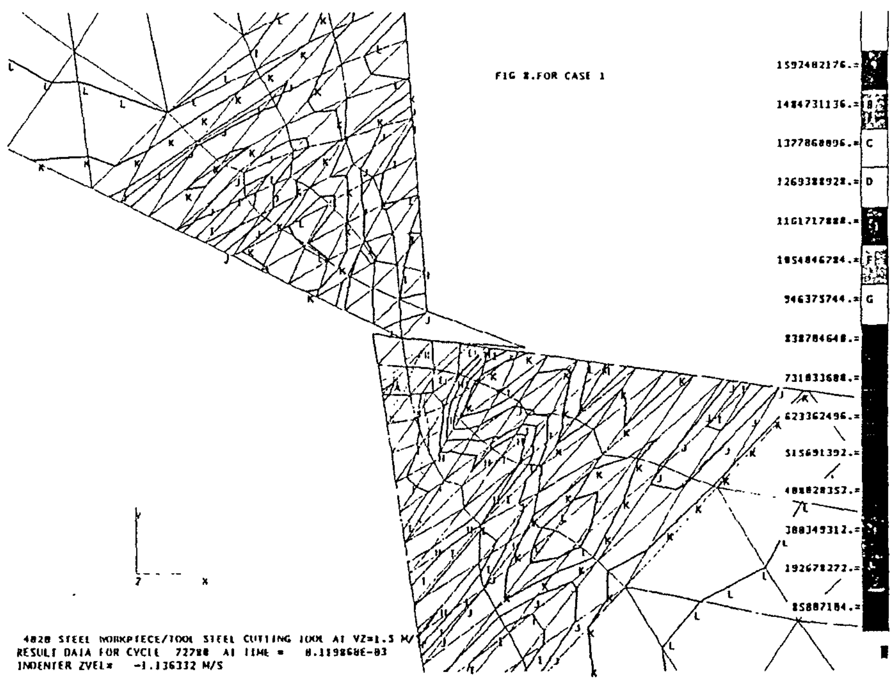

120μs

Fig. B.7 Stress Distribution in the Cutting Tool under Impact in the Intermittent Turning Process at 120 μs with 1.5m/s Cutting Speed

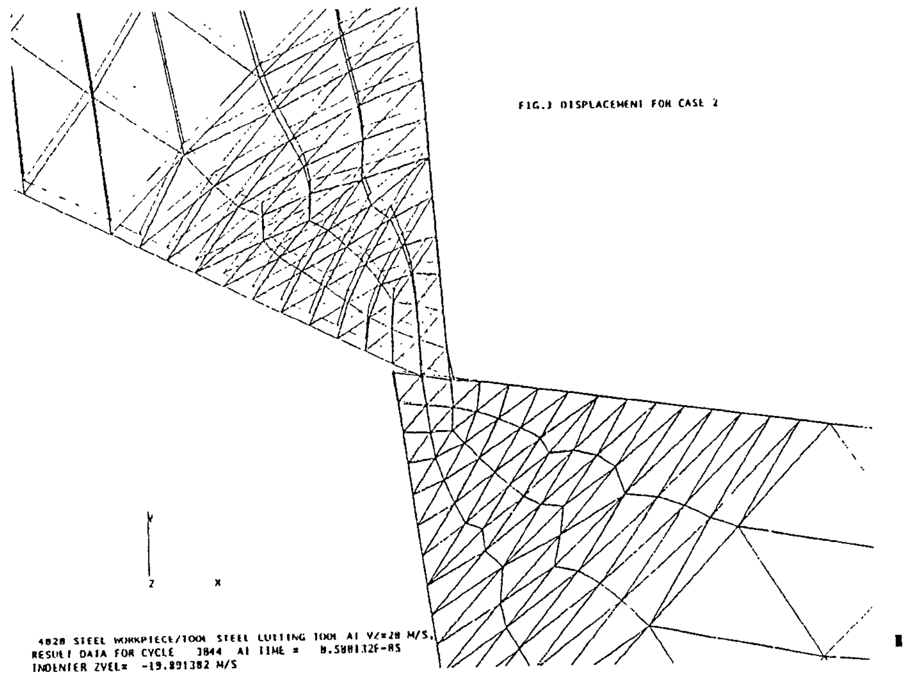

5 μs

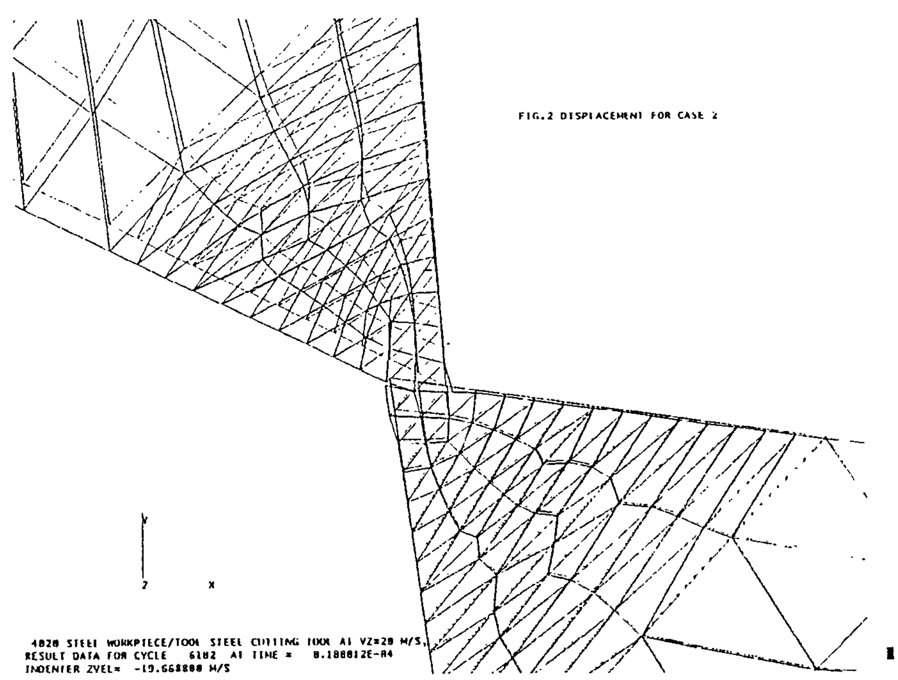

10 μs

Fig. B.8 Deformation Profiles of the Cutting Tool under Impact in the Intermittent Turning Process at 5 μs and 10 μs with 6m/s Cutting Speed

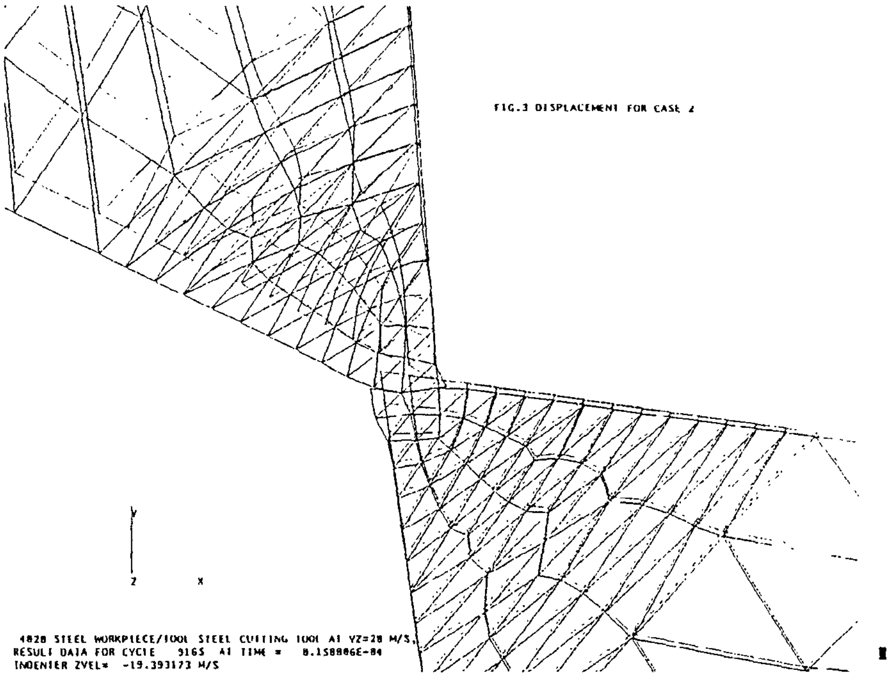

15 μs

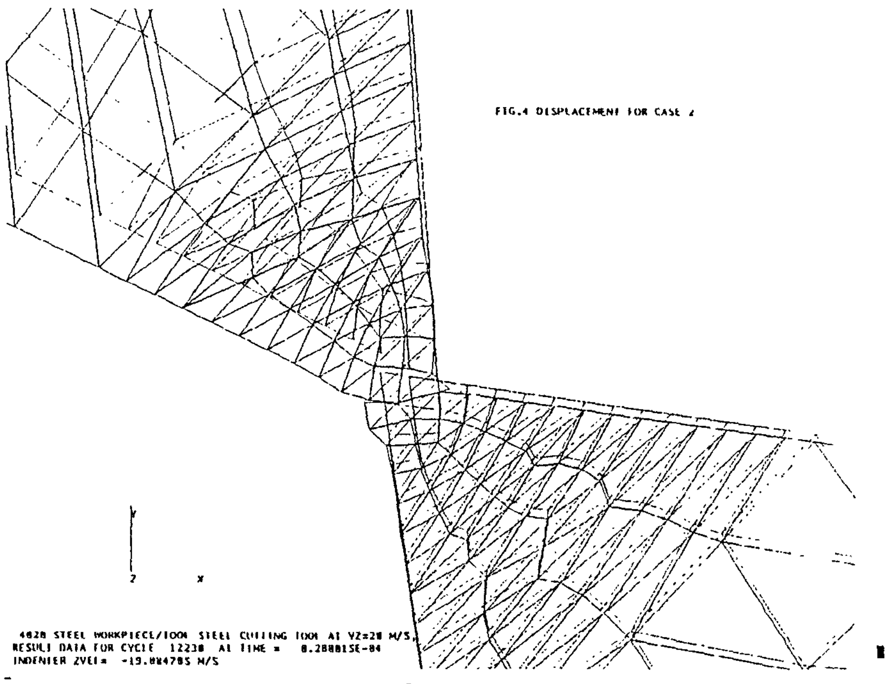

20μs

Fig. B.9 Deformation Profiles of the Cutting Tool under Impact in the Intermittent Turning Process at 15 μs and 20 μs with 6m/s Cutting Speed

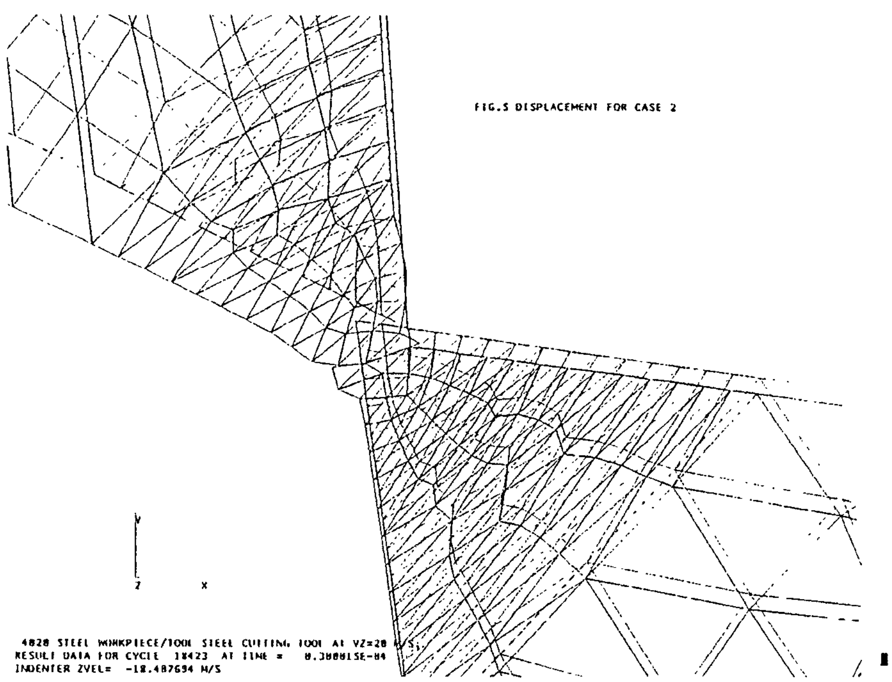

30 μs

Fig. B.10 Deformation Profiles of the Cutting Tool under Impact in the Intermittent Turning Process at 30 μs with 6m/s Cutting Speed

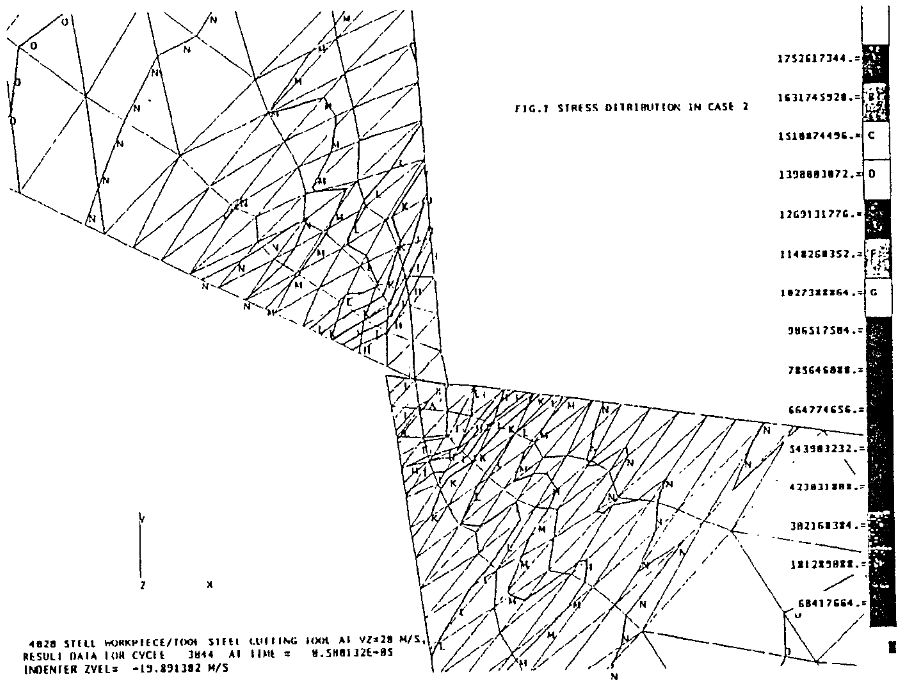

5 μs

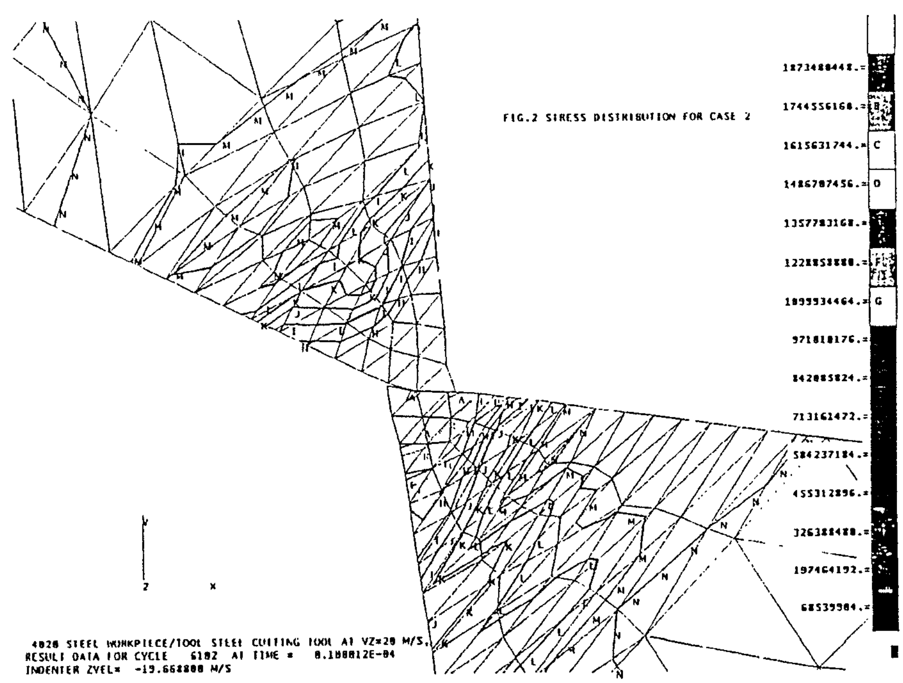

10 μs

Fig. B.11 Stress Distribution in the Cutting Tool under Impact in the Intermittent Turning Process at 5 μs and 10 μs with 6m/s Cutting Speed

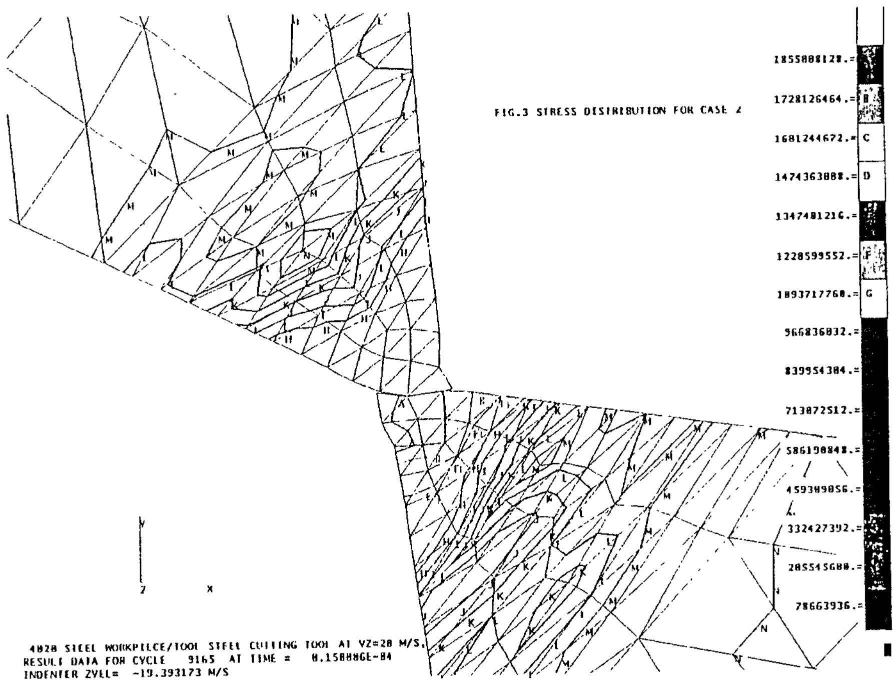

15 μs

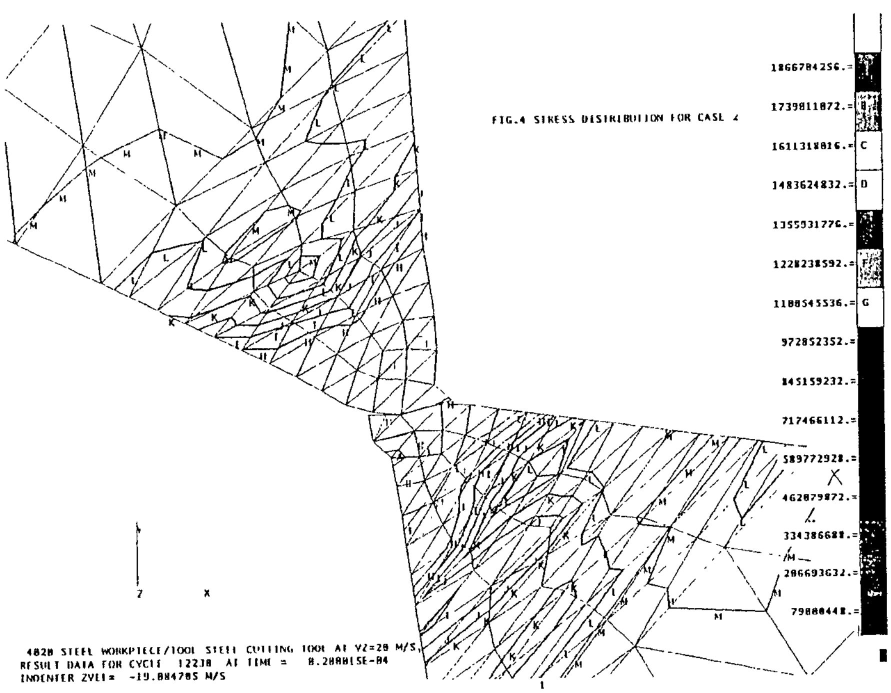

20μs

Fig.B.12 Stress Distribution in the Cutting Tool under Impact in the Intermittent Turning Process at 15 μs and 20 μs with 6m/s Cutting Speed